

**DISCRETIZATIONS AND SOLVERS FOR COUPLING
STOKES-DARCY FLOWS WITH TRANSPORT**

by

Danail Vassilev

M.S. in Physics, University of Sofia, Bulgaria, 2000

M.S. in Nuclear Engineering, University of Cincinnati, 2003

Submitted to the Graduate Faculty of
the Department of Mathematics in partial fulfillment
of the requirements for the degree of

Doctor of Philosophy

University of Pittsburgh

2010

UNIVERSITY OF PITTSBURGH
DEPARTMENT OF MATHEMATICS

This dissertation was presented

by

Danail Vassilev

It was defended on

July 16, 2010

and approved by

Prof. Ivan Yotov, Department of Mathematics, University of Pittsburgh

Prof. William Layton, Department of Mathematics, University of Pittsburgh

Prof. Catalin Trenchea, Department of Mathematics, University of Pittsburgh

Dr. Myron Sussman, Department of Mathematics, University of Pittsburgh

Dr. Konstantin Lipnikov, Theoretical Division, Los Alamos National Laboratory

Dissertation Director: Prof. Ivan Yotov, Department of Mathematics, University of Pittsburgh

DISCRETIZATIONS AND SOLVERS FOR COUPLING STOKES-DARCY FLOWS WITH TRANSPORT

Danail Vassilev, PhD

University of Pittsburgh, 2010

This thesis studies a mathematical model, in which Stokes-Darcy flow system is coupled with a transport equation. The objective is to develop stable and convergent numerical schemes that could be used in environmental applications. Special attention is given to discretization methods that conserve mass locally.

First, we present a global saddle point problem approach, which employs the discontinuous Galerkin method to discretize the Stokes equations and the mimetic finite difference method to discretize the Darcy equation. We show how the numerical scheme can be formulated on general polygonal (polyhedral in three dimensions) meshes if suitable operators mapping from degrees of freedom to functional spaces are constructed. The scheme is analyzed and error estimates are derived. A hybridization technique is used to solve the system effectively. We ran several numerical experiments to verify the theoretical convergence rates and depending on the mesh type we observed superconvergence of the computed solution in the Darcy region.

Another approach that we use to deal with the flow equations is based on non-overlapping domain decomposition. Domain decomposition enables us to solve the coupled Stokes-Darcy flow problem in parallel by partitioning the computational domain into subdomains, upon which families of coupled local problems of lower complexity are formulated. The coupling of the subdomain problems is removed through an iterative procedure. We investigate the properties of this method and derive estimates for the condition number of the associated algebraic system. Results from computer tests supporting the convergence analysis of the method are provided.

To discretize the transport equation we use the local discontinuous Galerkin (LDG) method,

which can be thought as a discontinuous mixed finite element method, since it approximates both the concentration and the diffusive flux. We develop stability and convergence analysis for the concentration and the diffusive flux in the transport equation. The numerical error is a combination of the LDG discretization error and the error from the discretization of the Stokes-Darcy velocity. Several examples verifying the theory and illustrating the capabilities of the method are presented.

TABLE OF CONTENTS

1.0 INTRODUCTION	1
1.1 Flow equations	2
1.1.1 Stokes equations	2
1.1.2 Darcy equations	4
1.1.3 Interface and boundary conditions	5
1.1.4 Formulation of the Stokes-Darcy flow problem	7
1.2 Transport equation	8
1.3 Methodology	9
2.0 A GLOBAL SADDLE POINT PROBLEM APPROACH FOR THE STOKES-DARCY FLOW	12
2.1 Coupling of two discretization methods	12
2.1.1 Notation, preliminaries	13
2.1.2 Discretization in the Stokes domain	14
2.1.3 Discretization in the Darcy domain	19
2.1.4 Discrete formulation of the coupled problem	23
2.2 Trace inequalities and interpolation results	24
2.3 Stability and well-posedness of the discrete problem	27
2.4 Error analysis	32
2.4.1 Error equation	33
2.4.2 Velocity estimate	34
2.4.3 Pressure Estimates	41
2.5 Implementation details	44

2.6 Numerical Results	45
2.6.1 Convergence tests	45
2.6.2 Simulation of coupled surface water and groundwater flows	48
3.0 DOMAIN DECOMPOSITION FOR THE STOKES-DARCY FLOW	52
3.1 Notation, preliminaries	52
3.2 Finite element discretization	54
3.3 Non-overlapping domain decomposition	57
3.3.1 Reduction to an interface problem	59
3.3.2 Floating Stokes subdomains	62
3.4 Analysis of the interface operator	65
3.5 Numerical Results	74
4.0 COUPLING THE STOKES-DARCY FLOW WITH TRANSPORT	80
4.1 Formulation of the LDG method for transport	82
4.2 Stability of the LDG scheme	84
4.3 Error analysis of the LDG scheme	90
4.4 Numerical results	97
4.4.1 Convergence tests	98
4.4.2 Contaminant transport examples	101
5.0 FUTURE WORK AND CONCLUSIONS	108
BIBLIOGRAPHY	112

LIST OF FIGURES

1.1 Computational domain.	2
2.1 Computed solution (left) and the associated error (right) for Test 1.	47
2.2 Computed solution (left) and the associated error (right) for Test 2.	48
2.3 Computed solution (left), permeability field (right) in the simulation.	51
3.1 Computed velocity field in Test 1: horizontal velocity (left); vertical velocity (right).	75
4.1 Permeability of the porous medium in the contaminant transport examples.	101
4.2 Computed velocity field in the contaminant transport examples: horizontal velocity (left); vertical velocity (right).	102
4.3 Initial plume, $t=0.0$. The arrows represent the computed Stokes-Darcy velocity.	103
4.4 The plume at early time is confined to the surface water region, $t=3.0$	103
4.5 The plume penetrates the porous medium, $t=5.0$	104
4.6 The plume spreads through the porous medium, $t=9.0$	104
4.7 Most of the plume has been transported to the porous medium, $t=16.0$	105
4.8 The front enters the surface water region, $t=2.0$. The arrows represent the computed Stokes-Darcy velocity.	106
4.9 The front reaches the porous medium, $t=11.0$	106
4.10 The front propagates inside the porous medium, $t=17.0$	107
5.1 Mortar multiscale example. Left: four subdomains with non-matching grids, right: permeability field	109
5.2 Mortar multiscale example. Computed solution.	109

LIST OF TABLES

1.1	Typical porosity and permeability values.	4
2.1	Numerical errors and convergence rates for Test 1 on unstructured grids.	49
2.2	Numerical errors and convergence rates for Test 1 on structured grids.	49
2.3	Numerical errors and convergence rates for Test 2 on unstructured grids.	50
2.4	Numerical errors and convergence rates for Test 2 on structured grids.	50
3.1	Convergence of the Taylor-Hood and RT0 finite elements for Test 1.	76
3.2	Convergence of CG iterations: $K=0.01$, varying the mesh size for 2 subdomains.	78
3.3	Convergence of CG iterations: $K=1.0$, varying the mesh size for 2 subdomains.	78
3.4	Convergence of CG iterations: $K=2.0$, varying the mesh size for 2 subdomains.	78
3.5	Convergence of CG iterations: $K=0.01$, varying the mesh size for 4 subdomains.	79
3.6	Convergence of CG iterations: $K=1.0$, varying the mesh size for 4 subdomains.	79
3.7	Convergence of CG iterations: $K=2.0$, varying the mesh size for 4 subdomains.	79
4.1	Convergence of the LDG scheme for Test 1: discontinuous tangential velocity.	99
4.2	Convergence of the LDG scheme for Test 2: smooth velocity.	100
4.3	Convergence of the LDG scheme for Test 3.	100

To my wife Ralitsa

Acknowledgements

I would like to express my deep gratitude to Prof. Ivan Yotov for giving me the exciting opportunity to be in his active research group. The confidence he has had in me over these years and his invaluable guidance enabled me to carry out this thesis.

A very special thank to Prof. William Layton for his stimulating and enthusiastic lectures, which gave me an insightful understanding of various topics in numerical analysis.

I am very grateful to Dr. Myron Sussman whose classes and discussions provided me with background to proceed with this research.

I would like to thank Dr. Konstantin Lipnikov for being my mentor for several months at the Los Alamos National Laboratory and giving me very helpful perspectives.

I would like to thank Prof. Catalin Trenchea for taking time to follow my progress as a Graduate Committee member.

I am in debt to Prof. H. Scott Dumas from the Department of Mathematical Sciences at the University of Cincinnati whose course on partial differential equations intensified my interest in the field and greatly influenced my decision to pursue a Ph.D. in Mathematics.

Many thanks to all the friends and colleagues at the Department of Mathematics at Pitt, especially to Evandro and Carolina Manica, Gergina Pencheva, Evgueni Trofimov, and Ben Ganis for creating a warm and inspiring atmosphere.

I would also like to thank my parents and my brother Stanislav for their constant love and support.

Above all, I thank my wife Ralitsa whose love, patience and understanding give me strength to be successful.

1.0 INTRODUCTION

Various problems originating in different fields of science and engineering are formulated and analyzed in terms of partial differential equations (PDE's). The adequate representation of physical systems often requires constructing multiphysics models, which means coupling several equations to represent different processes occurring at the same time in different parts of the domain of interest. The challenge is to develop models that are both physically justifiable and mathematically well-posed. The complexity of such models raises the importance of numerical methods for solving PDE's.

Coupling the Stokes and Darcy equations has a vast scope of practical applications. Such model can be used to describe hydrological systems in which surface water percolates through rocks and sand, physiological phenomena like the blood motion in the vessels, and various industrial problems involving filtration. In this thesis we assume the interaction between surface water and groundwater flows as the physical interpretation of the model. Fresh water is essential to human and other lifeforms. It is estimated that nearly 69 percent of the total fresh water on Earth is frozen in glaciers and permanent ice covers in the Antarctic and the Arctic regions [1]. About 96 percent of the total unfrozen fresh water in the world is groundwater [1], which resides in the pores of the soil or the rocks. A geologic formation containing water that can be withdrawn at wells or springs is called an *aquifer*. One serious problem today is contamination of groundwater. Many aquifers have been invaded by pollutants resulting from leaky underground storage tanks, chemical spills and other human activities. Coupling the Stokes-Darcy equations with a transport equation offers an effective tool for predicting the spread of the pollution and assessing the danger to the fresh water resources.

In our model we consider a fluid region $\Omega_f \subset \mathbb{R}^d$ and a saturated porous medium region $\Omega_p \subset \mathbb{R}^d$, where $d = 2, 3$. These are separated by an interface $\Gamma_{fp} := \overline{\Omega}_f \cap \overline{\Omega}_p$, through which the

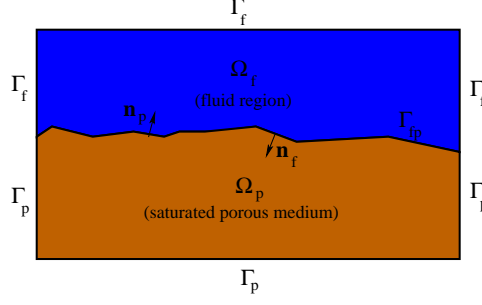


Figure 1.1: Computational domain.

fluid can flow in both directions. Both Ω_f and Ω_p are bounded domains with outward unit normal vectors \mathbf{n}_f and \mathbf{n}_p , respectively. We assume that Ω_f and Ω_p are polygonal for $d = 2$ or polyhedral for $d = 3$ with Lipschitz continuous boundaries. Let $\Gamma_f := \partial\Omega_f \setminus \Gamma_{fp}$ and $\Gamma_p := \partial\Omega_p \setminus \Gamma_{fp}$. We will also use the notation $\Omega := \Omega_f \cup \Omega_p$ and $\Gamma := \partial\Omega$ to represent the whole domain and its boundary. The velocity and the pressure in Ω_f , respectively Ω_p , are denoted by \mathbf{u}_f and p_f , respectively \mathbf{u}_p and p_p .

1.1 FLOW EQUATIONS

1.1.1 Stokes equations

Two important variables in the characterization of fluid motion are the deformation (or strain) rate tensor, which is defined as the symmetric part of the velocity gradient,

$$\mathbf{De} = \frac{1}{2}(\nabla\mathbf{u}_f + (\nabla\mathbf{u}_f)^T),$$

and the Cauchy stress tensor \mathbf{T} , which represents the forces exerted by the fluid per unit infinitesimal area. For a Newtonian fluid, like water, \mathbf{T} and \mathbf{De} are linearly related. Assuming that the fluid is incompressible,

$$\nabla \cdot \mathbf{u}_f = 0,$$

the stress-strain rate relation, also known as the Stokes law, is

$$\mathbf{T} = -p_f \mathbf{I} + 2\mu_f \mathbf{D}\mathbf{e},$$

where \mathbf{I} denotes the identity matrix and μ_f is the dynamic viscosity of the fluid. The time independent flow of a viscous incompressible Newtonian fluid is governed by the Navier-Stokes equations, see e.g. [45], consisting of the momentum equation (1.1) and the mass-conservation equation (1.2):

$$\rho_f(\mathbf{u}_f \cdot \nabla)\mathbf{u}_f - \mu_f \Delta \mathbf{u}_f + \nabla p_f = \mathbf{f}_f \quad \text{in } \Omega_f, \quad (1.1)$$

$$\nabla \cdot \mathbf{u}_f = 0 \quad \text{in } \Omega_f. \quad (1.2)$$

In the first equation ρ_f is the fluid density and \mathbf{f}_f represents a body force, which has the form $\mathbf{f}_f = \rho_f \mathbf{b}$, where \mathbf{b} is the force per unit mass of fluid. Let L_f and U_f be the characteristic length and the characteristic flow speed, respectively. The Reynolds number

$$Re_f = \frac{L_f U_f \rho_f}{\mu_f}$$

characterizes the ratio between the inertia and the viscous forces. In the limit of very small Reynolds number, $Re_f \ll 1$, the viscous term in the momentum equation is dominant and the convective term can be neglected. The resulting Stokes equations (1.3)–(1.4) are suitable to describe the *creeping flow* in a surface basin, e.g. lake.

$$-\mu_f \Delta \mathbf{u}_f + \nabla p_f = \mathbf{f}_f \quad \text{in } \Omega_f, \quad (1.3)$$

$$\nabla \cdot \mathbf{u}_f = 0 \quad \text{in } \Omega_f. \quad (1.4)$$

Table 1.1: Typical porosity and permeability values.

Material	Porosity ϕ	Permeability $K [cm^2]$
Brick	0.12 - 0.34	4.8e-11 - 2.2e-9
Limestone	0.04 - 0.10	2.0e-11 - 4.5e-10
Sand	0.37 - 0.50	2.0e-7 - 1.8e-6
Soil	0.43 - 0.54	2.9e-9 - 1.4e-7

1.1.2 Darcy equations

An aquifer performs two important functions. First, it stores water, serving as a reservoir. Second, it transmits water like a pipeline. The storage capacity of an aquifer depends on its *porosity* ϕ , which is defined as the fraction of the total volume of the aquifer that is occupied by void space. The pipeline function of an aquifer is characterized by the *permeability* of the medium. In Table 1.1 are reported the porosity and permeability values of common porous materials [76].

Darcy's experiments revealed a proportionality between the rate of unidirectional flow and the applied pressure in a uniform porous medium [38]. In three dimensions using modern notation this relationship is expressed by

$$\mathbf{u}_p = -\frac{\mathbf{K}}{\mu_f} \nabla p_p. \quad (1.5)$$

Here \mathbf{u}_p is the *seepage velocity*, which is the average velocity respective to a representative volume incorporating both solid and fluid material, and \mathbf{K} is a symmetric and positive definite tensor representing the permeability. The permeability tensor can be brought into diagonal form

$$\mathbf{K} = \text{diag}\{K_1, K_2, K_3\}$$

by introducing three mutually orthogonal axes called axes of principal directions of anisotropy. It is well known that Darcy's law can be obtained by averaging of the equations for incompressible

flow through porous medium. Darcy's equation holds for sufficiently small \mathbf{u}_p , which means that the Reynolds number

$$Re_p = \frac{L_p U_p \rho_f}{\mu_f},$$

based on the characteristic pore diameter L_p and the characteristic flow speed U_p in the porous medium, is of order unity or smaller. For $Re_p > 10$, the Dupuit-Forchheimer equation (1.6), see e.g. [76], is commonly used to describe a flow of a fluid in a porous medium with scalar permeability K ,

$$\nabla p_p = -K^{-1} \mu_f \mathbf{u}_p - c_F K^{-1/2} \rho_f |\mathbf{u}_p| \mathbf{u}_p, \quad (1.6)$$

where c_F is a dimensionless form-drag constant, which varies with the nature of the porous medium. An equation, which interpolates between Stokes equation and Darcy's law, was suggested by Brinkman [27]

$$\nabla p_p = -K^{-1} \mu_f \mathbf{u}_p + \mu_{eff} \Delta \mathbf{u}_p. \quad (1.7)$$

The coefficient μ_{eff} in (1.7) is the so-called effective viscosity, in general not equal to μ_f . Results presented in [47] suggest that Brinkman equation is valid for porosity values greater than 0.95, and inaccurate for smaller porosity values.

1.1.3 Interface and boundary conditions

In order to couple the flow equations in the free fluid region Ω_f with the equations governing the flow in the porous medium region Ω_p appropriate conditions must be specified on the interface Γ_{fp} . This is a challenging problem from both physical and mathematical point of view. One difficulty stems from the fact that the definitions of the variables differ in the two regions. Also there are no velocity derivatives involved in the Darcy's law while the Stokes equation is of second order for the velocity. Another question to consider is whether the interface conditions are compatible with the boundary conditions at $\Gamma_{fp} \cap \partial\Omega$ [65].

The first interface condition comes from mass conservation and can be written as follows

$$\mathbf{u}_f \cdot \mathbf{n}_f + \mathbf{u}_p \cdot \mathbf{n}_p = 0, \quad \text{on } \Gamma_{fp}. \quad (1.8)$$

Another condition is obtained by balancing the normal forces acting on the interface in each region. The force exerted by the free fluid in Ω_f on the boundary $\partial\Omega_f$ is equal to $-\mathbf{n}_f \cdot \mathbf{T}$. Since the only

force acting on Γ_{fp} from Ω_p is the Darcy pressure p_p , the second interface condition is

$$-\mathbf{n}_f \cdot \mathbf{T} \cdot \mathbf{n}_f = p_f - 2\mu_f \mathbf{n}_f \cdot \mathbf{De} \cdot \mathbf{n}_f = p_p, \quad \text{on } \Gamma_{fp}. \quad (1.9)$$

Due to the fact that the fluid is viscous a condition on the tangential velocity component is needed on the interface. The experimental work of Beavers and Joseph [11] indicated that the slip velocity along Γ_{fp} is proportional to the shear stress of the free fluid, which, mathematically, is expressed as

$$(\mathbf{u}_f - \mathbf{u}_p) \cdot \boldsymbol{\tau}_j = \frac{\sqrt{\tilde{k}_j}}{\mu_f \alpha_0} (-\mathbf{n}_f \cdot \mathbf{T}) \cdot \boldsymbol{\tau}_j, \quad 1 \leq j \leq (d-1) \quad \text{on } \Gamma_{fp}, \quad (1.10)$$

where $\{\boldsymbol{\tau}_j\}_{j=1}^{d-1}$ is an orthonormal system of tangent vectors Γ_{fp} , $\tilde{k}_j = \boldsymbol{\tau}_j \cdot \mu_f \mathbf{K} \cdot \boldsymbol{\tau}_j$, and α_0 is a parameter to be determined experimentally. Saffman [84] proposed a simplified condition by dropping the term $\mathbf{u}_p \cdot \boldsymbol{\tau}_j$ in (1.10). The resulting relationship

$$\mathbf{u}_f \cdot \boldsymbol{\tau}_j = -\frac{\sqrt{\tilde{k}_j}}{\mu_f \alpha_0} \mathbf{n}_f \cdot \mathbf{T} \cdot \boldsymbol{\tau}_j, \quad 1 \leq j \leq (d-1) \quad \text{on } \Gamma_{fp}, \quad (1.11)$$

is known as Beavers-Joseph-Saffman condition.

Depending on the particular flow problem in Ω_f there are different choices of possible boundary conditions on Γ_f . To facilitate the notation in the flow problem formulation we will use no slip boundary condition $\mathbf{u}_f = \mathbf{0}$ on Γ_f , but computational results with combinations of Dirichlet (prescribed velocity) and Neumann (prescribed normal and tangential stresses) boundary data will be presented. For the Darcy's equation we specify no flow boundary condition $\mathbf{u}_p \cdot \mathbf{n}_p = 0$ on Γ_p , which corresponds to an impermeable rock surrounding the aquifer.

1.1.4 Formulation of the Stokes-Darcy flow problem

Now we combine the flow equations in the two regions along with the boundary and the coupling conditions. Our flow model consists of the Stokes equations:

$$\begin{cases} -\nabla \cdot \mathbf{T} \equiv -2\mu_f \nabla \cdot \mathbf{De}(\mathbf{u}_f) + \nabla p_f = \mathbf{f}_f & \text{in } \Omega_f \quad (\text{momentum equation}), \\ \nabla \cdot \mathbf{u}_f = 0 & \text{in } \Omega_f \quad (\text{conservation of mass}), \\ \mathbf{u}_f = \mathbf{0} & \text{on } \Gamma_f, \end{cases} \quad (1.12)$$

Darcy's equations:

$$\begin{cases} \mu_f \mathbf{K}^{-1} \mathbf{u}_p + \nabla p_p = \mathbf{0} & \text{in } \Omega_p \quad (\text{Darcy's law}), \\ \nabla \cdot \mathbf{u}_p = f_p & \text{in } \Omega_p \quad (\text{conservation of mass}), \\ \mathbf{u}_p \cdot \mathbf{n}_p = 0 & \text{on } \Gamma_p, \end{cases} \quad (1.13)$$

solvability condition, which the source function f_p must satisfy:

$$\int_{\Omega_p} f_p \, d\mathbf{x} = 0, \quad (1.14)$$

and the interface conditions:

$$\begin{cases} \mathbf{u}_f \cdot \mathbf{n}_f + \mathbf{u}_p \cdot \mathbf{n}_p = 0 & \text{on } \Gamma_{fp}, \\ -\mathbf{n}_f \cdot \mathbf{T} \cdot \mathbf{n}_f \equiv p_f - 2\mu_f \mathbf{n}_f \cdot \mathbf{De}(\mathbf{u}_f) \cdot \mathbf{n}_f = p_p & \text{on } \Gamma_{fp}, \\ -\frac{\sqrt{k_j}}{\mu_f \alpha_0} \mathbf{n}_f \cdot \mathbf{T} \cdot \boldsymbol{\tau}_j \equiv -\frac{\sqrt{k_j}}{\alpha_0} 2\mathbf{n}_f \cdot \mathbf{De}(\mathbf{u}_f) \cdot \boldsymbol{\tau}_j = \mathbf{u}_f \cdot \boldsymbol{\tau}_j, \quad 1 \leq j \leq (d-1) & \text{on } \Gamma_{fp}. \end{cases} \quad (1.15)$$

1.2 TRANSPORT EQUATION

To model the transport of a contaminant we consider the following advection-diffusion equation

$$\phi c_t + \nabla \cdot (c\mathbf{u} - \mathbf{D}\nabla c) = \phi f_c, \quad \forall (\mathbf{x}, t) \in \Omega \times (0, T), \quad (1.16)$$

where $c(\mathbf{x}, t)$ is the concentration of some chemical component, $\mathbf{D}(\mathbf{x}, t)$ is the diffusion/dispersion tensor assumed to be symmetric and positive definite with smallest and largest eigenvalues D_* and D^* , respectively, $f_c(\mathbf{x}, t)$ is a source term, and \mathbf{u} is the velocity field defined by $\mathbf{u}|_{\Omega_f} = \mathbf{u}_f$ and $\mathbf{u}|_{\Omega_p} = \mathbf{u}_p$. We assume that the porosity in Ω_p satisfies

$$0 \leq \phi_* \leq \phi(\mathbf{x}) \leq \phi^*,$$

and it is set to 1 in Ω_f . The model is completed by the initial condition

$$c(\mathbf{x}, 0) = c^0(\mathbf{x}), \quad \forall \mathbf{x} \in \Omega \quad (1.17)$$

and the boundary conditions

$$(c\mathbf{u} - \mathbf{D}\nabla c) \cdot \mathbf{n} = (c_{in}\mathbf{u}) \cdot \mathbf{n} \quad \text{on } \Gamma_{in}, \quad (1.18)$$

$$(\mathbf{D}\nabla c) \cdot \mathbf{n} = 0 \quad \text{on } \Gamma_{out}. \quad (1.19)$$

Here $\Gamma_{in} := \{\mathbf{x} \in \partial\Omega : \mathbf{u} \cdot \mathbf{n} < 0\}$, $\Gamma_{out} := \{\mathbf{x} \in \partial\Omega : \mathbf{u} \cdot \mathbf{n} \geq 0\}$, and \mathbf{n} is the unit outward normal vector to $\partial\Omega$.

1.3 METHODOLOGY

There are number of stable and convergent numerical methods developed for the coupled Stokes-Darcy flow system, see e.g., [65, 42, 72, 81, 50]. For studying contaminant transport in groundwater flows it is critical to avoid creation of artificial mass sources, which necessitates utilizing locally mass conservative schemes for the porous medium region. Examples of such methods are the discontinuous Galerkin (DG) [80, 10, 70, 81, 93, 41, 88, 7], the mimetic finite difference (MFD) [14, 24, 26], the mixed finite element (MFE) [22, 21, 20, 4, 81, 23, 78], and the finite volume (FV) [57, 58] methods.

For the discretization of the Stokes-Darcy system we consider two different approaches. The first [69] solves a global saddle point problem and employs the DG method for the Stokes region and the MFD method for the Darcy equation. In addition to being locally mass conservative both methods allow to choose meshes that are most suitable for the particular problem. The original DG method was introduced in the early seventies by Reed and Hill [80] for solving the neutron transport equation. The first analysis of the DG method was carried out by Lasaint and Raviart [64]. Since then it has been actively researched and used to solve a wide range of problems: compressible [10] and incompressible [70, 81] fluid flows, magneto-hydrodynamics [93], contaminant transport [41] and elliptic problems [7]. The DG method is formulated on simplicial meshes, which can be unstructured with hanging nodes. It allows one to vary the degree of the approximating polynomials from element to element, which is important if local refinement is needed in some parts of the computational domain. The MFD method is a relatively new discretization technique originating from the support-operator algorithms [86, 62]. The method has been successfully applied to problems of continuum mechanics [73], electromagnetics [61], linear diffusion [62, 67], and recently fluid dynamics [12, 13]. The goal of the MFD discretization is to incorporate in the numerical model the physical principles (conservation laws, solution symmetries) of the underlying system. This is achieved by designing discrete operators that inherit the fundamental properties of the differential operators (grad, curl, div, etc.). The MFD method can handle general polygonal (or polyhedral in 3D) meshes with curved boundaries and possibly degenerate cells, which are well-suited to represent the irregular features of the porous medium. An equivalence between the MFD degrees of freedom and the lowest order Raviart-Thomas MFE spaces has been estab-

lished in [14]. By introducing lifting operators mapping from degrees of freedom to a functional space it is possible to interpret the lowest order DG method as a MFD method, which enables to formulate the DG method on general polygonal (or polyhedral in 3D) meshes [69]. Such meshes are attractive because in some flow problems they may lead to superior convergence rates and accuracy in comparison to the equivalent simplicial meshes. In [46] polygonal meshes are employed to discretize the Stokes and Navier-Stokes equations by using the mixed finite volume method.

In the second approach [91] for the coupled Stokes-Darcy flow problem we employ a non-overlapping domain decomposition method based on [65]. The computational domain is partitioned into several subdomains, on which local problems of lower complexity are introduced by using the governing equations and appropriate interface and boundary conditions. Each subdomain is covered by a local grid, which does not have to match with the grids of the neighbouring subdomains. This is achieved by using *mortar finite element spaces* to impose the interface conditions weakly [54]. Domain decomposition leads naturally to devising parallel algorithms, which are of great importance for large-scale problems. Domain decomposition is very suitable for multiphysics problems, e.g. coupling Stokes and Darcy equations, since different models may be associated with different computational units. Moreover, different numerical schemes within different subdomains can be employed and the reuse of legacy codes is possible. In our approach we use classical finite element spaces to discretize the Stokes equations and mixed finite element spaces to discretize the Darcy equations.

Domain decomposition approach for solving partial differential equations dates back to the nineteenth century, when Schwarz used his alternating method [85] as a theoretical tool to solve a certain class of elliptic problems. Although this idea seemed to be forgotten for a long period of time, domain decomposition has gained a lot of attention over the last decades due to the development of parallel computers. In 1988 Glowinski and Wheeler [55] proposed an algorithm, which combined mixed finite elements with domain decomposition. Domain decomposition for the coupled Stokes-Darcy problem is discussed in [50, 43, 44].

For the numerical approximation of the transport problem we employ the local discontinuous Galerkin (LDG) method [34, 32, 92], which conserves mass locally and accurately approximates sharp fronts. The method has a built-in upwinding mechanism that is used to handle the advective term. The LDG method like the other DG methods can be defined on unstructured grids and allows

one to vary the degree of the approximating polynomials from element to element. The LDG method can be thought of as a discontinuous mixed finite element method, since it approximates both the concentration and the diffusive flux.

2.0 A GLOBAL SADDLE POINT PROBLEM APPROACH FOR THE STOKES-DARCY FLOW

In this chapter we describe a coupled discretization scheme that is based on the DG method in the Stokes domain and the MFD method in the Darcy domain. The lowest order DG method can be viewed as a MFD method if suitable lifting operators mapping from degrees of freedom to functional spaces are constructed. Such unified approach can be used to define the DG method on general polygonal (or polyhedral in 3D) meshes. Ability to extend the discretization scheme for the coupled flow problem on general polyhedral meshes in the entire domain is attractive because it has practical advantages. First, the polyhedral meshes are known in some situations to give better approximation than the equivalent simplicial meshes. Second, using polyhedral elements in both the fluid region and the porous medium region may reduce the complexity of the implementation due to the mesh connectivity. The detailed construction of the unified approach is a topic for future work. In this chapter we derive optimal error estimates for the numerical scheme and provide numerical results to support the theory.

2.1 COUPLING OF TWO DISCRETIZATION METHODS

Finite dimensional approximations of processes taking place in infinite dimensional spaces may cause non-physical effects, e.g. failing to satisfy various physical principles in pointwise sense. Such effects can be treated by using discretization methods that confine them locally. For our model it is essential to conserve mass locally.

On a given mesh the DG method approximates the solution elementwise by polynomial functions that are discontinuous across interelement boundaries. To ensure stability and convergence

to the true solution a suitable penalty term is introduced in the formulation of the DG method. Because the incompressibility constraint, the second equation of (1.12), is enforced variationally with discontinuous test functions, the method conserves mass locally (per element) in integral sense.

The MFD method is based on approximating the differential operators in the governing equations by discrete operators that satisfy discrete versions of the fundamental identities of vector and tensor calculus, e.g. Gauss divergence theorem, to enforce local conservation laws and solution symmetries. A common framework for mimetic discretization using concepts from algebraic topology is discussed in [16].

2.1.1 Notation, preliminaries

For brevity we will use a subscript $\alpha = f, p$ to represent variables in either the free fluid region Ω_f or the porous medium region Ω_p . Let Ω_α^h be a partition of Ω_α , $\alpha = f, p$ into polygonal (or polyhedral in 3D) elements E with diameter h_E . Let $h_\alpha = \max_{E \in \Omega_\alpha^h} h_E$. We assume that this partition is shape-regular in the following sense.

Definition 2.1.1 *The polygonal (polyhedral) partition Ω_α^h is shape-regular if*

- *Each element E has at most N^* edges (faces), where N^* is independent of h_α*
- *Each element E is star-shaped with respect to every point of a ball of radius $\rho^* h_E$ centered at point $\mathbf{x}_E \in E$, where ρ^* is independent of h_α . Moreover, each edge (face) e of E is star-shaped with respect to every point of a ball of radius $\rho^* h_E$ centered at point $\mathbf{x}_e \in e$.*
- *Each element E can be split into shape-regular (in the sense of [31]) simplices and the union of all such simplices is a conformal mesh in Ω_α .*

The auxiliary simplicial mesh is used only in our analysis and does not need to be built explicitly. Meshes with non-convex elements may also satisfy the above definition. Note that partitions Ω_f^h and Ω_p^h do not have to match at the interface Γ_{fp} . Let $|E|$ and $|e|$ be the Lebesgue's measures of E and e , respectively. Hereafter, we shall use term *face* for both a face in 3D and an edge in 2D. Thus, for every element E and every face e we have

$$C h_E^d \leq |E| \leq h_E^d, \quad C h_E^{d-1} \leq |e| \leq h_E^{d-1}, \quad (2.1)$$

where the constant C is independent of h_E and E .

Let \mathcal{E}_α^h be the set of interior faces of Ω_α^h . For every mesh face e , we define a unit normal vector \mathbf{n}_e that will be fixed once and for all. If e belongs to Γ_α , we choose \mathbf{n}_e to be pointing outward to Ω_α . If e belongs to Γ_{fp} , we choose \mathbf{n}_e to be pointing outward to Ω_p . Let \mathbf{n}_E be the outward unit normal vector to E and $\chi_E^e = \mathbf{n}_e \cdot \mathbf{n}_E$. The mutual orientation of \mathbf{n}_e and \mathbf{n}_E is represented by $\chi_E^e \equiv \mathbf{n}_e \cdot \mathbf{n}_E$, which is either 1 or -1 .

2.1.2 Discretization in the Stokes domain

Let D be a domain in \mathbb{R}^d and $W^{s,t}(D)$, $s \geq 0$, $t \geq 1$, be the usual Sobolev space [2] with a norm $\|\cdot\|_{s,t,D}$ and a seminorm $|\cdot|_{s,t,D}$. The norm and seminorm in the Hilbert space $H^s(D) \equiv W^{s,2}(D)$ are denoted by $\|\cdot\|_{s,D}$ and $|\cdot|_{s,D}$, respectively. The Euclidean norm of algebraic vectors is denoted by $\|\cdot\|$, i.e. without a subscript.

We extend the formulation in [81] on simplicial elements to general polyhedra. Let X_f and Q_f be Sobolev spaces for the velocity and pressure, respectively, in the Stokes domain:

$$\begin{aligned} X_f &= \{\mathbf{v}_f \in (L^2(\Omega_f))^d : \mathbf{v}_f|_E \in (W^{2,3/2}(E))^d \ \forall E \in \Omega_f^h\}, \\ Q_f &= \{q_f \in L^2(\Omega_f) : q_f|_E \in W^{1,3/2}(E) \ \forall E \in \Omega_f^h\}. \end{aligned}$$

The functions in X_f and Q_f have double valued traces on the interior element faces. The trace inequality and the Sobolev imbedding theorem imply that $q|_e \in L^2(e)$. For a function w , we define its average $\{w\}_e$ and its jump $[w]_e$ across an interior face $e \in \mathcal{E}_1^h$ as follows:

$$\{w\}_e = \frac{1}{2}w|_{E_1} + \frac{1}{2}w|_{E_2}, \quad [w]_e = w|_{E_1} - w|_{E_2},$$

where E_1 and E_2 are two elements that share face e and such that \mathbf{n}_e is directed from E_1 to E_2 . For $e \in \partial\Omega_f^h$, the average and the jump are equal to the value of w .

Following [81], we introduce the following norms:

$$\begin{aligned} |||\mathbf{v}_f|||_{s,\Omega_f}^2 &= \sum_{E \in \Omega_f^h} \|\mathbf{v}_f\|_{s,E}^2, \\ \|\mathbf{v}_f\|_{X_f}^2 &= |||\nabla \mathbf{v}_f|||_{0,\Omega_f}^2 + \sum_{e \in \mathcal{E}_f^h \cup \Gamma_f} \frac{\sigma_e}{|e|} \|[\mathbf{v}_f]\|_{0,e}^2 + \sum_{e \in \Gamma_{fp}} \sum_{j=1}^{d-1} \frac{\mu_f}{G_j} \|\mathbf{v}_f \cdot \boldsymbol{\tau}_j\|_{0,e}^2, \\ \|q_f\|_{Q_f} &= \|q_f\|_{0,\Omega_f}, \end{aligned}$$

where $\sigma_e > 0$ is a parameter that is a constant on e and $G_j = \sqrt{\tilde{k}_j}/\alpha_0$, $j = 1, d-1$. The DG method for the Stokes equation is expressed in terms of the bilinear forms $a_f : X_f \times X_f \rightarrow \mathbb{R}$ and $b_f : X_f \times Q_f \rightarrow \mathbb{R}$ defined as follows:

$$\begin{aligned}
a_f(\mathbf{u}_f, \mathbf{v}_f) &= 2\mu_f \sum_{E \in \Omega_f^h} \int_E \mathbf{De}(\mathbf{u}_f) : \mathbf{De}(\mathbf{v}_f) dx + \sum_{e \in \mathcal{E}_f^h \cup \Gamma_f} \frac{\sigma_e}{h_e} \int_e [\mathbf{u}_f] \cdot [\mathbf{v}_f] ds \\
&\quad - 2\mu_f \sum_{e \in \mathcal{E}_f^h \cup \Gamma_f} \int_e \{\mathbf{De}(\mathbf{u}_f) \mathbf{n}_e\} \cdot [\mathbf{v}_f] ds + 2\mu_f \varepsilon \sum_{e \in \mathcal{E}_f^h \cup \Gamma_f} \int_e \{\mathbf{De}(\mathbf{v}_f) \mathbf{n}_e\} \cdot [\mathbf{u}_f] ds \\
&\quad + \sum_{e \in \Gamma_{fp}} \sum_{j=1}^{d-1} \frac{\mu_f}{G_j} \int_e (\mathbf{u}_f \cdot \boldsymbol{\tau}_j)(\mathbf{v}_f \cdot \boldsymbol{\tau}_j) ds, \quad \forall \mathbf{u}, \mathbf{v} \in X_f \\
b_f(\mathbf{v}_f, q_f) &= - \sum_{E \in \Omega_f^h} \int_E q_f \nabla \cdot \mathbf{v}_f dx + \sum_{e \in \mathcal{E}_f^h \cup \Gamma_f} \int_e \{q_f\} [\mathbf{v}_f] \cdot \mathbf{n}_e ds, \quad \forall \mathbf{v}_f \in X_f, \forall q_f \in Q_f.
\end{aligned}$$

The jump term involving σ_e is added for stabilization. We assume that for all faces e

$$\sigma_e \geq \sigma_0 > 0, \quad (2.2)$$

where σ_0 is chosen to be sufficiently large according to Lemma 2.3.3 in order to guarantee the coercivity of $a(\cdot, \cdot)$. The parameter ε controls the symmetry of the bilinear form and takes value -1 , 0 or 1 for the symmetric interior penalty Galerkin (SIPG) [6, 94], the incomplete interior penalty Galerkin (IIPG) [41], and the non-symmetric interior penalty Galerkin (NIPG) [77] methods, respectively.

Lemma 2.1.1 *The solution $(\mathbf{u}, p) = (\mathbf{u}_f, \mathbf{u}_p; p_f, p_p)$ to (1.12)–(1.15) satisfies*

$$a_f(\mathbf{u}_f, \mathbf{v}_f) + b_f(\mathbf{v}_f, p_f) + \int_{\Gamma_{fp}} p_p \mathbf{v}_f \cdot \mathbf{n}_f ds = \int_{\Omega_1} \mathbf{f}_f \cdot \mathbf{v}_f dx, \quad \forall \mathbf{v}_f \in X_f, \quad (2.3)$$

$$b_f(\mathbf{u}_f, q_f) = 0, \quad \forall q_f \in Q_f. \quad (2.4)$$

Proof. We use similar arguments as in [81]. Multiplying the momentum equation in (1.12) by $\mathbf{v}_f \in X_f$ and integrating by parts over one element E yields

$$\int_E (2\mu_f \mathbf{De}(\mathbf{u}_f) : \nabla \mathbf{v}_f - p_f \nabla \cdot \mathbf{v}_f) dx - \int_{\partial E} ((2\mu_f \mathbf{De}(\mathbf{u}_f) - p_f \mathbf{I}) \mathbf{n}_E) \cdot \mathbf{v}_f ds = \int_E \mathbf{f}_f \cdot \mathbf{v}_f dx. \quad (2.5)$$

Since the tensor $\mathbf{De}(\mathbf{u}_f)$ is symmetric and $\nabla \mathbf{v}_f$ can be expressed as a sum of symmetric and antisymmetric tensors

$$\nabla \mathbf{v}_f = \frac{1}{2}(\nabla \mathbf{v}_f + (\nabla \mathbf{v}_f)^T) + \frac{1}{2}(\nabla \mathbf{v}_f - (\nabla \mathbf{v}_f)^T),$$

we can write

$$\mathbf{De}(\mathbf{u}_f) : \nabla \mathbf{v}_f = \mathbf{De}(\mathbf{u}_f) : \frac{1}{2}(\nabla \mathbf{v}_f + (\nabla \mathbf{v}_f)^T) = \mathbf{De}(\mathbf{u}_f) : \mathbf{De}(\mathbf{v}_f). \quad (2.6)$$

Substituting (2.6) into (2.5) and summing over all the elements,

$$\begin{aligned} & \sum_{E \in \Omega_f^h} \int_E (2\mu_f \mathbf{De}(\mathbf{u}_f) : \mathbf{De}(\mathbf{v}_f) - p_f \nabla \cdot \mathbf{v}_f) dx \\ & - \sum_{e \in \mathcal{E}_f^h} \int_e \{(2\mu_f \mathbf{De}(\mathbf{u}_f) - p_f \mathbf{I}) \mathbf{n}_e\} \cdot [\mathbf{v}_f] ds - \sum_{e \in \mathcal{E}_f^h} \int_e [(2\mu_f \mathbf{De}(\mathbf{u}_f) - p_f \mathbf{I}) \mathbf{n}_e] \cdot \{\mathbf{v}_f\} ds \\ & - \int_{\Gamma_{fp}} ((2\mu_f \mathbf{De}(\mathbf{u}_f) - p_f \mathbf{I}) \mathbf{n}_f) \cdot \mathbf{v}_f ds - \int_{\Gamma_f} ((2\mu_f \mathbf{De}(\mathbf{u}_f) - p_f \mathbf{I}) \mathbf{n}_f) \cdot \mathbf{v}_f ds \\ & = \int_{\Omega_f} \mathbf{f}_f \cdot \mathbf{v}_f dx. \end{aligned}$$

Using the regularity of the true solution,

$$\begin{aligned} & \sum_{E \in \Omega_f^h} \int_E (2\mu_f \mathbf{De}(\mathbf{u}_f) : \mathbf{De}(\mathbf{v}_f) - p_f \nabla \cdot \mathbf{v}_f) dx + \sum_{e \in \mathcal{E}_f^h \cup \Gamma_f} \frac{\sigma_e}{h_e} \int_e [\mathbf{u}] \cdot [\mathbf{v}] ds \\ & - \sum_{e \in \mathcal{E}_f^h} \int_e \{(2\mu_f \mathbf{De}(\mathbf{u}_f) - p_f \mathbf{I}) \mathbf{n}_e\} \cdot [\mathbf{v}_f] ds + \epsilon \sum_{e \in \mathcal{E}_f^h \cup \Gamma_f} \int_e \{2\mu_f \mathbf{De}(\mathbf{v}_f) \mathbf{n}_e\} \cdot [\mathbf{u}_f] ds \\ & - \int_{\Gamma_{fp}} ((2\mu_f \mathbf{De}(\mathbf{u}_f) - p_f \mathbf{I}) \mathbf{n}_f) \cdot \mathbf{v}_f ds - \int_{\Gamma_f} ((2\mu_f \mathbf{De}(\mathbf{u}_f) - p_f \mathbf{I}) \mathbf{n}_f) \cdot \mathbf{v}_f ds \\ & = \int_{\Omega_f} \mathbf{f}_f \cdot \mathbf{v}_f dx. \end{aligned}$$

Decomposing the integrand in the interface term into normal and tangential components and applying the last two interface conditions in (1.15), we have

$$\begin{aligned}
& ((2\mu_f \mathbf{D}\mathbf{e}(\mathbf{u}_f) - p_f \mathbf{I}) \mathbf{n}_f) \cdot \mathbf{v}_f = \\
& ((2\mu_f \mathbf{D}\mathbf{e}(\mathbf{u}_f) - p_f \mathbf{I}) \mathbf{n}_f) \cdot \mathbf{n}_f (\mathbf{v}_f \cdot \mathbf{n}_f) + \sum_{j=1}^{d-1} ((2\mu_f \mathbf{D}\mathbf{e}(\mathbf{u}_f) - p_f \mathbf{I}) \mathbf{n}_f) \cdot \boldsymbol{\tau}_j (\mathbf{v}_f \cdot \boldsymbol{\tau}_j) = \\
& - p_p (\mathbf{v}_f \cdot \mathbf{n}_f) - \sum_{j=1}^{d-1} \frac{\mu_f}{G_j} (\mathbf{u}_f \cdot \boldsymbol{\tau}_j) (\mathbf{v}_f \cdot \boldsymbol{\tau}_j).
\end{aligned}$$

Thus, we obtain the variational equation

$$\begin{aligned}
& \sum_{E \in \Omega_f^h} \int_E 2\mu_f \mathbf{D}\mathbf{e}(\mathbf{u}_f) : \mathbf{D}\mathbf{e}(\mathbf{v}_f) dx + \sum_{e \in \mathcal{E}_f^h \cup \Gamma_f} \frac{\sigma_e}{h_e} \int_e [\mathbf{u}] \cdot [\mathbf{v}] ds \\
& + \int_{\Gamma_{fp}} p_p \mathbf{v}_f \cdot \mathbf{n}_f ds + \sum_{e \in \Gamma_{fp}} \sum_{j=1}^{d-1} \frac{\mu_f}{G_j} \int_e (\mathbf{u}_f \cdot \boldsymbol{\tau}_j) (\mathbf{v}_f \cdot \boldsymbol{\tau}_j) ds \\
& - \sum_{e \in \mathcal{E}_f^h \cup \Gamma_f} \int_e \{2\mu_f \mathbf{D}\mathbf{e}(\mathbf{u}_f) \mathbf{n}_e\} \cdot [\mathbf{v}_f] ds + \epsilon \sum_{e \in \mathcal{E}_f^h \cup \Gamma_f} \int_e \{2\mu_f \mathbf{D}\mathbf{e}(\mathbf{v}_f) \mathbf{n}_e\} \cdot [\mathbf{u}_f] ds \\
& - \sum_{E \in \Omega_f^h} \int_E p_f \nabla \cdot \mathbf{v}_f dx + \sum_{e \in \mathcal{E}_f^h \cup \Gamma_f} \{p_f\} [\mathbf{v}] \cdot \mathbf{n}_e ds = \int_{\Omega_f} \mathbf{f}_f \cdot \mathbf{v}_f dx, \quad \forall \mathbf{v}_f \in X_f,
\end{aligned}$$

which can be written as

$$a_f(\mathbf{u}_f, \mathbf{v}_f) + b_f(\mathbf{v}_f, p_f) + \int_{\Gamma_{fp}} p_p \mathbf{v}_f \cdot \mathbf{n}_f ds = \int_{\Omega_1} \mathbf{f}_f \cdot \mathbf{v}_f dx, \quad \forall \mathbf{v}_f \in X_f.$$

Similarly, the incompressibility condition in (1.12) combined with the regularity of the solution imply that

$$b_f(\mathbf{u}_f, q_f) = 0, \quad \forall q_f \in Q_f. \tag{2.7}$$

□

The case of simplicial elements has been studied extensively in the literature. Let \mathbb{P}_r denote the space of polynomials of degree at most r . The DG discrete spaces X_f^h and Q_f^h for the velocity and pressure, respectively, are defined as

$$\begin{aligned}
X_f^h &= \{\mathbf{v}_f^h \in X_f : \mathbf{v}_f^h|_E \in (\mathbb{P}_r(E))^d \quad \forall E \in \Omega_f^h\}, \\
Q_f^h &= \{q_f^h \in Q_f : q_f^h|_E \in \mathbb{P}_{r-1}(E) \quad \forall E \in \Omega_f^h\}.
\end{aligned}$$

We consider the cases $r = 1, 2, 3$ in two-dimensions and $r = 1$ in three-dimensions.

To develop a lowest order ($r = 1$) DG method for general polyhedra, we follow the mimetic approach and consider a lifting operator from degrees of freedom defined on faces to a functional space. For each element E and every face e of E , we associate d degrees of freedom (a vector in \mathbb{R}^d) representing the mean velocity on e :

$$\mathbf{V}_{f,E}^e = \frac{1}{|e|} \int_e \mathbf{v}_f ds.$$

Let $X_{f,MFD}^h$ be the vector space with the above degrees of freedom. For a vector $\mathbf{V}_f \in X_{f,MFD}^h$, let $\mathbf{V}_{f,E}$ be its restriction to element E .

On each E we need a lifting operator $\mathcal{R}_{f,E}$ acting on a vector $\mathbf{V}_{f,E}$ and returning a function in $H^1(E)$. We assume that the lifting operator has the following properties:

(L1) The lifted function has mean values on all faces e of E equal to the prescribed degrees of freedom:

$$\frac{1}{|e|} \int_e \mathcal{R}_{f,E}(\mathbf{V}_{f,E}) ds = \mathbf{V}_{f,E}^e.$$

(L2) The lifting operator is exact for linear functions. More precisely, if $\mathbf{V}_{f,E}^L$ is the vector of face mean values of the restriction on the element E of a linear function \mathbf{v}_f^L , then

$$\mathcal{R}_{f,E}(\mathbf{V}_{f,E}^L) = \mathbf{v}_f^L.$$

(L3) On every element $E \in \Omega_f^h$ the lifting operator satisfies

$$|\mathcal{R}_{f,E}(\mathbf{V}_{f,E})|_{m,E}^2 \leq Ch_E^{d-2m} \|\mathbf{V}_{f,E}\|^2, \quad \forall \mathbf{V}_{f,E} \in X_{f,MFD}^h(E),$$

where $m = 0, 1$.

Using the elemental lifting operators $\mathcal{R}_{1f,E}$, we define the following finite element spaces:

$$X_{f,LIFT}^h = \{\mathbf{v}_f^h: \mathbf{v}_f^h|_E = \mathcal{R}_{f,E}(\mathbf{V}_{f,E}), \quad \forall E \in \Omega_f^h, \forall \mathbf{V}_{f,E} \in X_{f,MFD}^h(E)\},$$

$$Q_{f,LIFT}^h = \{q_f^h: q_f^h|_E \in \mathbb{P}_0(E), \quad \forall E \in \Omega_f^h\}.$$

When E is a simplex, the lifting operator can be chosen to be the lowest order Crouzeix-Raviart finite element [37]. If the Crouzeix-Raviart finite element space is used for the DG space X_f^h , then $X_f^h \times Q_f^h$ for $r = 1$ coincide with $X_{f,LIFT}^h \times Q_{f,LIFT}^h$. The rigorous construction of lifting operators on polygonal (polyhedral in 3D) elements is a topic for future work.

The spaces $X_{f,LIFT}^h \times Q_{f,LIFT}^h$ are new DG spaces for Stokes on polygons or polyhedra. To keep the notation simple, for the rest of the paper we will denote the DG spaces on Stokes for both simplicial and polyhedral elements by $X_f^h \times Q_f^h$,

We are now ready to formulate the DG method in Ω_f . Given an approximation $\bar{\lambda}^h$ of p_2 on Γ_{fp} (to be defined later), the DG solution on Ω_f , $(\mathbf{u}_f^h, p_f^h) \in X_f^h \times Q_f^h$, satisfies

$$a_f(\mathbf{u}_f^h, \mathbf{v}_f^h) + b_f(\mathbf{v}_f^h, p_f^h) + \int_{\Gamma_{fp}} \bar{\lambda}^h \mathbf{v}_f^h \cdot \mathbf{n}_f ds = \int_{\Omega_f} \mathbf{f}_f \cdot \mathbf{v}_f^h dx, \quad \forall \mathbf{v}_f^h \in X_f^h, \quad (2.8)$$

$$b_f(\mathbf{u}_f^h, q_f^h) = 0, \quad \forall q_f^h \in Q_f^h. \quad (2.9)$$

2.1.3 Discretization in the Darcy domain

Let X_p and Q_p be the Sobolev spaces for the velocity and pressure in Ω_p , respectively, defined as follows:

$$X_p = \{\mathbf{v}_p \in (L^s(\Omega_p))^d, s > 2: \nabla \cdot \mathbf{v}_p \in L^2(\Omega_p)\}, \quad Q_p = L^2(\Omega_p).$$

We introduce the following L^2 -norms:

$$\|\mathbf{v}_p\|_{X_p} = \|\mathbf{v}_p\|_{0,\Omega_p}, \quad \|q_p\|_{Q_p} = \|q_p\|_{0,\Omega_p}.$$

It is easy to see that the solution (\mathbf{u}, p) to (1.12)–(1.15) satisfies

$$\int_{\Omega_p} \mathbf{K}^{-1} \mathbf{u}_p \cdot \mathbf{v}_p dx - \int_{\Omega_p} p_p \nabla \cdot \mathbf{v}_p dx + \int_{\Gamma_{fp}} p_p \mathbf{v}_p \cdot \mathbf{n}_p ds = 0, \quad \forall \mathbf{v}_p \in X_p, \quad (2.10)$$

$$\int_{\Omega_p} q_p \nabla \cdot \mathbf{u}_p dx = \int_{\Omega_p} f_p q_p dx, \quad \forall q_p \in Q_p. \quad (2.11)$$

Note that the boundary integral in (2.10) is well defined if $p_p \in H^1(\Omega_p)$.

We use the MFD method [25, 26] to define discrete forms of (2.10)–(2.11). The first step in the MFD method is the definition of degrees of freedom. For each face e in Ω_p^h , we prescribe one degree of freedom V_p^e representing the average flux across e . Let X_p^h be the vector space with these degrees of freedom. The dimension of X_p^h is equal to the number of faces in Ω_p^h .

For any $\mathbf{v}_p \in X_p$, we define its interpolant $\mathbf{v}_p^I \in X_p^h$ by

$$(\mathbf{v}_p^I)^e = \frac{1}{|e|} \int_e \mathbf{v}_p \cdot \mathbf{n}_e ds. \quad (2.12)$$

Lemma 2.1 in [68] guarantees the existence of this integral for every $\mathbf{v}_p \in X_p$.

For any $\mathbf{V}_p \in X_2^p$, let $\mathbf{V}_{p,E}$ denote the vector of degrees of freedom associated only with an element E . We denote its component associated with face e by $V_{p,E}^e$.

To approximate the pressure, on each element $E \in \Omega_p^h$, we introduce one degree of freedom $P_{p,E}$ representing the average pressure on E . Let Q_p^h be the vector space with these degrees of freedom. The dimension of Q_p^h is equal to the number of elements in Ω_p^h . For any $p_p \in Q_p$, we define its interpolant $p_p^I \in Q_p^h$ by

$$(p_p^I)_E = \frac{1}{|E|} \int_E p_p dx. \quad (2.13)$$

We also need to define a discrete mimetic space to approximate the pressure on the interface Γ_{fp} . This space will also serve the role of a Lagrange multiplier space for imposing weakly the normal flux continuity across Γ_{fp} . For each face $e \in \Gamma_{fp}^h = \Omega_p^h|_{\Gamma_{fp}}$ we introduce one degree of freedom λ^e representing the average pressure on e . Let Λ_{fp}^h be the vector space with these degrees of freedom. Note also that $\Lambda_{fp}^h = X_p^h|_{\Gamma_{fp}}$ and its dimension is equal to the number of faces of Γ_{fp} .

The second step in the MFD method is to equip the discrete spaces Q_p^h , X_p^h , and Λ_{fp}^h with inner products. The inner product in the space Q_p^h is relatively simple:

$$[\mathbf{P}, \mathbf{Q}]_{Q_p^h} = \sum_{E \in \Omega_p^h} |E| P_E Q_E, \quad \forall \mathbf{P}, \mathbf{Q} \in Q_p^h. \quad (2.14)$$

This inner product can be viewed as a quadrature rule for L^2 -product of two scalar functions. The inner product in X_p^h can be defined formally as

$$[\mathbf{U}, \mathbf{V}]_{X_p^h} = \mathbf{U}^T \mathbf{M}_p \mathbf{V}, \quad \forall \mathbf{U}, \mathbf{V} \in X_p^h, \quad (2.15)$$

where \mathbf{M}_p is a symmetric positive definite matrix. It can be viewed as a quadrature rule for the \mathbf{K}^{-1} -weighted L^2 -product of two vector functions. The mass matrix \mathbf{M}_p is assembled from element matrices $\mathbf{M}_{p,E}$:

$$\mathbf{U}^T \mathbf{M}_p \mathbf{V} = \sum_{E \in \Omega_2^h} \mathbf{U}_E^T \mathbf{M}_{p,E} \mathbf{V}_E, \quad \forall \mathbf{U}, \mathbf{V} \in X_p^h.$$

The symmetric and positive definite matrix $\mathbf{M}_{p,E}$ induces the local inner product

$$[\mathbf{U}_E, \mathbf{V}_E]_{X_p^h, E} = \mathbf{U}_E^T \mathbf{M}_{p,E} \mathbf{V}_E, \quad \forall \mathbf{U}_E, \mathbf{V}_E \in X_p^h(E). \quad (2.16)$$

The construction of matrix $\mathbf{M}_{p,E}$ for a general element E is at the heart of the mimetic method [26]. The inner product in Λ_{fp}^h is defined as

$$\langle \boldsymbol{\lambda}, \boldsymbol{\mu} \rangle_{\Lambda_{fp}^h} = \sum_{e \in \Gamma_{fp}^h} \lambda^e \mu^e |e|, \quad \forall \boldsymbol{\lambda}, \boldsymbol{\mu} \in \Lambda_{fp}^h. \quad (2.17)$$

Since $\mathbf{V}|_{\Gamma_{fp}} \in \Lambda_{fp}^h$ for every $\mathbf{V} \in X_p^h$, (2.17) can also be used to define $\langle \mathbf{V}, \boldsymbol{\mu} \rangle_{\Lambda_{fp}^h}$:

$$\langle \mathbf{V}, \boldsymbol{\mu} \rangle_{\Lambda_{fp}^h} = \sum_{e \in \Gamma_{fp}^h} V^e \mu^e |e|, \quad \forall \mathbf{V} \in X_p^h, \forall \boldsymbol{\mu} \in \Lambda_{fp}^h.$$

The third step in the mimetic method is discretization of the gradient and divergence operators. The degrees of freedom have been selected to provide a simple approximation of the divergence operator. The Gauss divergence theorem naturally leads to the following definition of the discrete divergence:

$$(\mathcal{DIV} \mathbf{V})_E = \frac{1}{|E|} \sum_{e \in \partial E} \chi_E^e V_E^e |e|, \quad \forall \mathbf{V} \in X_p^h. \quad (2.18)$$

We have the following useful commutative property of the interpolants:

$$(\mathcal{DIV} \mathbf{v}^I)_E = \frac{1}{|E|} \int_{\partial E} \mathbf{v} \cdot \mathbf{n}_E ds = \frac{1}{|E|} \int_E \nabla \cdot \mathbf{v} dx = (\nabla \cdot \mathbf{v})_E^I, \quad \forall \mathbf{v} \in X_p. \quad (2.19)$$

The discrete gradient operator must be a discretization of the continuous operator $-\mathbf{K}\nabla$. To provide a compatible discretization, the mimetic method derives this discrete operator from a discrete Gauss-Green formula:

$$[\mathbf{U}, \mathcal{GRAD}(\mathbf{P}, \boldsymbol{\lambda})]_{X_p^h} = [\mathcal{DIV} \mathbf{U}, \mathbf{P}]_{Q_p^h} - \langle \mathbf{U}, \boldsymbol{\lambda} \rangle_{\Lambda_{fp}^h}, \quad \forall \mathbf{U} \in X_p^h, \forall \mathbf{P} \in Q_p^h, \forall \boldsymbol{\lambda} \in \Lambda_{fp}^h.$$

The above equation mimics the continuous Gauss-Green formula

$$\int_{\Omega_p} \mathbf{u} \cdot \mathbf{K}^{-1}(-\mathbf{K}\nabla p) dx = \int_{\Omega_p} p \nabla \cdot \mathbf{u} dx - \int_{\Gamma_{fp}} p \mathbf{u} \cdot \mathbf{n} dx, \quad \forall \mathbf{u} \in X_p, \forall p \in H^1(\Omega_p).$$

Non-homogeneous velocity boundary conditions would require additional terms that represent non-zero boundary terms in the continuous Gauss-Green formula [60].

The construction of an admissible matrix $\mathbf{M}_{p,E}$ is based on the following *consistency condition* (see [26] for details). Let \mathbf{K}_E be the mean value of \mathbf{K} on element E . Then, we require

$$\begin{aligned} [\mathbf{V}, (-\mathbf{K}_E \nabla p^l)^I]_{X_p^h} &= [\mathcal{D}\mathcal{I}\mathcal{V} \mathbf{V}, (p^l)^I]_{Q_p^h} - \sum_{e \in \partial E} \chi_E^e V_E^e \int_e p^l ds, \\ \forall \mathbf{V} \in X_p^h, \forall p^l \in \mathbb{P}_1(E). \end{aligned} \quad (2.20)$$

The inner products (2.14) and (2.16) induce the following norms:

$$\|\mathbf{P}\|_{Q_p^h}^2 = [\mathbf{P}, \mathbf{P}]_{Q_p^h}, \quad \forall \mathbf{P} \in Q_p^h \quad \text{and} \quad \|\mathbf{V}\|_{X_p^h}^2 = [\mathbf{V}, \mathbf{V}]_{X_p^h}, \quad \forall \mathbf{V} \in X_p^h.$$

Lemma 2.1.2 ([26]) . *Under the assumptions of Definition 2.1.1, there exists the local inner product (2.16) such that*

$$\frac{1}{C} |E| \|\mathbf{V}_E\|^2 \leq \|\mathbf{V}\|_{X_p^h}^2 \leq C |E| \|\mathbf{V}_E\|^2, \quad \forall \mathbf{V} \in X_p^h, \quad (2.21)$$

where the constant C depends only on shape regularity of the auxiliary partition of E .

In the following, for consistency between the DG and the MFD notation, we will denote a vector $\mathbf{V}_p \in X_p^h$ by \mathbf{v}_p^h , a vector $\mathbf{Q}_p \in Q_p^h$ by q_p^h , and a vector $\boldsymbol{\lambda} \in \Lambda_{fp}^h$ by λ^h . We define the bilinear forms $a_p : X_p^h \times X_p^h \rightarrow \mathbb{R}$ and $b_p : X_p^h \times Q_p^h \rightarrow \mathbb{R}$ as follows

$$a_p(\mathbf{u}_p^h, \mathbf{v}_p^h) = [\mathbf{u}_p^h, \mathbf{v}_p^h]_{X_p^h}, \quad \forall \mathbf{u}_p^h, \mathbf{v}_p^h \in X_p^h,$$

and

$$b_p(\mathbf{v}_p^h, q_p^h) = -[\mathcal{D}\mathcal{I}\mathcal{V} \mathbf{v}_p^h, q_p^h]_{Q_p^h}, \quad \forall \mathbf{v}_p^h \in X_p^h, \forall q_p^h \in Q_p^h.$$

Given an approximation $\lambda^h \in \Lambda_{fp}^h$ of p_p on Γ_{fp} , the mimetic approximation of (2.10)–(2.11) reads:

Find $(\mathbf{u}_p^h, p_p^h) \in X_p^h \times Q_p^h$ such that

$$a_p(\mathbf{u}_p^h, \mathbf{v}_p^h) + b_p(\mathbf{v}_p^h, p_p^h) + \langle \mathbf{v}_p^h, \lambda^h \rangle_{\Lambda_{fp}^h} = 0, \quad \forall \mathbf{v}_p^h \in X_p^h, \quad (2.22)$$

$$b_p(\mathbf{u}_p^h, q_p^h) = -[f_p^I, q_p^h]_{Q_p^h}, \quad \forall q_p^h \in Q_p^h. \quad (2.23)$$

2.1.4 Discrete formulation of the coupled problem

In the previous two subsections we presented discretizations for the Stokes and the Darcy regions, (2.8)–(2.9) and (2.22)–(2.23), respectively, that are coupled through the approximations $\bar{\lambda}^h$ and λ^h of p_p on the interface Γ_{fp} . We impose the normal stress continuity condition (1.9) by taking $\bar{\lambda}^h$ to be the piecewise constant function on Γ_{fp}^h satisfying

$$\bar{\lambda}^h|_e = (\lambda^h)^e, \quad \forall e \in \Gamma_{fp}^h.$$

We impose the normal flux continuity (1.8) in a weak sense, using Λ_{fp}^h as the Lagrange multiplier space. The weak continuity is embedded in the definition of the global velocity space. More precisely, let $X^h = X_f^h \times X_p^h$, $Q^h = Q_p^h \times Q_p^h$, and

$$V^h = \left\{ \mathbf{v}^h \in X^h : \int_{\Gamma_{fp}} \mathbf{v}_f^h \cdot \mathbf{n}_f \bar{\mu}^h ds + \langle \mathbf{v}_p^h, \mu^h \rangle_{\Lambda_{fp}^h} = 0, \quad \forall \mu^h \in \Lambda_{fp}^h \right\}. \quad (2.24)$$

We also define the composite bilinear forms

$$\begin{aligned} a(\mathbf{u}^h, \mathbf{v}^h) &= a_f(\mathbf{u}_f^h, \mathbf{v}_f^h) + a_p(\mathbf{u}_p^h, \mathbf{v}_p^h), & \forall \mathbf{u}^h, \mathbf{v}^h \in X^h, \\ b(\mathbf{v}^h, q^h) &= b_f(\mathbf{v}_f^h, q_f^h) + b_p(\mathbf{v}_p^h, q_p^h), & \forall \mathbf{v}^h \in X^h, q^h \in Q^h. \end{aligned}$$

The weak formulation of the coupled problem is: find the pair $(\mathbf{u}^h, p^h) \in V^h \times Q^h$ such that

$$a(\mathbf{u}^h, \mathbf{v}^h) + b(\mathbf{v}^h, p^h) = \int_{\Omega_f} \mathbf{f}_f \cdot \mathbf{v}_f^h dx, \quad \forall \mathbf{v}^h \in V^h, \quad (2.25)$$

$$b(\mathbf{u}^h, q^h) = -[f_p^I, q_p^h]_{Q_p^h}, \quad \forall q^h \in Q^h. \quad (2.26)$$

Remark 2.1.1 *By constructing in the Stokes domain a lifting operator mapping from degrees of freedom to a functional space the DG method can be interpreted as a MFD method. A similar lifting operator can be used to define the MFD method in the Darcy domain as a finite element method.*

2.2 TRACE INEQUALITIES AND INTERPOLATION RESULTS

Throughout this article, we use a few well known inequalities. The Young's inequality reads:

$$ab \leq \frac{\epsilon}{2}a^2 + \frac{1}{2\epsilon}b^2, \quad a, b \geq 0, \quad \epsilon > 0. \quad (2.27)$$

A number of trace inequalities utilized in [81] on triangular meshes can be extended to polyhedral meshes using the auxiliary partition of an element E into shape-regular simplices. In particular, for any face e of element E , we have

$$\|\phi\|_{0,e}^2 \leq C (h_E^{-1} \|\phi\|_{0,E}^2 + h_E |\phi|_{1,E}^2), \quad \forall \phi \in H^1(E), \quad (2.28)$$

and its immediate consequence

$$\|\nabla \phi \cdot \mathbf{n}_e\|_{0,e}^2 \leq C (h_E^{-1} \|\phi\|_{1,E}^2 + h_E |\phi|_{2,E}^2), \quad \forall \phi \in H^2(E). \quad (2.29)$$

For polynomial functions, we have the trace inequality

$$\|\nabla \phi \cdot \mathbf{n}_e\|_{0,e} \leq C h_E^{-1/2} |\phi|_{1,E}, \quad \forall \phi \in \mathbb{P}_r(E). \quad (2.30)$$

For $\phi \in (H^s(E))^2$, $0 \leq s \leq 1$, with $\nabla \cdot \phi \in L^2(E)$ we use Lemma 3.1 from [68] that gives

$$\|\phi \cdot \mathbf{n}_e\|_{s-\frac{1}{2},e}^2 \leq C (h_E^{-1} \|\phi\|_{0,E}^2 + h_E^{2s-1} \|\phi\|_{s,E}^2 + h_E \|\nabla \cdot \phi\|_{0,E}^2). \quad (2.31)$$

Lemma 2.2.1 *Let $\mathbf{v}_f \in (H^1(\Omega_f))^d$. There exists an interpolant $\pi_f^h : (H^1(\Omega_f))^d \rightarrow X_f^h$ such that*

$$b_1(\pi_f^h(\mathbf{v}_f) - \mathbf{v}_f, q_f^h) = 0, \quad \forall q_f^h \in Q_f^h, \quad (2.32)$$

$$\int_e [\pi_f^h \mathbf{v}_f] \cdot \mathbf{w} \, ds = 0, \quad \forall \mathbf{w} \in (\mathbb{P}_{r-1}(e))^d, \quad (2.33)$$

for every face $e \in \mathcal{E}_1^h \cup \Gamma_f$, and

$$\|\pi_f^h(\mathbf{v}_f)\|_{1,\Omega_f} \leq C \|\mathbf{v}_f\|_{1,\Omega_f}. \quad (2.34)$$

The interpolant has optimal approximation properties for $\mathbf{v}_f \in (H^s(\Omega_f))^d$, $1 \leq s \leq r+1$:

$$|\pi_f^h(\mathbf{v}_f) - \mathbf{v}_f|_{m,E} \leq C h_E^{s-m} |\mathbf{v}_f|_{s,\delta(E)}, \quad m = 0, 1, \quad (2.35)$$

where either $\delta(E)$ is the union of E with all its closest neighbours in the case of simplicies or $\delta(E) = E$ in the case of the lifted DG spaces on polyhedra.

Furthermore, the following estimates hold for $\mathbf{v}_f \in (H^s(\Omega_f))^d$, $1 \leq s \leq r + 1$:

$$\|\pi_f^h(\mathbf{v}_f) - \mathbf{v}_f\|_{X_f} \leq Ch_f^{s-1} |\mathbf{v}_f|_{s,\Omega_f}, \quad (2.36)$$

$$\|\pi_f^h(\mathbf{v}_f)\|_{X_f} \leq C\|\mathbf{v}_f\|_{1,\Omega_f}. \quad (2.37)$$

Proof. On triangles for $r = 1, 2, 3$ and tetrahedra for $r = 1$ the existence of such an interpolant is shown in [37, 49, 36, 53, 81].

It remains to consider the case of polyhedral meshes with $r = 1$. Let $\mathbf{v}_f \in (H^1(\Omega_f))^d$ and let \mathbf{V}_f be the corresponding vector of degrees of freedom. We introduce the interpolant π_f^h such that $\pi_f^h(\mathbf{v}_f) = \mathcal{R}_f(\mathbf{V}_f)$. Due to the lifting property **(L1)**, we immediately get condition (2.33) with $\mathbf{w} \in (\mathbb{P}_0(e))^d$. Then, for every $q_f^h \in Q_f^h$, the lifting property **(L2)** gives

$$\begin{aligned} b_f(\pi_f^h(\mathbf{v}_f) - \mathbf{v}_f, q_f^h) &= - \sum_{E \in \Omega_f^h} \int_E q_f^h \nabla \cdot (\pi_f^h \mathbf{v}_f - \mathbf{v}_f) dx \\ &= - \sum_{E \in \Omega_f^h} q_{f,E} \int_{\partial E} (\mathcal{R}_{f,E}(\mathbf{V}_{f,E}) - \mathbf{v}_f) \cdot \mathbf{n}_E ds = 0. \end{aligned} \quad (2.38)$$

To show (2.34), let \mathbf{v}_f^c be the L^2 -projection of \mathbf{v}_f onto the space of piecewise constant functions on Ω_f^h . We have

$$\|\mathbf{v}_f^c\|_{0,E} \leq \|\mathbf{v}_f - \mathbf{v}_f^c\|_{0,E} + \|\mathbf{v}_f\|_{0,E} \leq Ch_E |\mathbf{v}_f|_{1,E} + \|\mathbf{v}_f\|_{0,E} \leq C\|\mathbf{v}_f\|_{1,E}.$$

For every element E , the triangle inequality and lifting properties **(L2)** and **(L3)** give

$$\begin{aligned} \|\pi_f^h(\mathbf{v}_f)\|_{0,E}^2 &\leq 2\|\pi_f^h(\mathbf{v}_f - \mathbf{v}_f^c)\|_{0,E}^2 + 2\|\mathbf{v}_f^c\|_{0,E}^2 \\ &\leq C \left(|E| \sum_{e \in \partial E} \left(\frac{1}{|e|} \int_e |\mathbf{v}_f - \mathbf{v}_f^c| ds \right)^2 + \|\mathbf{v}_f\|_{1,E}^2 \right). \end{aligned}$$

Applying the the trace inequality (2.28) to each component of \mathbf{v}_f and using the standard approximation property of the L^2 -projection, we bound each of the edge integrals:

$$\begin{aligned} \left(\int_e |\mathbf{v}_f - \mathbf{v}_f^c| ds \right)^2 &\leq |e| \int_e |\mathbf{v}_f - \mathbf{v}_f^c|^2 ds \\ &\leq C|e| (h_E^{-1} \|\mathbf{v}_f - \mathbf{v}_f^c\|_{0,E}^2 + h_E |\mathbf{v}_f|_{1,E}^2) \leq C|e| h_E |\mathbf{v}_f|_{1,E}^2. \end{aligned} \quad (2.39)$$

Combining the last two inequalities and using the shape regularity of E (2.1), we get

$$\|\pi_f^h(\mathbf{v}_f)\|_{0,E}^2 \leq C \left(\frac{h_E |E|}{|e|} |\mathbf{v}_f|_{1,E}^2 + \|\mathbf{v}_f\|_{1,E}^2 \right) \leq C \|\mathbf{v}_f\|_{1,E}^2.$$

To bound the H^1 -seminorm of $\pi_f^h(\mathbf{v}_f)$, we use **(L3)** to obtain

$$|\pi_f^h(\mathbf{v}_f) - \mathbf{v}_f^c|_{1,E}^2 \leq Ch_E^{d-2} \|\mathbf{V}_{f,E} - \mathbf{V}_{f,E}^c\|^2 \leq Ch_E^{d-2} \sum_{e \in \partial E} \left(\frac{1}{|e|} \int_e |\mathbf{v}_f - \mathbf{v}_f^c| ds \right)^2,$$

where $\mathbf{V}_{f,E}^c$ is the vector of degrees of freedom for the constant function \mathbf{v}_f^c . Combining the above inequality and (2.39), and using the shape regularity of E (2.1), we conclude that

$$|\pi_f^h(\mathbf{v}_f)|_{1,E} \leq C |\mathbf{v}_f|_{1,E},$$

which completes the proof of (2.34).

Since **(L2)** implies that π_f^h is exact for all linear functions on E , an application of the Bramble-Hilbert lemma [19] gives (2.35).

It remains to show (2.36) and (2.37). Note that **(L1)** implies that for all faces e of E

$$\int_e (\pi_f^h \mathbf{v}_f - \mathbf{v}_f) ds = 0, \quad \forall \mathbf{v}_f \in (H^1(E))^d.$$

Therefore we can employ Lemma 3.9 of [53] to conclude that

$$\|\pi_f^h(\mathbf{v}_f) - \mathbf{v}_f\|_{X_f} \leq C \|\nabla(\pi_h^1(\mathbf{v}_1) - \mathbf{v}_1)\|_{0,\Omega_1},$$

which, combined with (2.35), implies (2.36). The continuity bound (2.37) follows from the triangle inequality, (2.36), and the bound $\|\mathbf{v}_f\|_{X_f} \leq C \|\mathbf{v}_f\|_{1,\Omega_f}$. \square

2.3 STABILITY AND WELL-POSEDNESS OF THE DISCRETE PROBLEM

In this section we prove a discrete inf-sup condition and show that the discrete problem (2.25)–(2.26) has a unique solution. Let $X^h = X_f^h \times X_p^h$ and $Q^h = Q_f^h \times Q_p^h$ with norms

$$\begin{aligned}\|\mathbf{v}^h\|_{X^h}^2 &= \|\mathbf{v}_f^h\|_{X_f^h}^2 + \|\mathbf{v}_p^h\|_{div}^2, \quad \forall \mathbf{v}^h = (\mathbf{v}_f^h, \mathbf{v}_p^h) \in X^h, \\ \|q^h\|_{Q^h}^2 &= \|q_f^h\|_{0,\Omega_f}^2 + \|q_p^h\|_{Q_p^h}^2, \quad \forall q^h = (q_f^h, q_p^h) \in Q^h,\end{aligned}$$

where

$$\|\mathbf{v}_p^h\|_{div}^2 = \|\mathbf{v}_p^h\|_{X_p^h}^2 + \|\mathcal{DIV} \mathbf{v}_p^h\|_{Q_p^h}^2, \quad \forall \mathbf{v}_p^h \in X_p^h.$$

Lemma 2.3.1 *Let $\mathbf{v} \in (H^1(\Omega))^d$ and $\mathbf{v}_\alpha = \mathbf{v}|_{\Omega_\alpha}$, $\alpha = f, p$. Then, there exists an operator $\pi^h : (X_f \times X_p) \cap (H^1(\Omega))^d \rightarrow V^h$, $\pi^h(\mathbf{v}) = (\pi_f^h(\mathbf{v}_f), \pi_p^h(\mathbf{v}_p))$, such that*

$$b(\pi^h(\mathbf{v}) - \mathbf{v}, q^h) = 0, \quad \forall q^h \in Q^h, \quad (2.40)$$

and

$$\|\pi_f^h(\mathbf{v}_f)\|_{X_f} \leq C\|\mathbf{v}_f\|_{1,\Omega_f}, \quad \|\pi_p^h(\mathbf{v}_p)\|_{X_p^h} \leq C\|\mathbf{v}\|_{1,\Omega}. \quad (2.41)$$

Proof. Let π_f^h be the operator defined in Lemma 2.2.1. The property (2.32) gives (2.40) for any $q^h = (q_f^h, 0)$. Due to (2.37), we get automatically the first inequality in (2.41). To construct $\pi_p^h(\mathbf{v}_p)$, we solve the following boundary value problem:

$$\begin{aligned}\Delta\varphi &= 0 && \text{in } \Omega_p, \\ \nabla\varphi \cdot \mathbf{n}_p &= 0 && \text{on } \Gamma_p, \\ \nabla\varphi \cdot \mathbf{n}_p &= (\mathbf{v} - \pi_f^h(\mathbf{v}_f)) \cdot \mathbf{n}_f && \text{on } \Gamma_{fp},\end{aligned} \quad (2.42)$$

and define

$$\pi_p^h(\mathbf{v}_p) = \mathbf{v}_p^I + (\nabla\varphi)^I.$$

By elliptic regularity [66],

$$\|\nabla\varphi\|_{H^\theta(\Omega_p)} \leq C\|(\mathbf{v} - \pi_f^h(\mathbf{v}_f)) \cdot \mathbf{n}_f\|_{H^{\theta-1/2}(\Gamma_{fp})}, \quad 0 \leq \theta \leq 1/2. \quad (2.43)$$

For all $q_p^h \in Q_p^h$, using definition of π_p^h and the commutative property (2.19), we get

$$b_p(\pi_p^h(\mathbf{v}) - \mathbf{v}_p^I, q_p^h) = b_p((\nabla\varphi)^I, q_p^h) = -[D\mathcal{IV}(\nabla\varphi)^I, q_p^h]_{Q_p^h} = -[(\nabla \cdot \nabla\varphi)^I, q_p^h]_{Q_p^h} = 0.$$

To prove the second inequality in (2.41), we start with the triangle inequality

$$\|\|\|\pi_p^h(\mathbf{v})\|\|\|_{X_p^h} \leq \|\|\|\mathbf{v}_p^I\|\|\|_{X_p^h} + \|\|\|(\nabla\varphi)^I\|\|\|_{X_p^h} \quad (2.44)$$

and bound every term. From the stability estimate (2.21), the trace inequality (2.28), and the shape regularity estimates (2.1), we obtain

$$\begin{aligned} \|\|\|\mathbf{v}_p^I\|\|\|_{X_p^h}^2 &= [\mathbf{v}_p^I, \mathbf{v}_p^I]_{X_p^h} \leq C \sum_{E \in \Omega_p^h} |E| \sum_{e \subset \partial E} |(\mathbf{v}_p^I)_e|^2 \\ &\leq C \sum_{E \in \Omega_p^h} \sum_{e \subset \partial E} \frac{|E|}{|e|} (h_E^{-1} \|\mathbf{v}_p\|_{0,E}^2 + h_E |\mathbf{v}_p|_{1,E}^2) \\ &\leq C \sum_{E \in \Omega_p^h} (\|\mathbf{v}_p\|_{0,E}^2 + h_E^2 |\mathbf{v}_p|_{1,E}^2) \\ &\leq C \|\mathbf{v}_p\|_{1,\Omega_p}^2. \end{aligned} \quad (2.45)$$

Using the same arguments plus inequality (2.31) with $s = 1/2$, we get

$$\begin{aligned} \|\|\|(\nabla\varphi)^I\|\|\|_{X_p^h}^2 &\leq C \sum_{E \in \Omega_p^h} |E| \sum_{e \subset \partial E} \left(\frac{1}{|e|} \int_e \nabla\varphi \cdot \mathbf{n}_e \, ds \right)^2 \\ &\leq C \sum_{E \in \Omega_p^h} \sum_{e \subset \partial E} \frac{|E|}{|e|} \left(h_E^{-1} \|\nabla\varphi\|_{0,E}^2 + \|\nabla\varphi\|_{\frac{1}{2},E}^2 \right) \\ &\leq C \left(\|\nabla\varphi\|_{0,\Omega_p}^2 + h_p \|\nabla\varphi\|_{\frac{1}{2},\Omega_p}^2 \right). \end{aligned} \quad (2.46)$$

To bound the first and the second term on the right hand side in (2.46) we apply (2.43) with $\theta = 0$ and $\theta = 1/2$, respectively:

$$\begin{aligned} \|\|\|(\nabla\varphi)^I\|\|\|_{X_p^h}^2 &\leq C \left(\|(\mathbf{v}_f - \pi_f^h(\mathbf{v}_f)) \cdot \mathbf{n}_f\|_{-\frac{1}{2},\Gamma_{fp}}^2 + h_p \|(\mathbf{v}_f - \pi_f^h(\mathbf{v}_f)) \cdot \mathbf{n}_f\|_{0,\Gamma_{fp}}^2 \right) \\ &\leq C \|(\mathbf{v}_f - \pi_f^h(\mathbf{v}_f)) \cdot \mathbf{n}_f\|_{0,\Gamma_{fp}}^2. \end{aligned} \quad (2.47)$$

Using the trace inequality (2.28) for every $e \in \Gamma_{fp}^h$ and the approximation result (2.35), we have that

$$\begin{aligned} \|(\mathbf{v}_f - \pi_f^h(\mathbf{v}_f)) \cdot \mathbf{n}_f\|_{L^2(e)} &\leq C \left(h_E^{-1/2} \|\mathbf{v}_f - \pi_f^h(\mathbf{v}_f)\|_{0,E} + h_E^{1/2} |\mathbf{v}_f - \pi_f^h(\mathbf{v}_f)|_{1,E} \right) \\ &\leq Ch_E^{s-1/2} |\mathbf{v}_f|_{s,\delta(E)}, \quad 1 \leq s \leq r+1. \end{aligned} \quad (2.48)$$

Thus,

$$\|(\nabla\varphi)^I\|_{X_p^h} \leq Ch_f^{s-1/2} \|\mathbf{v}_f\|_{s,\Omega_f}, \quad 1 \leq s \leq r+1. \quad (2.49)$$

Combining (2.44) with estimates (2.45) and (2.49), we conclude that $\|\pi_p^h(\mathbf{v})\|_{X_p^h} \leq C\|\mathbf{v}\|_{1,\Omega}$.

It remains to show that $\pi^h(\mathbf{v}) \in V^h$. Let $\mu_h \in \Lambda_{fp}^h$. From definition of the inner product (2.17), definition of the interpolant (2.12), the boundary conditions in (2.42), and the regularity assumption $\mathbf{v} \in (H^1(\Omega))^d$, it follows that

$$\begin{aligned} \langle \pi_p^h \mathbf{v}, \mu^h \rangle_{\Lambda_{fp}^h} &= \langle \mathbf{v}_p^I, \mu^h \rangle_{\Lambda_{fp}^h} + \langle (\nabla\varphi)^I, \mu^h \rangle_{\Lambda_{fp}^h} \\ &= \sum_{e \in \Gamma_{fp}^h} (\mu^h)^e \int_e \mathbf{v}_p \cdot \mathbf{n}_p \, ds + \sum_{e \in \Gamma_{fp}^h} (\mu^h)^e \int_e \nabla\varphi \cdot \mathbf{n}_p \, ds \\ &= \int_{\Gamma_{fp}} \mathbf{v}_p \cdot \mathbf{n}_p \, \bar{\mu}^h \, ds + \int_{\Gamma_{fp}} \mathbf{v}_f \cdot \mathbf{n}_f \, \bar{\mu}^h \, ds - \int_{\Gamma_{fp}} \pi_f^h(\mathbf{v}_f) \cdot \mathbf{n}_f \, \bar{\mu}^h \, ds \\ &= - \int_{\Gamma_{fp}} \pi_f^h(\mathbf{v}_f) \cdot \mathbf{n}_f \, \bar{\mu}^h \, ds. \end{aligned}$$

Therefore $\pi^h(\mathbf{v}) \in V^h$. This proves the assertion of the lemma. \square

Next, we prove a discrete inf-sup condition, which guarantees that the approximating spaces are compatible with one another.

Lemma 2.3.2 *There exists a positive constant β such that*

$$\inf_{q^h \in Q^h} \sup_{\mathbf{v}^h \in V^h} \frac{b_f(\mathbf{v}_f^h, q_f^h) + b_p(\mathbf{v}_p^h, q_p^h)}{\|\mathbf{v}^h\|_{X^h} \|q^h\|_{Q^h}} \geq \beta. \quad (2.50)$$

Proof. For a given $q^h \in Q^h$, let us define $\ell \in L^2(\Omega)$ by

$$\ell = (\ell_f, \ell_p), \quad \text{where } \ell_f = -q_f^h \quad \text{and} \quad \ell_p|_E = -(q_p^h)_E, \quad \forall E \in \Omega_p^h.$$

Note that $\ell_p^I = -q_p^h$ and $\|\ell_p\|_{0,\Omega_p} = \|q_p^h\|_{Q_p^h}$. We can construct $\mathbf{v} \in (H^1(\Omega))^d$ [52] for which

$$\nabla \cdot \mathbf{v} = \ell, \quad \text{and} \quad \|\mathbf{v}\|_{1,\Omega} \leq C\|\ell\|_{0,\Omega}. \quad (2.51)$$

Let $\pi^h(\mathbf{v}) = (\pi_f^h(\mathbf{v}_f), \pi_p^h(\mathbf{v}_p))$ be the interpolant constructed in Lemma 2.3.1. Using (2.40) and the commutative property (2.19), we get

$$\begin{aligned} b_f(\pi_f^h \mathbf{v}, q_f^h) + b_p(\pi_p^h \mathbf{v}, q_p^h) &= b_f(\mathbf{v}_f, q_f^h) + b_p(\mathbf{v}_p^I, q_p^h) \\ &= - \int_{\Omega_f} (\operatorname{div} \mathbf{v}_f) q_f^h dx - [\mathcal{D}\mathcal{I}\mathcal{V} \mathbf{v}_p^I, q_p^h]_{Q_p^h} \\ &= \int_{\Omega_f} (q_f^h)^2 dx + [q_p^h, q_p^h]_{Q_p^h} \\ &= \|q_f^h\|_{0,\Omega_f}^2 + \|q_p^h\|_{Q_p^h}^2 = \|q^h\|_{Q^h}^2. \end{aligned} \quad (2.52)$$

The definition of π_p^h and (2.19) imply that

$$\mathcal{D}\mathcal{I}\mathcal{V}(\pi_p^h(\mathbf{v})) = \mathcal{D}\mathcal{I}\mathcal{V}(\mathbf{v}_p^I + (\nabla\varphi)^I) = (\nabla \cdot \mathbf{v}_p)^I + (\nabla \cdot \nabla\varphi)^I = -q_p^h.$$

Using estimate (2.41) from Lemma 2.3.1, we bound $\pi^h(\mathbf{v})$:

$$\begin{aligned} \|\pi^h(\mathbf{v})\|_{X^h}^2 &= \|\pi_f^h(\mathbf{v}_f)\|_{X_f^h}^2 + \|\pi_p^h(\mathbf{v}_p)\|_{X_p^h}^2 + \|\mathcal{D}\mathcal{I}\mathcal{V}(\pi_p^h(\mathbf{v}_p))\|_{Q_p^h}^2 \\ &\leq C \left(\|\mathbf{v}\|_{f,\Omega}^2 + \|q_p^h\|_{Q_p^h}^2 \right) \\ &\leq C \left(\|q_f^h\|_{0,\Omega}^2 + \|q_p^h\|_{Q_p^h}^2 \right) \leq C \|q^h\|_{Q^h}^2. \end{aligned} \quad (2.53)$$

Combining (2.52) and (2.53) yields

$$b_f(\pi_f^h(\mathbf{v}_f), q_f^h) + b_p(\pi_p^h(\mathbf{v}_p), q_p^h) \geq C \|\pi^h(\mathbf{v})\|_{X^h} \|q^h\|_{Q^h}, \quad (2.54)$$

which proves the assertion of the lemma. □

To prove that the method is well-posed we will also need the coercivity property established in the next lemma.

Lemma 2.3.3 Assuming (2.2) there exists a positive constant α_c dependent on σ_0 but independent of h_f such that

$$a_f(\mathbf{v}_f^h, \mathbf{v}_f^h) \geq \alpha_c \|\mathbf{v}_f^h\|_{X_f^h}, \quad \forall \mathbf{v}_f^h \in X_f^h. \quad (2.55)$$

Proof. Let $\mathbf{v}_f^h \in X_f^h$. From the definition of $a_f(\cdot, \cdot)$ we have

$$\begin{aligned} a_f(\mathbf{v}_f^h, \mathbf{v}_f^h) &= 2\mu_f \sum_{E \in \Omega_f^h} \int_E \mathbf{De}(\mathbf{v}_f^h) : \mathbf{De}(\mathbf{v}_f^h) dx + \sum_{e \in \mathcal{E}_f^h \cup \Gamma_f} \frac{\sigma_e}{h_e} \int_e [\mathbf{v}_f^h] \cdot [\mathbf{v}_f^h] ds \\ &\quad - 2\mu_f(1 - \varepsilon) \sum_{e \in \mathcal{E}_f^h \cup \Gamma_f} \int_e \{\mathbf{De}(\mathbf{v}_f^h) \mathbf{n}_e\} \cdot [\mathbf{v}_f^h] ds + \sum_{e \in \Gamma_{fp}} \sum_{j=1}^{d-1} \frac{\mu_f}{G_j} \int_e (\mathbf{v}_f^h \cdot \boldsymbol{\tau}_j)(\mathbf{v}_f^h \cdot \boldsymbol{\tau}_j) ds. \end{aligned}$$

For piecewise H^1 vector fields the following Korn's holds [18]:

$$\|\|\mathbf{v}_f^h\|\|_{1, \Omega_f}^2 \leq K_0 \left(\|\|\mathbf{De}(\mathbf{v}_f^h)\|\|_{0, \Omega_f}^2 + \sum_{e \in \mathcal{E}_f^h \cup \Gamma_f} \frac{1}{h_e} \|\|[\mathbf{v}_f^h]\|\|_{0, e}^2 \right), \quad \forall \mathbf{v}_f^h \in X_f^h. \quad (2.56)$$

Thus,

$$\begin{aligned} a_f(\mathbf{v}_f^h, \mathbf{v}_f^h) &\geq \frac{2\mu_f}{K_0} \|\|\mathbf{v}_f^h\|\|_{1, \Omega_f}^2 + \sum_{e \in \mathcal{E}_f^h \cup \Gamma_f} \frac{\sigma_0 - 2\mu_f}{h_e} \|\|[\mathbf{v}_f^h]\|\|_{0, e}^2 \\ &\quad - 2\mu_f(1 - \varepsilon) \sum_{e \in \mathcal{E}_f^h \cup \Gamma_f} \int_e \{\mathbf{De}(\mathbf{v}_f^h) \mathbf{n}_e\} \cdot [\mathbf{v}_f^h] ds + \sum_{e \in \Gamma_{fp}} \sum_{j=1}^{d-1} \frac{\mu_f}{G_j} \|\|\mathbf{v}_f^h \cdot \boldsymbol{\tau}_j\|\|_{0, e}^2. \end{aligned}$$

Clearly, the coercivity property holds when $\varepsilon = 1$ and $\sigma_0 > 2\mu_f$. To address the case when $\varepsilon = -1$ or 0, we use the trace inequality (2.30) and the Young's inequality (2.27) to estimate the third term:

$$\begin{aligned} \sum_{e \in \mathcal{E}_f^h \cup \Gamma_f} \int_e \{\mathbf{De}(\mathbf{v}_f^h) \mathbf{n}_e\} \cdot [\mathbf{v}_f^h] ds &\leq C_1 \sum_{e \in \mathcal{E}_f^h \cup \Gamma_f} h_{E^e}^{-1/2} \|\|\nabla \mathbf{v}_f^h\|\|_{E^e} \left(\frac{|h_e|}{|h_e|} \right)^{1/2} \|\|[\mathbf{v}_f^h]\|\|_{0, e} \\ &\leq C_2 \sum_{e \in \mathcal{E}_f^h \cup \Gamma_f} \left(\frac{1}{2C_3} \|\|\nabla \mathbf{v}_f^h\|\|_{0, E^e}^2 + \frac{C_3}{2h_e} \|\|[\mathbf{v}_f^h]\|\|_{0, e}^2 \right) \\ &\leq \frac{C_2}{2C_3} \|\|\mathbf{v}_f^h\|\|_{1, \Omega_f}^2 + \frac{C_2 C_3}{2} \sum_{e \in \mathcal{E}_f^h \cup \Gamma_f} \frac{\|\|[\mathbf{v}_f^h]\|\|_{0, e}^2}{h_e} \end{aligned}$$

Then,

$$a_f(\mathbf{v}_f^h, \mathbf{v}_f^h) \geq \mu_f \left(\frac{2}{K_0} - \frac{C_2(1-\varepsilon)}{C_3} \right) \|\mathbf{v}_f^h\|_{1,\Omega_f}^2 \\ + (\sigma_0 - \mu_f(2 + C_2C_3(1-\varepsilon))) \sum_{e \in \mathcal{E}_f^h \cup \Gamma_f} \frac{\|[\mathbf{v}_f^h]\|_{0,e}^2}{h_e} + \sum_{e \in \Gamma_{fp}} \sum_{j=1}^{d-1} \frac{\mu_f}{G_j} \|\mathbf{v}_f^h \cdot \boldsymbol{\tau}_j\|_{0,e}^2.$$

Setting $C_3 = 2K_0C_2$ ensures that the first term is positive for both $\varepsilon = 0$ and $\varepsilon = -1$. Then to control the second term it is sufficient to choose $\sigma_0 > 2\mu_f(1 + C_2C_3) = 2\mu_f(1 + 2K_0C_2^2)$. \square

Theorem 2.3.1 *The problem (2.25)–(2.26) has a unique solution.*

Proof. It is sufficient to show that solution of the homogeneous problem (2.25)–(2.26) is zero. By choosing $\mathbf{v}^h = \mathbf{u}^h$ and $q^h = p^h$ we get

$$a_f(\mathbf{u}_f^h, \mathbf{u}_1^h) + a_p(\mathbf{u}_p^h, \mathbf{u}_p^h) = 0,$$

which combined with (2.55) implies that $\mathbf{u}^h = 0$. The remainder of (2.25) together with the inf-sup condition (2.50) imply that $p^h = 0$. \square

2.4 ERROR ANALYSIS

Let the pair (\mathbf{u}, p) be the solution to (1.12)–(1.15) and let $\mathbf{u}_\alpha = \mathbf{u}|_{\Omega_\alpha}$, $\alpha = f, p$. We define functions $\tilde{\mathbf{u}} \in V^h$ and $\tilde{p} \in Q^h$ as follows:

$$\tilde{\mathbf{u}} = (\tilde{\mathbf{u}}_f, \tilde{\mathbf{u}}_p) = (\pi_1^h(\mathbf{u}_f), \pi_p^h(\mathbf{u}_p)), \quad \tilde{p} = (\tilde{p}_f, \tilde{p}_p),$$

where π^h is the operator introduced in Lemma (2.3.1), $\tilde{p}_p = p_p^I \in Q_p^h$ is the interpolant of p_p introduced in (2.13) and \tilde{p}_f is the L^2 -projection of p_f :

$$\int_E (\tilde{p}_f - p_f) q_f dx = 0, \quad \forall q_f \in \mathbb{P}_{r-1}(E), \quad \forall E \in \Omega_f^h. \quad (2.57)$$

For any $p_f \in H^s(\Omega_f)$ we have the approximation result:

$$\|p_f - \tilde{p}_f\|_{m,E} \leq Ch_E^{s-m} |p_f|_{s,E}, \quad m = 0, 1, \quad 1 \leq s \leq r \quad (2.58)$$

We also need the approximation result (3.4) from [68]: for any $\phi \in H^s(E)$, $0 \leq s \leq 1$, there exists a linear function ϕ_E^1 such that

$$\|\phi - \phi_E^1\|_{m,E} \leq Ch_E^{s-m} |\phi|_{s,E}, \quad m = 0, 1. \quad (2.59)$$

Applying (2.28) to $\phi - \phi_E^1$ and using (2.59), we obtain the estimate for a face e :

$$\|\phi - \phi_E^1\|_{0,e}^2 \leq Ch_E^{2s-1} |\phi|_{s,E}^2. \quad (2.60)$$

Let $\bar{\mathbf{K}}$ be a piecewise constant tensor equal to \mathbf{K}_E on element E . Recall that \mathbf{K}_E is the mean of value of \mathbf{K} on E . We assume that $\mathbf{K} \in (W^{1,\infty}(E))^{d \times d}$, $\forall E \in \Omega_p^h$, and that $\max_{E \in \Omega_p^h} \|\mathbf{K}\|_{1,\infty,E}$ is uniformly bounded independent of h_2 , where $\|\mathbf{K}\|_{1,\infty,E} = \max_{1 \leq i,j \leq d} \|\mathbf{K}_{i,j}\|_{W^{1,\infty}(E)}$. From Taylor's theorem it follows that

$$\max_{x \in E} |\mathbf{K}_{ij}(x) - \mathbf{K}_{E,ij}| \leq Ch_E \|\mathbf{K}_{ij}\|_{W^{1,\infty}(E)}. \quad (2.61)$$

2.4.1 Error equation

Subtracting the weak formulation (2.3)–(2.4) from the discrete equations (2.25)–(2.26), we obtain

$$\begin{aligned} a_f(\mathbf{u}_f^h - \mathbf{u}_f, \mathbf{v}_f^h) + b_f(\mathbf{v}_f^h, p_f^h - p_f) - \sum_{e \in \Gamma_{fp}^h} \int_e p_p \mathbf{v}_f^h \cdot \mathbf{n}_f ds \\ + a_p(\mathbf{u}_p^h, \mathbf{v}_p^h) + b_p(\mathbf{v}_p^h, p_p^h) = 0, \quad \forall \mathbf{v}^h \in V^h, \end{aligned} \quad (2.62)$$

$$b_f(\mathbf{u}_f^h - \mathbf{u}_f, q_f^h) + b_p(\mathbf{u}_p^h, q_p^h) = -[f_p^I, q_p^h]_{Q_p^h}, \quad \forall q^h \in Q^h.$$

If we take $q_f^h = 0$ in the second equation, we recover the weak form of the mass balance equation for the Darcy region (2.23). Using this, plus adding and subtracting $\tilde{\mathbf{u}}_f$, \tilde{p}_f , and \mathbf{u}_p^I in the appropriate terms of (2.62), we obtain

$$\begin{aligned} a_f(\mathbf{u}_f^h - \tilde{\mathbf{u}}_f, \mathbf{v}_f^h) + b_f(\mathbf{v}_f^h, p_f^h - \tilde{p}_f) + a_p(\mathbf{u}_p^h - \mathbf{u}_p^I, \mathbf{v}_p^h) + b_p(\mathbf{v}_p^h, p_p^h) \\ = a_f(\mathbf{u}_f - \tilde{\mathbf{u}}_f, \mathbf{v}_f^h) + b_f(\mathbf{v}_f^h, p_f - \tilde{p}_f) \\ + \sum_{e \in \Gamma_{fp}^h} \int_e p_p \mathbf{v}_f^h \cdot \mathbf{n}_f ds - a_p(\mathbf{u}_p^I, \mathbf{v}_p^h), \quad \forall \mathbf{v}^h \in V^h, \end{aligned} \quad (2.63)$$

$$b_f(\mathbf{u}_f^h - \tilde{\mathbf{u}}_f, q_f^h) = b_f(\mathbf{u}_f - \tilde{\mathbf{u}}_f, q_f^h), \quad \forall q_h \in Q_h.$$

2.4.2 Velocity estimate

Theorem 2.4.1 *Let (\mathbf{u}, p) be the solution to (1.12)–(1.15) and (\mathbf{u}^h, p^h) be the solution to (2.25)–(2.26). Furthermore, let $\mathbf{u}_f \in (H^{r+1}(\Omega_f))^d$, $p_f \in H^r(\Omega_f)$, $\mathbf{u}_p \in (H^1(\Omega_p))^d$, and $p_p \in H^2(\Omega_p)$. If Ω_f^h is a polyhedral mesh, we assume that $\varepsilon = 0$. Then, the following error bound holds*

$$\|\mathbf{u}_f^h - \mathbf{u}_f\|_{X_f} + \|\|\mathbf{u}_p^h - \mathbf{u}_p^I\|\|_{X_p^h}^2 \leq C (\varepsilon_1 + \varepsilon_2), \quad (2.64)$$

where

$$\begin{aligned} \varepsilon_1 &= h_f^r (|\mathbf{u}_f|_{r+1, \Omega_f} + |p_f|_{r, \Omega_f}) \\ \varepsilon_2 &= h_p (|p_p|_{1, \Omega_p} + |p_p|_{2, \Omega_p} + |\mathbf{u}_p|_{1, \Omega_p}) + h_p^{1/2} (h_p h_f^{-1/2} + h_f^{1/2}) \|p_p\|_{1, \Omega_p}. \end{aligned}$$

Proof. We choose the test functions in (2.63) to be $\mathbf{v}^h = \mathbf{u}^h - \tilde{\mathbf{u}}$ and $q^h = p^h - \tilde{p}$. The definition of $\pi_f^h(\mathbf{u}_f)$ implies that the right-hand side of the second equation in (2.63) is zero:

$$b_f(\mathbf{u}_f^h - \tilde{\mathbf{u}}_f, p_f^h - \tilde{p}_f) = 0.$$

Using the commutative property (2.19) and (2.42) we conclude that

$$\begin{aligned} \mathcal{DIV}(\mathbf{u}_p^h - \tilde{\mathbf{u}}_p) &= \mathcal{DIV}(\mathbf{u}_p^h - \mathbf{u}_p^I - (\nabla \varphi)^I) \\ &= \mathcal{DIV} \mathbf{u}_p^h - (\nabla \cdot \mathbf{u}_p)^I - (\nabla \cdot \nabla \varphi)^I = f_p^I - f_p^I - 0 = 0. \end{aligned}$$

Plugging the last two results results in the first equation of (2.63), we eliminate terms in the left-hand side that contain bilinear forms $b_f(\cdot, \cdot)$ and $b_p(\cdot, \cdot)$. Using the definition of $\tilde{\mathbf{u}}_p$, we break the third term in the left-hand side into three pieces:

$$\begin{aligned} a_f(\mathbf{u}_f^h - \tilde{\mathbf{u}}_f, \mathbf{u}_f^h - \tilde{\mathbf{u}}_f) + a_p(\mathbf{u}_p^h - \mathbf{u}_p^I, \mathbf{u}_p^h - \mathbf{u}_p^I) &= \\ a_f(\mathbf{u}_f - \tilde{\mathbf{u}}_f, \mathbf{u}_f^h - \tilde{\mathbf{u}}_f) + b_f(\mathbf{u}_f^h - \tilde{\mathbf{u}}_f, p_f - \tilde{p}_f) & \\ + \sum_{e \in \Gamma_{fp}^h} \int_e p_p(\mathbf{u}_f^h - \tilde{\mathbf{u}}_f) \cdot \mathbf{n}_f ds - a_p(\mathbf{u}_p^I, \mathbf{u}_p^h - \mathbf{u}_p^I) + a_p(\mathbf{u}_p^I, (\nabla \varphi)^I) & \\ + a_p(\mathbf{u}_p^h - \mathbf{u}_p^I, (\nabla \varphi)^I) \equiv T_1 + T_2 + T_3 + T_4 + T_5 + T_6. & \end{aligned} \quad (2.65)$$

To bound T_1 , we follow the analysis of a similar term in [81]. We expand it as follows:

$$\begin{aligned}
a_f(\mathbf{u}_f - \tilde{\mathbf{u}}_f, \mathbf{u}_f^h - \tilde{\mathbf{u}}_f^h) &= 2\mu_f \sum_{E \in \Omega_f^h} \int_E \mathbf{D}(\mathbf{u}_f - \tilde{\mathbf{u}}_f) : \mathbf{D}(\mathbf{u}_f^h - \tilde{\mathbf{u}}_f^h) dx \\
&\quad - 2\mu_f \sum_{e \in \mathcal{E}_f^h \cup \Gamma_f^h} \int_e \{\mathbf{D}(\mathbf{u}_f - \tilde{\mathbf{u}}_f)\} \mathbf{n}_e \cdot [\mathbf{u}_f^h - \tilde{\mathbf{u}}_f^h] ds \\
&\quad + 2\mu_f \varepsilon \sum_{e \in \mathcal{E}_f^h \cup \Gamma_f^h} \int_e \{\mathbf{D}(\mathbf{u}_f^h - \tilde{\mathbf{u}}_f^h)\} \mathbf{n}_e \cdot [\mathbf{u}_f - \tilde{\mathbf{u}}_f] ds \\
&\quad + \sum_{e \in \mathcal{E}_1^h \cup \Gamma_f^h} \frac{\sigma_e}{h_e} \int_e [\mathbf{u}_f - \tilde{\mathbf{u}}_f] \cdot [\mathbf{u}_f^h - \tilde{\mathbf{u}}_f^h] ds \\
&\quad + \sum_{e \in \Gamma_{fp}^h} \sum_{j=1}^{d-1} \frac{\mu_f}{G_j} \int_e (\mathbf{u}_f - \tilde{\mathbf{u}}_f) \cdot \boldsymbol{\tau}_j (\mathbf{u}_f^h - \tilde{\mathbf{u}}_f^h) \cdot \boldsymbol{\tau}_j ds \\
&\equiv T_{11} + T_{12} + T_{13} + T_{14} + T_{15}.
\end{aligned} \tag{2.66}$$

To estimate T_{11} , we apply the Cauchy-Schwarz inequality, the Young's inequality (2.27), and the approximation property (2.36):

$$\begin{aligned}
|T_{11}| &\leq 2\mu_f \sum_{E \in \Omega_f^h} \|\nabla(\mathbf{u}_f - \tilde{\mathbf{u}}_f)\|_{0,E} \|\nabla(\mathbf{u}_f^h - \tilde{\mathbf{u}}_f^h)\|_{0,E} \\
&\leq C \|\nabla(\mathbf{u}_f - \tilde{\mathbf{u}}_f)\|_{0,\Omega_f}^2 + \frac{1}{8} \|\nabla(\mathbf{u}_f^h - \tilde{\mathbf{u}}_f^h)\|_{0,\Omega_f}^2 \\
&\leq C h_f^{2r} |\mathbf{u}_f|_{r+1,\Omega_f}^2 + \frac{1}{8} \|\nabla(\mathbf{u}_f^h - \tilde{\mathbf{u}}_f^h)\|_{0,\Omega_f}^2.
\end{aligned} \tag{2.67}$$

To bound T_{12} , we introduce the Lagrange interpolant $\mathcal{L}_h(\mathbf{u}_f)$ of degree r satisfying

$$|\mathbf{u}_f - \mathcal{L}_h(\mathbf{u}_f)|_{m,E} \leq C h_E^{s-m} |\mathbf{u}_f|_{s,E}, \quad 2 \leq s \leq r+1, \quad m = 0, 1, 2. \tag{2.68}$$

Let $\delta(e)$ be the union of elements having the face e . We split T_{12} in two pieces T_{12}^a and T_{12}^b by adding and subtracting $\mathcal{L}_h(\mathbf{u}_f)$ inside the average factor $\{\cdot\}$. Using the Cauchy-Schwarz

inequality, the Young's inequality (2.27), the trace inequality (2.30), and (2.68), we obtain

$$\begin{aligned}
|T_{12}^a| &= \left| \sum_{e \in \mathcal{E}_f^h \cup \Gamma_f^h} \int_e \{\mathbf{D}(\mathcal{L}_h(\mathbf{u}_f) - \tilde{\mathbf{u}}_f)\} \mathbf{n}_e \cdot [\mathbf{u}_f^h - \tilde{\mathbf{u}}_f] ds \right| \\
&\leq \sum_{e \in \mathcal{E}_f^h \cup \Gamma_f^h} \frac{h_e^{1/2}}{\sigma_e^{1/2}} \|\{\mathbf{D}(\mathcal{L}_h(\mathbf{u}_f) - \tilde{\mathbf{u}}_f)\} \mathbf{n}_e\|_{0,e} \frac{\sigma_e^{1/2}}{h_e^{1/2}} \|\mathbf{u}_f^h - \tilde{\mathbf{u}}_f\|_{0,e} \\
&\leq C \sum_{e \in \mathcal{E}_f^h \cup \Gamma_f^h} |\mathcal{L}_h(\mathbf{u}_f) - \tilde{\mathbf{u}}_f|_{1,\delta(e)}^2 + \frac{1}{8} \sum_{e \in \mathcal{E}_f^h \cup \Gamma_f^h} \frac{\sigma_e}{h_e} \|\mathbf{u}_f^h - \tilde{\mathbf{u}}_f\|_{0,e}^2 \\
&\leq C h_f^{2r} |\mathbf{u}_f|_{r+1,\Omega_f}^2 + \frac{1}{8} \sum_{e \in \mathcal{E}_f^h \cup \Gamma_f^h} \frac{\sigma_e}{h_e} \|\mathbf{u}_f^h - \tilde{\mathbf{u}}_f\|_{0,e}^2.
\end{aligned} \tag{2.69}$$

The other term is estimated similarly using the trace inequality (2.29):

$$\begin{aligned}
|T_{12}^b| &= \left| \sum_{e \in \mathcal{E}_f^h \cup \Gamma_f^h} \int_e \{\mathbf{D}(\mathbf{u}_f - \mathcal{L}_h(\mathbf{u}_f))\} \mathbf{n}_e \cdot [\mathbf{u}_f^h - \tilde{\mathbf{u}}_f] ds \right| \\
&\leq C \sum_{e \in \mathcal{E}_f^h \cup \Gamma_f^h} \frac{h_e}{\sigma_e} (h_e^{-1} |\mathbf{u}_f - \mathcal{L}_h(\mathbf{u}_f)|_{1,\delta(e)}^2 + h_e |\mathbf{u}_f - \mathcal{L}_h(\mathbf{u}_f)|_{2,\delta(e)}^2) \\
&\quad + \frac{1}{8} \sum_{e \in \mathcal{E}_f^h \cup \Gamma_f^h} \frac{\sigma_e}{h_e} \|\mathbf{u}_f^h - \tilde{\mathbf{u}}_f\|_{0,e}^2 \\
&\leq C h_f^{2r} |\mathbf{u}_f|_{r+1,\Omega_f}^2 + \frac{1}{8} \sum_{e \in \mathcal{E}_f^h \cup \Gamma_f^h} \frac{\sigma_e}{h_e} \|\mathbf{u}_f^h - \tilde{\mathbf{u}}_f\|_{0,e}^2.
\end{aligned} \tag{2.70}$$

We conclude that

$$|T_{12}| \leq C h_f^{2r} |\mathbf{u}_f|_{r+1,\Omega_f}^2 + \frac{1}{4} \sum_{e \in \mathcal{E}_f^h \cup \Gamma_f^h} \frac{\sigma_e}{h_e} \|\mathbf{u}_f^h - \tilde{\mathbf{u}}_f\|_{0,e}^2. \tag{2.71}$$

The third term in (2.66) is zero, $T_{13} = 0$, due to the continuity of \mathbf{u}_f and the property (2.33). The fourth term is estimated by applying the Cauchy-Schwarz inequality, the approximation property (2.35), and the trace inequality (2.28):

$$\begin{aligned}
|T_{14}| &\leq C \sum_{e \in \mathcal{E}_f^h \cup \Gamma_f^h} \frac{\sigma_e}{h_e} \|\mathbf{u}_f - \tilde{\mathbf{u}}_f\|_{0,e}^2 + \frac{1}{8} \sum_{e \in \mathcal{E}_f^h \cup \Gamma_f^h} \frac{\sigma_e}{h_e} \|\mathbf{u}_f^h - \tilde{\mathbf{u}}_f\|_{0,e}^2 \\
&\leq C h_1^{2r} |\mathbf{u}_f|_{r+1,\Omega_f}^2 + \frac{1}{8} \sum_{e \in \mathcal{E}_f^h \cup \Gamma_f^h} \frac{\sigma_e}{h_e} \|\mathbf{u}_f^h - \tilde{\mathbf{u}}_f\|_{0,e}^2.
\end{aligned} \tag{2.72}$$

Using the same arguments, we bound the fifth term:

$$\begin{aligned}
|T_{15}| &\leq \sum_{e \in \Gamma_{fp}^h} \sum_{j=1}^{d-1} \frac{\mu_f}{G_j} \|\mathbf{u}_f - \tilde{\mathbf{u}}_f\|_{0,e} \|(\mathbf{u}_f^h - \tilde{\mathbf{u}}_f) \cdot \boldsymbol{\tau}_j\|_{0,e} \\
&\leq C h_f^{2r} |\mathbf{u}_f|_{r+1, \Omega_f}^2 + \sum_{e \in \Gamma_{fp}^h} \sum_{j=1}^{d-1} \frac{\mu_f}{2G_j} \|(\mathbf{u}_f^h - \tilde{\mathbf{u}}_f) \cdot \boldsymbol{\tau}_j\|_{0,e}^2.
\end{aligned} \tag{2.73}$$

To handle the term T_2 , we use the property (2.57) of the L^2 -projection \tilde{p}_1 :

$$\begin{aligned}
b_f(\mathbf{u}_f^h - \tilde{\mathbf{u}}_f, p_f - \tilde{p}_f) &= - \sum_{E \in \Omega_f^h} \int_E (p_f - \tilde{p}_f) \nabla \cdot (\mathbf{u}_f^h - \tilde{\mathbf{u}}_f) dx \\
&\quad + \sum_{e \in \mathcal{E}_f^h \cup \Gamma_f^h} \int_e \{p_f - \tilde{p}_f\} [\mathbf{u}_f^h - \tilde{\mathbf{u}}_f] \cdot \mathbf{n}_e ds \\
&= \sum_{e \in \mathcal{E}_1^h \cup \Gamma_f^h} \int_e \{p_f - \tilde{p}_f\} [\mathbf{u}_f^h - \tilde{\mathbf{u}}_f] \cdot \mathbf{n}_e ds.
\end{aligned} \tag{2.74}$$

Thus, using the trace inequality (2.28) and the property (2.58) of the L^2 projection \tilde{p}_f , we get

$$|T_2| \leq C h_f^{2r} |p_f|_{r, \Omega_f}^2 + \frac{1}{8} \sum_{e \in \mathcal{E}_f^h \cup \Gamma_f^h} \frac{\sigma_e}{h_e} \int_e [\mathbf{u}_f^h - \tilde{\mathbf{u}}_f]^2 ds. \tag{2.75}$$

The remaining terms in the error equation (2.65) requires to use analysis developed for mimetic discretizations of elliptic equations [24, 68]. We use the piecewise constant tensor $\bar{\mathbf{K}}$ defined at the beginning of this section.

Let p_p^1 be a discontinuous piecewise linear function defined on Ω_p^h such that (2.59) holds on every element $E \in \Omega_p^h$. Then, adding and subtracting $\bar{\mathbf{K}} \nabla p_p^1$, we obtain

$$T_4 = a_p((\mathbf{u}_p + \bar{\mathbf{K}} \nabla p_p^1)^I, \mathbf{u}_p^I - \mathbf{u}_p^h) - a_p((\bar{\mathbf{K}} \nabla p_p^1)^I, \mathbf{u}_p^I - \mathbf{u}_p^h) \equiv T_{41} + T_{42}. \tag{2.76}$$

Applying the Cauchy-Schwarz inequality, the stability assumption (2.21), and the trace inequality (2.28), we get

$$\begin{aligned}
|T_{41}| &\leq \|(\mathbf{u}_p + \bar{\mathbf{K}} \nabla p_p^1)^I\|_{X_p^h} \|\mathbf{u}_p^h - \mathbf{u}_p^I\|_{X_p^h} \\
&\leq C \left(\sum_{E \in \Omega_p^h} |E| \sum_{e \subset \partial E} \left| \frac{1}{|e|} \int_e (\mathbf{u}_p + \bar{\mathbf{K}} \nabla p_p^1) \cdot \mathbf{n}_e ds \right|^2 \right)^{1/2} \|\mathbf{u}_p^h - \mathbf{u}_p^I\|_{X_p^h} \\
&\leq C \left(\sum_{E \in \Omega_p^h} [\|\mathbf{u}_p + \bar{\mathbf{K}} \nabla p_p^1\|_{0,E}^2 + h_E^2 |\mathbf{u}_p|_{1,E}^2] \right)^{1/2} \|\mathbf{u}_p^h - \mathbf{u}_p^I\|_{X_p^h}.
\end{aligned} \tag{2.77}$$

Using the triangle inequality and then estimates (2.61) and (2.59), we obtain

$$\begin{aligned}
\|\mathbf{u}_p + \overline{\mathbf{K}}\nabla p_p^1\|_{0,E}^2 &\leq \|\mathbf{K}\nabla(p_p - p_p^1)\|_{0,E} + \|(\mathbf{K} - \overline{\mathbf{K}})\nabla p_p^1\|_{0,E} \\
&\leq C (h_E |p_p|_{2,E} + h_E \|\nabla p_p^1\|_{0,E}) \\
&\leq Ch_E (|p_p|_{2,E} + \|\nabla p_p\|_{0,E} + \|\nabla(p_p - p_p^1)\|_{0,E}) \\
&\leq Ch_E (|p_p|_{2,E} + |p_p|_{1,E}).
\end{aligned}$$

Combining the two last inequalities and applying the Young's inequality (2.27), we get

$$|T_{41}| \leq C h_p^2 \left(|p_p|_{1,\Omega_p} + |p_p|_{2,\Omega_p} + |\mathbf{u}_p|_{1,\Omega_p} \right)^2 + \frac{1}{8} \|\mathbf{u}_p^h - \mathbf{u}_p^I\|_{X_p^h}^2. \quad (2.78)$$

The consistency condition (2.20) and continuity of p_p allow us to rewrite T_{42} as follows:

$$\begin{aligned}
T_{42} &= \sum_{E \in \Omega_p^h} \sum_{e \subset \partial E} \chi_E^e (\mathbf{u}_p^h - \mathbf{u}_p^I)_E^e \int_e p_{p,E}^1 ds \\
&= \sum_{E \in \Omega_p^h} \sum_{e \subset \partial E} \chi_E^e (\mathbf{u}_p^h - \mathbf{u}_p^I)_E^e \int_e (p_{p,E}^1 - p_p) ds + \sum_{e \in \Gamma_{fp}^h} \chi_E^e (\mathbf{u}_p^h - \mathbf{u}_p^I)_E^e \int_e p_p ds \\
&\equiv T_{42}^a + T_{42}^b.
\end{aligned} \quad (2.79)$$

We estimate T_{42}^a using (2.60) and the stability property (2.21):

$$\begin{aligned}
|T_{42}^a| &\leq \sum_{E \in \Omega_p^h} \sum_{e \subset \partial E} |e|^{1/2} |(\mathbf{u}_p^h - \mathbf{u}_p^I)_E^e| \|p_{p,E}^1 - p_p\|_{0,e} \\
&\leq C \sum_{E \in \Omega_p^h} h_E \left(|E| \sum_{e \subset \partial E} |(\mathbf{u}_p^h - \mathbf{u}_p^I)_E^e|^2 \right)^{1/2} |p_p|_{2,E} \\
&\leq C h_p |p_p|_{2,\Omega_p} \|\mathbf{u}_p^h - \mathbf{u}_p^I\|_{X_p^h} \leq C h_p^2 |p_p|_{2,\Omega_p}^2 + \frac{1}{8} \|\mathbf{u}_p^h - \mathbf{u}_p^I\|_{X_p^h}^2.
\end{aligned} \quad (2.80)$$

The term T_{42}^b will be combined with other terms later. Now we proceed with the fifth term in the error equation. Adding and subtracting $\overline{\mathbf{K}}\nabla p_p^1$, we get

$$T_5 = a_p((\mathbf{u}_p + \overline{\mathbf{K}}\nabla p_p^1)^I, (\nabla\varphi)^I) - a_p((\overline{\mathbf{K}}\nabla p_p^1)^I, (\nabla\varphi)^I) \equiv T_{51} + T_{52}. \quad (2.81)$$

The term T_{51} is similar to T_{41} ; therefore, we use the same approach to bound it:

$$|T_{51}| \leq C h_p \left(|p_p|_{1,\Omega_p} + |p_p|_{2,\Omega_p} + |\mathbf{u}_p|_{1,\Omega_p} \right) \|(\nabla\varphi)^I\|_{X_p^h}.$$

Using estimate (2.49), we conclude that

$$|T_{51}| \leq C h_p h_f \left(|p_p|_{1,\Omega_p} + |p_p|_{2,\Omega_p} + |\mathbf{u}_p|_{1,\Omega_p} \right) |\mathbf{u}_f|_{3/2,\Omega_f}. \quad (2.82)$$

For the term T_{52} , we apply estimate (2.60) and the consistency condition (2.20):

$$\begin{aligned} T_{52} &= - \sum_{E \in \Omega_p^h} \sum_{e \subset \partial E} \chi_E^e ((\nabla \varphi)^I)_E^e \int_e p_{p,E}^1 ds \\ &= \sum_{E \in \Omega_p^h} \sum_{e \subset \partial E} \chi_E^e ((\nabla \varphi)^I)_E^e \int_e (p_p - p_{p,E}^1) ds - \sum_{e \in \Gamma_{fp}^h} \chi_E^e ((\nabla \varphi)^I)_E^e \int_e p_p ds \\ &\equiv T_{52}^a + T_{52}^b. \end{aligned} \quad (2.83)$$

To estimate T_{52}^a , we repeat arguments used for terms T_{42}^a and T_{51} . We obtain

$$|T_{52}^a| \leq C h_p |p_p|_{2,\Omega_p} \| |(\nabla \varphi)^I| \|_{X_p^h} \leq C h_p h_f |p_p|_{2,\Omega_p} |\mathbf{u}_f|_{3/2,\Omega_f}. \quad (2.84)$$

The term T_{52}^b will be combined with other terms later.

The sixth term in the error equation is bounded using the Cauchy-Schwartz inequality and estimate (2.49):

$$|T_6| \leq \| |\mathbf{u}_p^h - \mathbf{u}_p^I| \|_{X_p^h} \| |(\nabla \varphi)^I| \|_{X_p^h} \leq \frac{1}{8} \| |\mathbf{u}_p^h - \mathbf{u}_p^I| \|_{X_p^h}^2 + C h_f^2 |\mathbf{u}_f|_{3/2,\Omega_f}^2. \quad (2.85)$$

Finally, the third term in the error equation (2.65) is combined with T_{42}^b and T_{52}^b . Let $p_p^* \in \Lambda_{fp}^h$ such that $(p_p^*)^e$ is the L^2 -projection of p_p on $\mathbb{P}_0(e)$ and let \bar{p}_p^* be the piecewise constant function on Γ_{fp}^h satisfying

$$\bar{p}_p^*|_e = (p_p^*)^e, \quad \forall e \in \Gamma_{fp}^h.$$

Because $\mathbf{u}^h - \tilde{\mathbf{u}}^h \in V^h$,

$$\int_{\Gamma_{fp}} \bar{p}_p^* (\mathbf{u}_f^h - \tilde{\mathbf{u}}_f) \cdot \mathbf{n}_f ds + \langle p_p^*, \mathbf{u}_p^h - \tilde{\mathbf{u}}_p \rangle_{\Lambda_{fp}^h} = 0.$$

Using the above equation, the definition of operator π_p^h and the property of the L^2 projection, we obtain

$$\begin{aligned}
T_3 + T_{42}^g + T_{52}^b &= \sum_{e \in \Gamma_{fp}^h} \left(\int_e p_p(\mathbf{u}_f^h - \tilde{\mathbf{u}}_f) \cdot \mathbf{n}_f ds + \chi_E^e (\mathbf{u}_p^h - \mathbf{u}_p^I - (\nabla \varphi)^I)_E^e \int_e p_p ds \right) \\
&= \sum_{e \in \Gamma_{fp}^h} \left(\int_e p_p(\mathbf{u}_f^h - \tilde{\mathbf{u}}_f) \cdot \mathbf{n}_f ds + (\mathbf{u}_p^h - \tilde{\mathbf{u}}_p)_E^e \int_e p_p ds \right) \\
&= \sum_{e \in \Gamma_{fp}^h} \left(\int_e (p_p - \bar{p}_p^*)(\mathbf{u}_f^h - \tilde{\mathbf{u}}_f) \cdot \mathbf{n}_f ds + (\mathbf{u}_p^h - \tilde{\mathbf{u}}_p)_E^e \int_e (p_p - (\bar{p}_p^*)^e) ds \right) \\
&= \sum_{e \in \Gamma_{fp}^h} \int_e (p_p - \bar{p}_p^*)(\mathbf{u}_f^h - \tilde{\mathbf{u}}_f) \cdot \mathbf{n}_f ds.
\end{aligned}$$

For each face $e \in \Gamma_{fp}^h$ we define \mathbf{c}^e to be the L^2 -projection of $\mathbf{u}^h - \tilde{\mathbf{u}}$ on $\mathbb{P}_0(e)$. Let us assume that $e = E_p^e \cap \bigcup_{i=1}^{n_e} E_{f,i}^e$, where $E_p^e \in \Omega_p^h$, and $E_{f,i}^e \in \Omega_f^h$ for $i = 1, \dots, n_e$. Using properties of the L^2 -projection, the approximation properties and the trace inequality (2.28), we obtain

$$\begin{aligned}
|T_3 + T_{42}^b + T_{52}^b| &= \sum_{e \in \Gamma_{fp}^h} \int_e (p_p - \bar{p}_p^*|_e)(\mathbf{u}_f^h - \tilde{\mathbf{u}}_f - \mathbf{c}^e) \cdot \mathbf{n}_f ds \\
&\leq C \sum_{e \in \Gamma_{fp}^h} h_p^{1/2} \|p_p\|_{1,E_p^e} \sum_{i=1}^{n_e} \left(h_f^{-1/2} \|\mathbf{u}_f^h - \tilde{\mathbf{u}}_f - \mathbf{c}^e\|_{0,E_{f,i}^e} + h_f^{1/2} |\mathbf{u}_f^h - \tilde{\mathbf{u}}_f|_{1,E_{f,i}^e} \right) \\
&\leq C \sum_{e \in \Gamma_{fp}^h} h_p^{1/2} \|p_p\|_{1,E_p^e} \sum_{i=1}^{n_e} (h_* h_f^{-1/2} + h_f^{1/2}) |\mathbf{u}_f^h - \tilde{\mathbf{u}}_f|_{1,E_{f,i}^e} \\
&\leq C h_p \left(h_* h_f^{-1/2} + h_f^{1/2} \right)^2 \|p_p\|_{1,\Omega_p}^2 + \frac{1}{8} \|\nabla(\mathbf{u}_f^h - \tilde{\mathbf{u}}_f)\|_{0,\Omega_f}^2,
\end{aligned} \tag{2.86}$$

where

$$h_* = \max(h_p, h_f).$$

We recall that the velocity \mathbf{u}_p is understood as an average over large enough representative volume, which is much larger than the one needed to define \mathbf{u}_f . Hence, it is relevant to assume that the grid in the porous medium region is coarser than the one in the fluid region, meaning that $h_* = h_p$. Collecting the estimates of all terms in the right hand side of error equation (2.65), we prove the assertion of the theorem. \square

2.4.3 Pressure Estimates

Theorem 2.4.2 *Under the assumptions of Theorem 2.4.1, the following error bound holds:*

$$\|p^h - p\|_{Q^h} \leq C(\varepsilon_1 + \varepsilon_2) \quad (2.87)$$

where

$$\begin{aligned} \varepsilon_1 &= h_f^r (|p_f|_{r,\Omega_f} + |\mathbf{u}_f|_{r+1,\Omega_f}), \\ \varepsilon_2 &= h_p (|p_p|_{1,\Omega_p} + |p_p|_{2,\Omega_p} + |\mathbf{u}_p|_{1,\Omega_p}) + h_p^{1/2} (h_p h_f^{-1/2} + h_f^{1/2}) \|p_p\|_{1,\Omega_f}. \end{aligned}$$

Proof. Taking $q^h = (p_f^h - \tilde{p}_f, p_p^h - \tilde{p}_p)$ in the inf-sup condition (2.50), we get

$$\|p^h - \tilde{p}\|_{Q^h} \leq \frac{1}{\beta} \sup_{\mathbf{v}^h \in V^h} \frac{b_f(\mathbf{v}_f^h, p_f^h - \tilde{p}_f) + b_p(\mathbf{v}_p^h, p_p^h - \tilde{p}_p)}{\|\mathbf{v}^h\|_{X^h}}. \quad (2.88)$$

From (2.63), we get

$$\begin{aligned} b_f(\mathbf{v}_f^h, p_f^h - \tilde{p}_f) + b_p(\mathbf{v}_p^h, p_p^h - \tilde{p}_p) &= a_f(\mathbf{u}_f - \mathbf{u}_f^h, \mathbf{v}_f^h) + b_f(\mathbf{v}_f^h, p_f - \tilde{p}_f) \\ &\quad + \sum_{e \in \Gamma_{fp}^h} \int_e p_p \mathbf{v}_f^h \cdot \mathbf{n}_f ds - a_p(\mathbf{u}_p^h, \mathbf{v}_p^h) - b_p(\mathbf{v}_p^h, \tilde{p}_p) \\ &\equiv J_1 + J_2 + J_3 + J_4 + J_5. \end{aligned}$$

By adding and subtracting terms, and using the consistency condition (2.20), we obtain

$$\begin{aligned} J_4 + J_5 &= -a_p((\mathbf{u}_p + \bar{\mathbf{K}}\nabla p_p^l)^I, \mathbf{v}_p^h) + a_p((\bar{\mathbf{K}}\nabla p_p^l)^I, \mathbf{v}_p^h) \\ &\quad + [\mathcal{D}\mathcal{I}\mathcal{V} \mathbf{v}_p^h, (p_p - p_p^l)^I]_{Q_p^h} + [\mathcal{D}\mathcal{I}\mathcal{V} \mathbf{v}_p^h, (p_p^l)^I]_{Q_p^h} - a_p(\mathbf{u}_p^h - \mathbf{u}_p^I, \mathbf{v}_p^h) \\ &= -a_p((\mathbf{u}_p + \bar{\mathbf{K}}\nabla p_p^l)^I, \mathbf{v}_p^h) + \sum_{e \subset \partial E} \chi_E^e(\mathbf{v}_p^h)_E^e \int_e p_p^l ds \\ &\quad + [\mathcal{D}\mathcal{I}\mathcal{V} \mathbf{v}_p^h, (p_p - p_p^l)^I]_{Q_p^h} - a_p(\mathbf{u}_p^h - \mathbf{u}_p^I, \mathbf{v}_p^h) \\ &= J_6 + J_7 + J_8 + J_9. \end{aligned} \quad (2.89)$$

Thus, we need to estimate seven terms. We expand J_1 as follows:

$$\begin{aligned}
J_1 &= a_f(\mathbf{u}_f - \mathbf{u}_f^h, \mathbf{v}_f^h) = 2\mu_f \sum_{E \in \Omega_f^h} \int_E \mathbf{De}(\mathbf{u}_f - \mathbf{u}_f^h) : \mathbf{De}(\mathbf{v}_f^h) dx \\
&\quad - 2\mu_f \sum_{e \in \mathcal{E}_f^h \cup \Gamma_f^h} \int_e \{\mathbf{De}(\mathbf{u}_f - \mathbf{u}_f^h) \mathbf{n}_e\} \cdot [\mathbf{v}_f^h] ds \\
&\quad + 2\mu_f \varepsilon \sum_{e \in \mathcal{E}_f^h \cup \Gamma_f^h} \int_e \{\mathbf{De}(\mathbf{v}_f^h) \mathbf{n}_e\} \cdot [\mathbf{u}_f - \mathbf{u}_f^h] ds \\
&\quad + \sum_{e \in \mathcal{E}_1^h \cup \Gamma_f^h} \frac{\sigma_e}{h_e} \int_e [\mathbf{u}_f - \mathbf{u}_f^h] \cdot [\mathbf{v}_f^h] ds \\
&\quad + \sum_{e \in \Gamma_{fp}^h} \sum_{j=1}^{d-1} \frac{\mu_f}{G_j} \int_e ((\mathbf{u}_f - \mathbf{u}_f^h) \cdot \boldsymbol{\tau}_j) (\mathbf{v}_f^h \cdot \boldsymbol{\tau}_j) ds \\
&= J_{11} + J_{12} + J_{13} + J_{14} + J_{15}.
\end{aligned} \tag{2.90}$$

From Cauchy-Schwarz inequality, we immediately get bounds for three terms:

$$|J_{11} + J_{14} + J_{15}| \leq C \|\mathbf{u}_f - \mathbf{u}_f^h\|_{X_f} \|\mathbf{v}_f^h\|_{X_f}. \tag{2.91}$$

We bound J_{12} by taking similar approach as the one used for T_{12} ,

$$\begin{aligned}
|J_{12}| &\leq C \sum_{e \in \mathcal{E}_f^h \cup \Gamma_f^h} \left(\frac{h_e}{\sigma_e} \right)^{1/2} \|\nabla(\mathbf{u}_f - \mathbf{u}_f^h)\|_{0,e} \left(\frac{\sigma_e}{h_e} \right)^{1/2} \|[\mathbf{v}_f^h]\|_{0,e} \\
&\leq C \left(\sum_{e \in \mathcal{E}_f^h \cup \Gamma_f^h} \frac{h_e}{\sigma_e} (\|\nabla(\mathbf{u}_f - \tilde{\mathbf{u}}_f)\|_{0,e}^2 + \|\nabla(\tilde{\mathbf{u}}_f - \mathbf{u}_f^h)\|_{0,e}^2) \right)^{1/2} \|\mathbf{v}_f^h\|_{X_f} \\
&\leq C \left(h_f^{2r} |\mathbf{u}_f|_{r+1, \Omega_f}^2 + \|\tilde{\mathbf{u}}_f - \mathbf{u}_f^h\|_{X_f}^2 \right)^{1/2} \|\mathbf{v}_f^h\|_{X_f}.
\end{aligned} \tag{2.92}$$

To bound the term J_{13} , we use the trace inequality (2.30), and shape regularity of element E^e having face e :

$$\begin{aligned}
|J_{13}| &\leq C \sum_{e \in \mathcal{E}_f^h \cup \Gamma_f^h} \| \{\mathbf{De}(\mathbf{v}_f^h) \mathbf{n}_e\} \|_{0,e} \|[\mathbf{u}_f - \mathbf{u}_f^h]\|_{0,e} \\
&\leq C \sum_{e \in \mathcal{E}_f^h \cup \Gamma_f^h} h_{E^e}^{-1/2} \left(\frac{h_e}{\sigma_e} \right)^{1/2} \|\nabla \mathbf{v}_f^h\|_{0,E^e} \left(\frac{\sigma_e}{h_e} \right)^{1/2} \|[\mathbf{u}_f - \mathbf{u}_f^h]\|_{0,e} \\
&\leq C \|\mathbf{v}_f^h\|_{X_f^h} \|\mathbf{u}_f - \mathbf{u}_f^h\|_{X_f}.
\end{aligned} \tag{2.93}$$

We proceed with J_2 by applying the trace inequality (2.28) and the property (2.58) of the L^2 projection:

$$\begin{aligned}
|J_2| &= |b_f(\mathbf{v}_f^h, p_f - \tilde{p}_f)| = \left| \sum_{e \in \mathcal{E}_f^h \cup \Gamma_f^h} \int_e \{p_f - \tilde{p}_f\} [\mathbf{v}_f^h] \cdot \mathbf{n}_e ds \right| \\
&\leq \sum_{e \in \mathcal{E}_f^h \cup \Gamma_f^h} \left(\frac{h_e}{\sigma_e} \right)^{1/2} \|\{p_f - \tilde{p}_f\}\|_{0,e} \left(\frac{\sigma_e}{h_e} \right)^{1/2} \|\mathbf{v}_f\|_{0,e} \\
&\leq Ch_f^r |p|_{r, \Omega_f} \|\mathbf{v}_f^h\|_{X_f}.
\end{aligned} \tag{2.94}$$

By combining J_3 with J_7 and repeating the steps we followed to bound T_{42} , we get

$$|J_3 + J_7| \leq C \left(h_p |p_p|_{2, \Omega_p} \|\mathbf{v}_p^h\|_{X_p^h} + h_p^{1/2} \left(h_p h_f^{-1/2} + h_f^{1/2} \right) \|p_p\|_{1, \Omega_p} \|\nabla \mathbf{v}_f^h\|_{0, \Omega_f} \right).$$

Since J_6 is similar to T_{51} , we can write:

$$|J_6| \leq C h_p \left(|p_p|_{1, \Omega_p} + |p_p|_{2, \Omega_p} + |\mathbf{u}_p|_{1, \Omega_p} \right) \|\mathbf{v}_p^h\|_{X_p^h}. \tag{2.95}$$

The term J_8 is estimated by using Cauchy-Schwartz inequality and the approximation properties (2.59):

$$|J_8| \leq C h_p^2 \|\mathbf{v}_p^h\|_{div} |p_2|_{2, \Omega_p}. \tag{2.96}$$

Next, for the term J_9 , using Cauchy-Schwarz inequality and the velocity estimates, we find that

$$\begin{aligned}
|J_9| &\leq C \left(h_f (|\mathbf{u}_f|_{2, \Omega_f} + |p_f|_{1, \Omega_f}) + h_p (|p_p|_{1, \Omega_p} + |p_p|_{2, \Omega_p} + |\mathbf{u}_p|_{1, \Omega_p}) \right. \\
&\quad \left. + h_p^{1/2} \left(h_p h_f^{-1/2} + h_f^{1/2} \right) \|p_p\|_{1, \Omega_f} \right) \|\mathbf{v}_p^h\|_{X_p^h}.
\end{aligned} \tag{2.97}$$

Combining all the bounds and dividing by $\|\mathbf{v}^h\|_{X^h}$ yields the assertion of the theorem. \square

2.5 IMPLEMENTATION DETAILS

The global velocity space V^h , which embeds the interface continuity constraint, is not convenient for a computer program. Instead, the continuity constraints on the velocity are imposed weakly and additional variables, the Lagrange multipliers are added to the system.

Efficient solution of Darcy's law uses the hybridization procedure that is the standard in numerical method for mixed discretizations. We relax flux continuity condition on all mesh faces in the Darcy region. Two flux dregrees of freedom $(U_p)_{E_1}^e$ and $(U_p)_{E_2}^e$ are prescribed to every interior face e . Then the following continuity condition is added to the system

$$\lambda^e (U_p)_{E_1}^e + \lambda^e (U_p)_{E_2}^e = 0,$$

where λ^e is a Lagrange multiplier associated with the face e . The new system is algebraically equivalent to the original system; however, it has a special structure that allows to eliminate efficiently the primary pressure and velocity unknowns in the Darcy region.

Each continuity constraint results in one Lagrange multiplier. We collect the Lagrange multipliers in a single vector $\mathbf{L} = (\lambda^{e_1}, \dots, \lambda^{e_J})$, where J is the number of the mesh edges in Ω_p^h .

Let us define the block-diagonal matrix $\mathbf{M}_p = \text{diag}\{\mathbf{M}_{p,E_1}, \dots, \mathbf{M}_{p,E_N}\}$ and the diagonal matrix $\mathbf{C}_p = \text{diag}\{|e_1|, \dots, |e_J|\}$. Let \mathbf{A}_f and \mathbf{B}_f be the matrices associated with the bilinear forms $a_f(\cdot, \cdot)$ and $b_f(\cdot, \cdot)$, respectively. The matrix associated with the interface term is denoted by \mathbf{C}_1 . The matrix equations are

$$\begin{pmatrix} \mathbf{A}_f & \mathbf{B}_f & \mathbf{0} & \mathbf{0} & \mathbf{C}_f \\ \mathbf{B}_f^T & \mathbf{0} & \mathbf{0} & \mathbf{0} & \mathbf{0} \\ \mathbf{0} & \mathbf{0} & \mathbf{M}_p & \mathbf{B}_p & \mathbf{C}_p \\ \mathbf{0} & \mathbf{0} & \mathbf{B}_p^T & \mathbf{0} & \mathbf{0} \\ \mathbf{C}_f^T & \mathbf{0} & \mathbf{C}_p^T & \mathbf{0} & \mathbf{0} \end{pmatrix} \begin{pmatrix} \mathbf{U}_f \\ \mathbf{P}_f \\ \mathbf{U}_p \\ \mathbf{P}_p \\ \mathbf{L} \end{pmatrix} = \begin{pmatrix} \mathbf{F}_f \\ 0 \\ 0 \\ -\mathbf{F}_p \\ 0 \end{pmatrix}, \quad (2.98)$$

where \mathbf{F}_p is a vector of size N consisting of the cell averages of the source term.

The first pair of equations is the matrix form of the discrete Stokes problem. The second pair of equations represents elemental equations for the Darcy region. The last block equation represents the flux continuity constraints.

The matrix of system (2.98) is symmetric. The hybridization procedure results in the block-diagonal matrix \mathbf{B}_p with as many blocks as the number of elements in Ω_p^h . Thus, the unknowns \mathbf{U}_p and \mathbf{P}_p may be easily eliminated. Changing the order of remaining unknowns, we get the following saddle point problem:

$$\begin{pmatrix} \mathbf{A}_f & \mathbf{C}_f & \mathbf{B}_f \\ \mathbf{C}_f^T & -\mathbf{A}_p & \mathbf{0} \\ \mathbf{B}_f^T & \mathbf{0} & \mathbf{0} \end{pmatrix} \begin{pmatrix} \mathbf{U}_f \\ \mathbf{L} \\ \mathbf{P}_f \end{pmatrix} = \begin{pmatrix} \mathbf{F}_f \\ \mathbf{G}_p \\ \mathbf{0} \end{pmatrix}, \quad (2.99)$$

where

$$\mathbf{A}_p = \mathbf{C}_p^T (\mathbf{M}_p^{-1} - \mathbf{M}_p^{-1} \mathbf{C}_p \mathbf{B}_p (\mathbf{B}_p^T \mathbf{M}_p^{-1} \mathbf{B}_p)^{-1} \mathbf{B}_p^T \mathbf{M}_p^{-1} \mathbf{C}_p) \mathbf{C}_p$$

is a symmetric positive definite (SPD) matrix. This matrix is a special approximation of the elliptic operator in the Darcy region. Note, that only \mathbf{M}_p^{-1} is used in the above formula which suggests its direct calculation as discribed in [26].

2.6 NUMERICAL RESULTS

We present three computer experiments, the first two of which confirm the convergence of the method. The third experiment demonstrates the ability of the method to be applied to realistic coupled Stokes-Darcy flow problems.

2.6.1 Convergence tests

Here we choose the computational domain to be $\Omega = \Omega_f \cup \Omega_p$, where $\Omega_f = [0, 1] \times [0, \frac{1}{2}]$ and $\Omega_p = [0, 1] \times [\frac{1}{2}, 1]$. In the Stokes equation the stress tensor is taken to be

$$\mathbf{T}(\mathbf{u}_f, p_f) = -p_f \mathbf{I} + \mu_f \nabla \mathbf{u}_f.$$

Each coverage test uses a manufactured solution that satisfies the coupled system (1.12)–(1.15) with the Dirichlet boundary conditions on $\partial\Omega$. We consider a scalar permeability field $\mathbf{K} = K\mathbf{I}$.

In *Test 1*, the normal velocity is continuous, but the tangential velocity is discontinuous, across the interface:

$$\mathbf{u}_f = \begin{bmatrix} (2-x)(1.5-y)(y-\xi) \\ -\frac{y^3}{3} + \frac{y^2}{2}(\xi+1.5) - 1.5\xi y - 0.5 + \sin(\omega x) \end{bmatrix},$$

$$\mathbf{u}_p = \begin{bmatrix} \omega \cos(\omega x) y \\ \chi(y+0.5) + \sin(\omega x) \end{bmatrix},$$

$$p_f = -\frac{\sin(\omega x) + \chi}{2K} + \mu_f(0.5 - \xi) + \cos(\pi y), \quad p_p = -\frac{\chi}{K} \frac{(y+0.5)^2}{2} - \frac{\sin(\omega x) y}{K},$$

where

$$\mu_f = 0.1, \quad K = 1, \quad \alpha_0 = 0.5, \quad G = \frac{\sqrt{\mu_f K}}{\alpha_0}, \quad \xi = \frac{1-G}{2(1+G)}, \quad \chi = \frac{-30\xi - 17}{48}, \quad \omega = 6.$$

In *Test 2* the velocity field is chosen to be smooth across the interface:

$$\mathbf{u}_f = \mathbf{u}_p = \begin{bmatrix} \sin\left(\frac{x}{G} + \omega\right) e^{y/G} \\ -\cos\left(\frac{x}{G} + \omega\right) e^{y/G} \end{bmatrix},$$

$$p_f = \left(\frac{G}{K} - \frac{\mu_f}{G}\right) \cos\left(\frac{x}{G} + \omega\right) e^{1/(2G)} + y - 0.5, \quad p_p = \frac{G}{K} \cos\left(\frac{x}{G} + \omega\right) e^{y/G},$$

where $\omega = 1.05$ and μ_f, K, α_0, G are the same as in the *Test 1*.

The convergence test problems are solved using two different grid sequences: one consisting of unstructured grids and the other consisting of structured grids. All of the grids consist of triangles in the Stokes region and polygons (rectangles if structured) in the Darcy region. The subdomain grids Ω_f^h and Ω_p^h are chosen to match on the interface Γ_{fp} . The structured grids are obtained by first partitioning Ω into rectangles and then dividing each rectangle in Ω_f along its diagonal into two triangles.

The computed solution along with the associated numerical error for the two tests are plotted in Figure 2.1 and Figure 2.2, respectively. The convergence rates based on the unstructured grids are reported in Table 2.1 and Table 2.3, respectively. The convergence rates based on the structured grids are reported in Table 2.2 and Table 2.4, respectively. These experimental results verify the theoretically predicted convergence rate of order one. The slight discrepancy in the convergence rate for the pressure in the Stokes region when the coupled problem is solved on unstructured grids

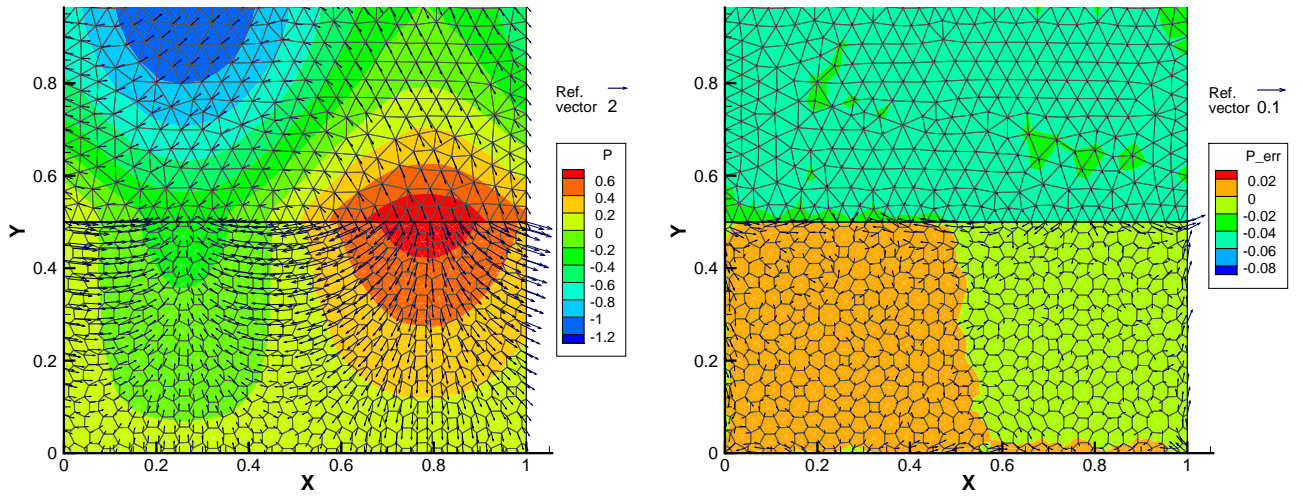


Figure 2.1: Computed solution (left) and the associated error (right) for Test 1.

may be attributed to different shape regularity constants of the unstructured triangular meshes. Table 2.1 and Table 2.3 show superconvergence of the pressure in Ω_p . Table 2.2 and Table 2.4 show superconvergence of both the velocity and the pressure in Ω_p when a rectangular mesh is used in the porous medium. It is well known that the MFD and the MFE methods for the Darcy equation alone are superconvergent on rectangular grids [15, 82]. Investigation of the similar behavior for the coupled Stokes-Darcy problem is a possible topic of future work.

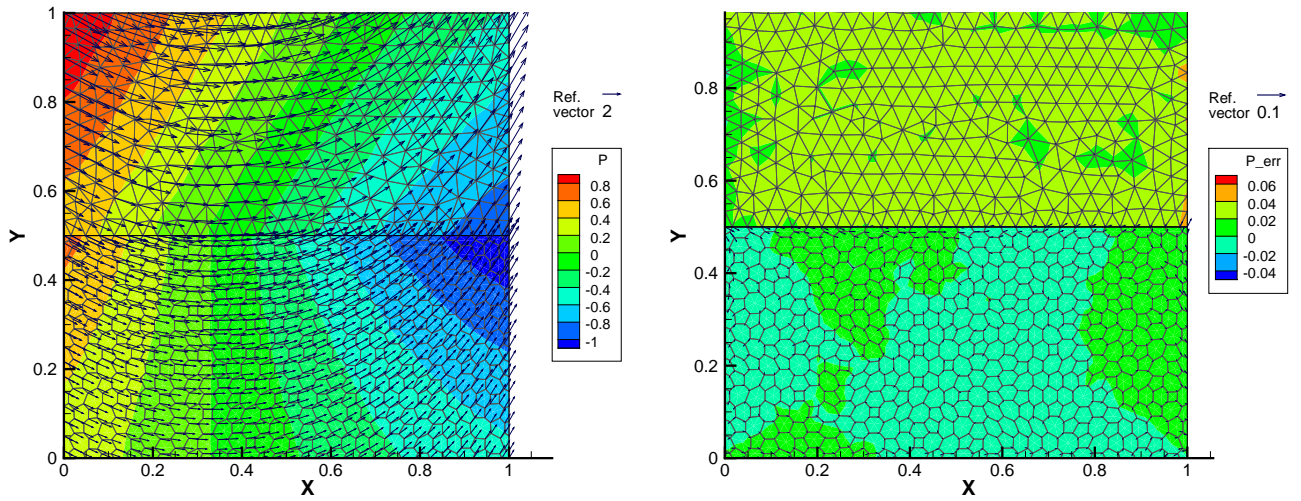


Figure 2.2: Computed solution (left) and the associated error (right) for Test 2.

2.6.2 Simulation of coupled surface water and groundwater flows

In this experiment we present a more realistic model of the coupled surface and subsurface flows. The flow domain is decomposed into two subdomains. The top half represents a lake or a slow flowing river (the Stokes region) and the bottom half represents an aquifer (the Darcy region). The surface fluid flows from left to right, with a parabolic inflow condition on the left boundary, no flow on the top, and zero stress on the right (outflow) boundary. No flow condition is imposed on the left and right boundaries of the aquifer. The pressure is specified on the bottom to simulate gravity. The permeability of the porous media is set to one. The computed pressure and velocity are shown on Figure 2.3. As expected, the pressure and the tangential velocity are discontinuous across the interface, while the normal velocity is continuous. After the surface fluid enters the aquifer, it does not move as fast in the tangential direction, but percolates toward the bottom.

Table 2.1: Numerical errors and convergence rates for Test 1 on unstructured grids.

Stokes region:					
$elements$	h_f	$\ \mathbf{u}_f - \mathbf{u}_f^h\ _{1,\Omega_f}$	$rate$	$\ p_f - p_f^h\ _{0,\Omega_f}$	$rate$
44	0.2170	6.5442e-01		1.4657e-01	
164	0.1330	3.5368e-01	1.26	8.7418e-02	1.06
652	0.0662	1.8798e-01	0.91	5.5335e-02	0.66
2468	0.0363	9.8347e-02	1.08	2.9591e-02	1.04
Darcy region:					
$elements$	h_p	$\ \mathbf{u}_p^I - \mathbf{u}_p^h\ _{X_p^h}$	$rate$	$\ p_p^I - p_p^h\ _{Q_p^h}$	$rate$
32	0.2489	1.4530e-01		2.1906e-02	
128	0.1111	5.3651e-02	1.24	5.3156e-03	1.76
512	0.0530	2.4535e-02	1.06	1.2140e-03	2.00
2048	0.0259	1.1917e-02	1.01	2.9045e-04	2.00

Table 2.2: Numerical errors and convergence rates for Test 1 on structured grids.

Stokes region:					
$elements$	h_f	$\ \mathbf{u}_f - \mathbf{u}_f^h\ _{1,\Omega_f}$	$rate$	$\ p_f - p_f^h\ _{0,\Omega_f}$	$rate$
36	0.2357	8.4380e-01		2.8244e-01	
100	0.1414	5.0922e-01	0.99	1.7391e-01	0.95
576	0.0589	2.1303e-01	1.00	7.3116e-02	0.99
2304	0.0295	1.0664e-01	1.00	3.6566e-02	1.00
Darcy region:					
$elements$	h_p	$\ \mathbf{u}_p^I - \mathbf{u}_p^h\ _{X_p^h}$	$rate$	$\ p_p^I - p_p^h\ _{Q_p^h}$	$rate$
18	0.2357	7.2054e-02		8.8162e-03	
50	0.1414	2.6670e-02	1.95	3.2124e-03	1.98
288	0.0589	4.6994e-03	1.98	5.5936e-04	2.00
1152	0.0295	1.1785e-03	2.00	1.3966e-04	2.01

Table 2.3: Numerical errors and convergence rates for Test 2 on unstructured grids.

Stokes region:					
$elements$	h_f	$\ \mathbf{u}_f - \mathbf{u}_f^h\ _{1,\Omega_f}$	$rate$	$\ p - p_f^h\ _{0,\Omega_f}$	$rate$
44	0.2170	5.4501e-01		1.5488e-01	
164	0.1330	2.9432e-01	1.26	6.5413e-02	1.76
652	0.0662	1.4152e-01	1.05	4.1093e-02	0.67
2468	0.0363	7.2480e-02	1.11	2.3073e-02	0.96
Darcy region:					
$elements$	h_p	$\ \mathbf{u}_p^I - \mathbf{u}_p^h\ _{X_p^h}$	$rate$	$\ p_p^I - p_p^h\ _{Q_p^h}$	$rate$
32	0.2489	5.9883e-02		2.1452e-03	
128	0.1111	2.0731e-02	1.32	5.2424e-04	1.75
512	0.0530	9.6960e-03	1.03	1.2789e-04	1.91
2048	0.0259	4.8383e-03	0.98	3.4431e-05	1.83

Table 2.4: Numerical errors and convergence rates for Test 2 on structured grids.

Stokes region:					
$elements$	h_f	$\ \mathbf{u}_f - \mathbf{u}_f^h\ _{1,\Omega_f}$	$rate$	$\ p_f - p_f^h\ _{0,\Omega_f}$	$rate$
36	0.2357	6.0192e-01		1.6431e-01	
100	0.1414	3.6005e-01	1.01	1.1073e-01	0.77
576	0.0589	1.4896e-01	1.01	5.1783e-02	0.87
2304	0.0295	7.4275e-02	1.01	2.7083e-02	0.94
Darcy region:					
$elements$	h_p	$\ \mathbf{u}_p^I - \mathbf{u}_p^h\ _{X_p^h}$	$rate$	$\ p_p^I - p_p^h\ _{Q_p^h}$	$rate$
18	0.2357	3.2312e-02		3.0839e-03	
50	0.1414	1.2691e-02	1.83	1.1787e-03	1.88
288	0.0589	2.4612e-03	1.87	2.0925e-04	1.97
1152	0.0295	6.5882e-04	1.91	5.2467e-05	2.00

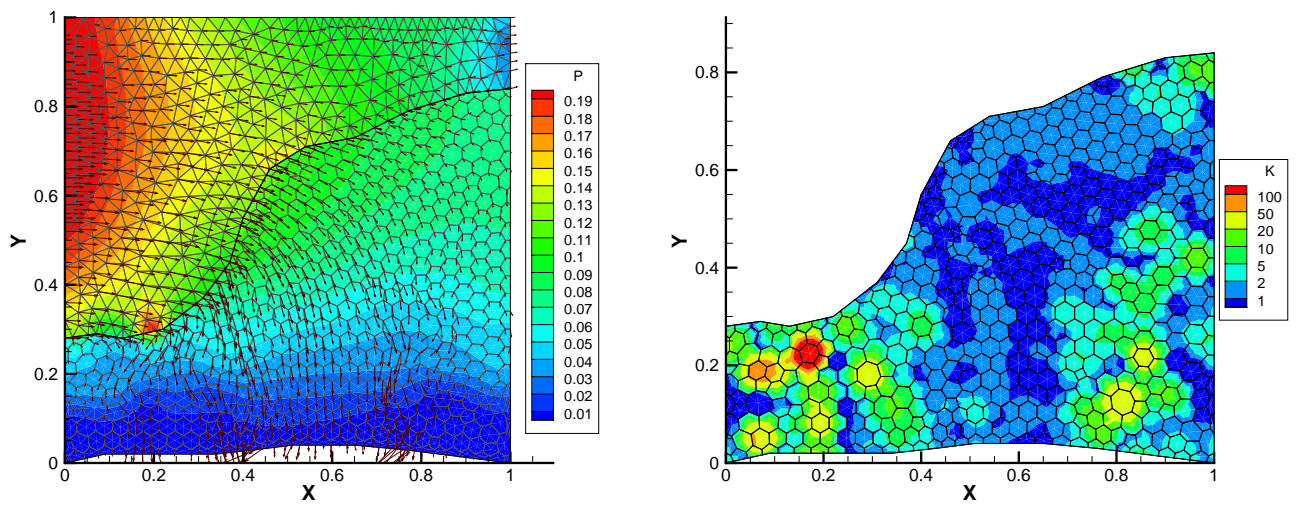


Figure 2.3: Computed solution (left), permeability field (right) in the simulation.

3.0 DOMAIN DECOMPOSITION FOR THE STOKES-DARCY FLOW

Our goal in this chapter is to develop a robust and efficient algorithm for solving the coupled Stokes-Darcy flow system in parallel. The computational domain is partitioned into several non-overlapping subdomains and the original problem is reduced to a problem involving Lagrange multipliers that are defined on the interfaces between the subdomains. We analyze the interface problem and estimate its condition number.

3.1 NOTATION, PRELIMINARIES

We recall the variational formulation of (1.12)–(1.15) derived in [65]. The velocity–pressure spaces in the fluid region Ω_f are

$$X_f = \{\mathbf{v}_f \in (H^1(\Omega_f))^d, \mathbf{v}_f = 0 \text{ on } \Gamma_f\} \text{ and } Q_f = L^2(\Omega_f),$$

equipped with the norms

$$\|\mathbf{v}_f\|_{X_f} = \left(\|\mathbf{v}_f\|_{0,\Omega_f}^2 + \|\mathbf{v}_f\|_{1,\Omega_f}^2 \right)^{1/2} \text{ and } \|q_f\|_{Q_f} = \|q_f\|_{0,\Omega_f}, \text{ respectively.}$$

In the porous medium region Ω_p we introduce the spaces

$$X_p = \{\mathbf{v}_p \in H(\text{div}; \Omega_p) : \langle \mathbf{v}_p \cdot \mathbf{n}_p, \varphi \rangle_{\partial\Omega_p} = 0, \forall \varphi \in H_{0,\Gamma_{fp}}^1(\Omega_p)\} \text{ and } Q_p = L^2(\Omega_p),$$

where

$$H(\text{div}; \Omega_p) = \{\mathbf{v}_p \in (L^2(\Omega_p))^d : \nabla \cdot \mathbf{v}_p \in L^2(\Omega_p)\}$$

and

$$H_{0,\Gamma_{fp}}^1(\Omega_p) = \{\varphi \in H^1(\Omega_p) : \varphi = 0 \text{ on } \Gamma_{fp}\}.$$

The norms on X_p and Q_p are

$$\|\mathbf{v}_p\|_{X_p} = \left(\|\mathbf{v}_p\|_{0,\Omega_p}^2 + \|\nabla \cdot \mathbf{v}_p\|_{0,\Omega_p}^2 \right)^{1/2} \quad \text{and} \quad \|q_p\|_{Q_p} = \|q_p\|_{0,\Omega_p}, \quad \text{respectively.}$$

We define $X = X_f \times X_p$ and

$$Q = \{q = (q_f, q_p) \in Q_f \times Q_p : \int_{\Omega} q \, dx = 0\}.$$

We also consider the space of continuous-normal-trace velocities

$$V = \{\mathbf{v} = (\mathbf{v}_f, \mathbf{v}_p) \in X : b_{fp}(\mathbf{v}, \mu) = 0, \forall \mu \in \Lambda_{fp}\},$$

where

$$\Lambda_{fp} = H^{1/2}(\Gamma_{fp})$$

and

$$b_{fp}(\mathbf{v}, \mu) = \langle \mathbf{v}_f \cdot \mathbf{n}_f + \mathbf{v}_p \cdot \mathbf{n}_p, \mu \rangle_{\Gamma_{fp}} : V \times \Lambda_{fp} \rightarrow \mathbb{R}.$$

A function $\lambda \in \Lambda_{fp}$ can be interpreted physically as the normal stress on the interface separating the two regions:

$$p_f - 2\mu_f \mathbf{n}_f \cdot \mathbf{De}(\mathbf{u}_f) \cdot \mathbf{n}_f = \lambda = p_p \quad \text{on } \Gamma_{fp}.$$

Remark 3.1.1 *Due to the choice of Λ_{fp} the pairing $b_{fp}(\cdot, \cdot)$ is well-defined. If $\mathbf{v}_p \in H(\text{div}; \Omega_p)$ and $\mathbf{v}_p \cdot \mathbf{n}_p = 0$ on $\partial\Omega_p \setminus \Gamma_{fp}$, then $\mathbf{v}_p \cdot \mathbf{n}_p \in H^{-1/2}(\Gamma_{fp})$, see [50].*

The weak form solution is: find $(\mathbf{u}, p) \in V \times Q$ satisfying

$$a(\mathbf{u}, \mathbf{v}) + b(\mathbf{v}, p) = \int_{\Omega_f} \mathbf{f}_f \cdot \mathbf{v}_f \, dx, \quad \mathbf{v} \in \mathbf{V}, \quad (3.1)$$

$$b(\mathbf{u}, q) = - \int_{\Omega_p} f_p q \, dx, \quad q \in Q, \quad (3.2)$$

where

$$a(\mathbf{u}, \mathbf{v}) = a_f(\mathbf{u}_f, \mathbf{v}_f) + a_p(\mathbf{u}_p, \mathbf{v}_p) : X \times X \rightarrow \mathbb{R},$$

$$b(\mathbf{v}, q) = b_f(\mathbf{v}_f, q_f) + b_p(\mathbf{v}_p, q_p) : X \times Q \rightarrow \mathbb{R},$$

$$\begin{aligned} a_f(\mathbf{u}_f, \mathbf{v}_f) &= \int_{\Omega_f} 2\mu_f \mathbf{De}(\mathbf{u}_f) : \mathbf{De}(\mathbf{v}_f) dx + \sum_{j=1}^{d-1} \int_{\Gamma_{fp}} \frac{\mu_f \alpha_0}{\sqrt{\tilde{k}_j}} (\mathbf{u}_f \cdot \boldsymbol{\tau}_j) (\mathbf{v}_f \cdot \boldsymbol{\tau}_j) ds, \\ b_f(\mathbf{v}_f, q_f) &= - \int_{\Omega_f} q_f \nabla \cdot \mathbf{v}_f dx, \\ a_p(\mathbf{u}_p, \mathbf{v}_p) &= \int_{\Omega_p} \mu_f \mathbf{K}^{-1} \mathbf{u}_p \cdot \mathbf{v}_p dx, \quad \text{and} \\ b_p(\mathbf{v}_p, q_p) &= - \int_{\Omega_p} q_p \nabla \cdot \mathbf{v}_p dx. \end{aligned}$$

We note that the definitions of the above bilinear forms differ from these in Chapter 2.

The continuity of flux (1.8) is an essential condition for the velocity space, while (1.9) and (1.11) are natural conditions. Existence and uniqueness of a solution to (3.1)–(3.2) is established in [65].

3.2 FINITE ELEMENT DISCRETIZATION

Let Ω_f , respectively Ω_p , be decomposed into N_f , respectively N_p , non-overlapping Lipschitz subdomains:

$$\Omega_f = \bigcup_{i=1}^{N_f} \Omega_i, \quad \Omega_p = \bigcup_{i=N_f+1}^N \Omega_i, \quad N = N_f + N_p.$$

For $1 \leq i \leq N$, let \mathbf{n}_i be the outward unit normal vector to subdomain Ω_i . The exterior boundary pieces of Ω_i , possibly with zero measure, are denoted by $\Gamma_{i,ext}$:

$$\Gamma_{i,ext} = \partial\Omega_i \cap \partial\Omega, \quad 1 \leq i \leq N.$$

Let Γ_{ij} be the interfaces between the subdomains, again possibly with zero measure:

$$\Gamma_{ij} = \partial\Omega_i \cap \partial\Omega_j, \quad 1 \leq i < j \leq N.$$

We also introduce the following notations to represent the union of the interfaces between the subdomains of the same type:

$$\Gamma_{ff} = \bigcup_{1 \leq i < j \leq N_f} (\partial\Omega_i \cap \partial\Omega_j),$$

$$\Gamma_{pp} = \bigcup_{N_f+1 \leq i < j \leq N} (\partial\Omega_i \cap \partial\Omega_j).$$

The union of all the interfaces is denoted by Γ_I :

$$\Gamma_I = \Gamma_{fp} \cup \Gamma_{pp} \cup \Gamma_{ff}.$$

Let Ω_i^h be a shape-regular affine finite element partition of Ω_i , $i = 1, N$. We allow for the traces of the grids on Γ_{fp} to be non-matching and assume that no point of the interface boundary $\partial\Gamma_{fp}$ belongs to the interior of a face of an element of Ω_i^h . We assume at this point that the traces of the grids on Γ_{ff} and Γ_{pp} are matching.

Remark 3.2.1 *Although the discretization presented here is based on finite elements, it is possible to use the numerical schemes from Section 2.1 and thus employ polygonal (polyhedral in 3D) meshes with less assumptions on the regularity.*

For all $1 \leq i \leq N_f$ let $X_i = X_f|_{\Omega_i}$, let $Q_i = Q_f|_{\Omega_i}$, and let $X_i^h \times Q_i^h \subset X_i \times Q_i$, be any Stokes finite element spaces satisfying the inf-sup condition

$$\inf_{0 \neq q_i^h \in Q_i^h} \sup_{0 \neq \mathbf{v}_i^h \in X_i^h} \frac{\int_{\Omega_i} q_i^h \operatorname{div} \mathbf{v}_i^h \, dx}{\|\mathbf{v}_i^h\|_{H^1(\Omega_i)} \|q_i^h\|_{L^2(\Omega_i)}} \geq \beta_f > 0 \quad (3.3)$$

and a discrete Korn inequality

$$(\operatorname{De}(\mathbf{v}_i^h), \operatorname{De}(\mathbf{v}_i^h))_{\Omega_i} \geq C_{K,i} |\mathbf{v}_i^h|_{1,\Omega_i}^2, \quad \forall \mathbf{v}_i^h \in X_i^h. \quad (3.4)$$

Examples of such spaces include the MINI elements [8], the Taylor–Hood elements [89], and the conforming Crouzeix–Raviart elements [37]. For the analysis we will need a projection operator $\Pi_{f,i}^h : (H^1(\Omega_i))^d \rightarrow X_i^h$ such that for all $\mathbf{w}_i \in (H^1(\Omega_i))^d$

$$(\nabla \cdot (\mathbf{w}_i - \Pi_{f,i}^h(\mathbf{w}_i)), q_i^h)_{\Omega_i} = 0, \quad \forall q_i^h \in Q_i^h. \quad (3.5)$$

The existence of such operator is shown in [23].

Similarly, for all $N_f + 1 \leq i \leq N$, let $X_i = X_p|_{\Omega_i}$, let $Q_i = Q_p|_{\Omega_i}$, and let $X_i^h \times Q_i^h \subset X_i \times Q_i$ be any of the well-known mixed finite element spaces on Ω_i (see [23, section III.3]), the RT spaces [79, 75], the BDM spaces [22], the BDFM spaces [21], the BDDF spaces [20], or the CD spaces [30]. All of the above spaces satisfy $\nabla \cdot X_i^h = Q_i^h$ and the inf-sup condition

$$\inf_{0 \neq q_i^h \in Q_i^h} \sup_{0 \neq \mathbf{v}_i^h \in X_i^h} \frac{\int_{\Omega_i} q_i^h \operatorname{div} \mathbf{v}_i^h \, dx}{\|\operatorname{div} \mathbf{v}_i^h\|_{L^2(\Omega_i)} \|q_i^h\|_{L^2(\Omega_i)}} \geq \beta_p > 0. \quad (3.6)$$

Moreover, there exist a projection operator $\Pi_{p,i}^h : (H^1(\Omega_i))^d \rightarrow X_i^h$ such that for all $\mathbf{w}_i \in (H^1(\Omega_i))^d$

$$(\nabla \cdot (\mathbf{w}_i - \Pi_{p,i}^h(\mathbf{w}_i)), q_i^h)_{\Omega_i} = 0, \quad \forall q_i^h \in Q_{h,i} \quad (3.7)$$

and, for any element face e ,

$$\langle (\mathbf{w}_i - \Pi_{p,i}^h(\mathbf{w}_i)) \cdot \mathbf{n}_i, \mu^h \rangle_e = 0, \quad \forall \mu^h \in X_i^h \cdot \mathbf{n}_i|_e. \quad (3.8)$$

We also note that, if $\mathbf{w}_i \in (H^\varepsilon(\Omega_i))^d \cap X_i$, $0 < \varepsilon < 1$, then $\Pi_{p,i}^h(\mathbf{q}_i)$ is well defined and [74, 4],

$$\|\Pi_{p,i}^h(\mathbf{q}_i)\|_{\Omega_i} \leq C(\|\mathbf{q}_i\|_{\varepsilon, \Omega_i} + \|\nabla \cdot \mathbf{q}_i\|_{\Omega_i}). \quad (3.9)$$

The finite element spaces on Ω are

$$\begin{aligned} X_f^h &= \{\mathbf{v}^h \in (H^1(\Omega_f))^d : \mathbf{v}^h|_{\Omega_i} \in X_i^h, 1 \leq i \leq N_f, \mathbf{v}^h = 0 \text{ on } \Gamma_f\}, \\ X_p^h &= \{\mathbf{v}^h \in (H(\operatorname{div}; \Omega_p))^d : \mathbf{v}^h|_{\Omega_i} \in X_i^h, N_f + 1 \leq i \leq N, \mathbf{v}^h \cdot \mathbf{n}_p = 0 \text{ on } \Gamma_p\}, \\ X^h &= \{\mathbf{v}^h \in (L^2(\Omega))^d : \mathbf{v}^h|_{\Omega_f} \in X_f^h, \mathbf{v}^h|_{\Omega_p} \in X_p^h\}, \\ Q_f^h &= \{q^h \in L^2(\Omega_f) : q^h|_{\Omega_i} \in Q_i^h, 1 \leq i \leq N_f\}, \\ Q_p^h &= \{q^h \in L^2(\Omega_p) : q^h|_{\Omega_i} \in Q_i^h, N_f + 1 \leq i \leq N\}, \\ Q^h &= \{q^h \in L^2_0(\Omega) : q^h|_{\Omega_f} \in Q_f^h, q^h|_{\Omega_p} \in Q_p^h\}, \\ \Lambda_{fp}^h &= X_p^h \cdot \mathbf{n}_p \text{ on } \Gamma_{fp}, \end{aligned}$$

and

$$V^h = \{\mathbf{v}^h \in X^h : b_{fp}(\mathbf{v}^h, \mu^h) = 0, \forall \mu^h \in \Lambda_{fp}^h\}.$$

Remark 3.2.2 Since a function $\mu^h \in \Lambda_{fp}^h$ can be discontinuous, $\Lambda_{fp}^h \not\subset \Lambda_{fp}$. Therefore $V^h \not\subset V$, resulting in a non-conforming and exterior approximation.

The finite element discretization of (3.1)–(3.2) is the following: find $(\mathbf{u}_h, p_h) \in V_h \times W_h$ satisfying

$$a(\mathbf{u}^h, \mathbf{v}^h) + b(\mathbf{v}^h, p^h) = \int_{\Omega_f} \mathbf{f}_f \cdot \mathbf{v}^h dx, \quad \mathbf{v}^h \in V^h, \quad (3.10)$$

$$b(\mathbf{u}^h, q^h) = - \int_{\Omega_p} f_p q^h dx, \quad q^h \in Q^h. \quad (3.11)$$

Existence, uniqueness, and the optimal error estimate (3.12) for the variational problem (3.10)–(3.11) are proved in [65].

$$\|\mathbf{u} - \mathbf{u}^h\|_X + \|p - p^h\|_Q \leq C \left(h_f^{k_f} + h_p^{k_p+1} + h_p^{l_p+1} \right), \quad (3.12)$$

where h_α , $\alpha = f, p$, characterizes the mesh used in Ω_α , k_f is the polynomial degree of the velocity space in the fluid region, k_p is the polynomial degree of the velocity space in the porous region, and l_p is the polynomial degree of the pressure space in the porous region.

Remark 3.2.3 Although the convergence theory in [65] is stated under the assumption that the grids match on the interface Γ_{fp} , it is easy to check that, with the above choice of Λ_{fp}^h , the results in [65] hold for non-matching grids as well.

3.3 NON-OVERLAPPING DOMAIN DECOMPOSITION

In this section we present a domain decomposition algorithm for the solution of the algebraic system arising from (3.10)–(3.11). The goal is to design an algorithm that

- (1) performs well on distributed parallel computers and
- (2) can utilize existing and optimized software for solving the Stokes and the Darcy equations.

Using ideas from [55], we use Lagrange multiplier spaces Λ_{fp}^h , respectively Λ_{pp}^h , to impose the continuity of the normal velocity components on Γ_{fp} , respectively Γ_{pp} . The space Λ_{pp}^h is defined analogously to Λ_{fp}^h :

$$\Lambda_{pp}^h = X_p^h \cdot \mathbf{n}_p \text{ on } \Gamma_{pp}.$$

Both spaces consist of functions, which are constant on each edge and approximate either the normal stresses or the pressures on the subdomain interfaces $\Gamma_{ij} \in \Gamma_{fp} \cup \Gamma_{pp}$. We also need the Lagrange multiplier space $\Lambda_{ff}^h = X_f^h|_{\Gamma_{ff}}$ on the interfaces between adjacent Stokes subdomains. Since the velocity has to be continuous in Ω_f , on these interfaces we need to impose d conditions (constraints). Thus, the functions $\boldsymbol{\lambda}^h \in \Lambda_{ff}^h$ are d -dimensional vectors. For example, if $d = 2$, $\boldsymbol{\lambda}^h = (\lambda_n^h, \lambda_\tau^h)$, where λ_n^h and λ_τ^h are approximations to the normal and the tangential components, respectively, of the stress vector on Γ_{ff} . It is convenient to define the space

$$\tilde{\Lambda}^h = \Lambda_{fp}^h \times \Lambda_{pp}^h \times \Lambda_{ff}^h.$$

To simplify the notations we will omit whenever it is possible the superscript h on the functions from the discrete spaces. We introduce the bilinear forms

$$b_{pp}(\mathbf{v}, \mu_n) = \sum_{\Gamma_{ij} \subset \Gamma_{pp}} \langle \mathbf{v}_i \cdot \mathbf{n}_i + \mathbf{v}_j \cdot \mathbf{n}_j, \mu_n \rangle_{\Gamma_{ij}}, \quad \forall \mathbf{v} \in X^h, \forall \mu_n \in \Lambda_{pp}^h,$$

and

$$b_{ff}(\mathbf{v}, \boldsymbol{\mu}) = \sum_{\Gamma_{ij} \subset \Gamma_{ff}} \langle \mathbf{v}_i \cdot \mathbf{n}_i + \mathbf{v}_j \cdot \mathbf{n}_j, \mu_n \rangle_{\Gamma_{ij}} + \sum_{\Gamma_{ij} \subset \Gamma_{ff}} \langle \mathbf{v}_i \cdot \boldsymbol{\tau}_i + \mathbf{v}_j \cdot \boldsymbol{\tau}_j, \mu_\tau \rangle_{\Gamma_{ij}},$$

$$\forall \mathbf{v} \in X^h, \forall \boldsymbol{\mu} = (\mu_n, \mu_\tau) \in \Lambda_{ff}^h,$$

where $\boldsymbol{\tau}_i$ is a unit vector, which is tangential to $\partial\Omega_i$ and is oriented counterclockwise relative to Ω_i . Let us also introduce a bilinear form to represent the dual pairing on all subdomain interfaces:

$$b_I(\mathbf{v}, \tilde{\boldsymbol{\lambda}}) = b_{fp}(\mathbf{v}, \lambda_{fp}) + b_{pp}(\mathbf{v}, \lambda_{pp}) + b_{ff}(\mathbf{v}, \boldsymbol{\lambda}_{ff}),$$

$$\forall \mathbf{v} \in X^h, \forall \tilde{\boldsymbol{\lambda}} = (\lambda_{fp}, \lambda_{pp}, \boldsymbol{\lambda}_{ff}) \in \tilde{\Lambda}^h.$$

For $1 \leq i \leq N_f$, let $a_i(\cdot, \cdot) = a_f(\cdot, \cdot)|_{X_i^h \times X_i^h}$ and $b_i(\cdot, \cdot) = b_f(\cdot, \cdot)|_{X_i^h \times Q_i^h}$. Similarly, for $N_f + 1 \leq i \leq N$, let $a_i(\cdot, \cdot) = a_p(\cdot, \cdot)|_{X_i^h \times X_i^h}$ and $b_i(\cdot, \cdot) = b_p(\cdot, \cdot)|_{X_i^h \times Q_i^h}$. The restrictions of the right-hand side functions in (1.12) and (1.13) on the subdomains are denoted by

$$\mathbf{f}_i = \begin{cases} \mathbf{f}_f|_{\Omega_i}, & 1 \leq i \leq N_f \\ \mathbf{0}, & N_f + 1 \leq i \leq N \end{cases}$$

and

$$f_i = \begin{cases} 0, & 1 \leq i \leq N_f \\ f_p|_{\Omega_i}, & N_f + 1 \leq i \leq N \end{cases},$$

respectively. Finally, let \mathbf{v}_i and q_i represent the restrictions of $\mathbf{v} \in X^h$ and $q \in Q^h$, respectively, on the subdomain Ω_i , $1 \leq i \leq N$.

It is easy to see that (3.10)–(3.11) is equivalent to the following discrete formulation: find $(\mathbf{u}^h, p^h, \tilde{\boldsymbol{\lambda}}) \in X^h \times Q^h \times \tilde{\Lambda}^h$ satisfying

$$\begin{aligned} \sum_{i=1}^N a_i(\mathbf{u}_i^h, \mathbf{v}_i) + \sum_{i=1}^N b_i(\mathbf{v}_i, p_i^h) + b_I(\mathbf{v}, \tilde{\boldsymbol{\lambda}}) &= \sum_{i=1}^N \int_{\Omega_i} \mathbf{f}_i \cdot \mathbf{v}_i \, dx, \quad \forall \mathbf{v} \in X^h \\ \sum_{i=1}^N b_i(\mathbf{u}_i^h, q_i) &= - \sum_{i=1}^N \int_{\Omega_i} q_i f_i \, dx, \quad \forall q \in Q^h \\ b_I(\mathbf{u}^h, \tilde{\boldsymbol{\mu}}) &= 0, \quad \forall \tilde{\boldsymbol{\mu}} \in \tilde{\Lambda}^h. \end{aligned} \tag{3.13}$$

3.3.1 Reduction to an interface problem

We show that the algebraic system (3.13) can be reduced to a symmetric and positive semi-definite interface problem. To do that we introduce families of local problems on each subdomain Ω_i .

Consider the set of Darcy subdomain problems on Ω_i , $N_f + 1 \leq i \leq N$, with specified normal stress λ_n on Γ_{ij} : find $(\mathbf{u}_i^*(\lambda_n), p_i^*(\lambda_n)) \in X_i^h \times Q_i^h$ such that

$$a_i(\mathbf{u}_i^*(\lambda_n), \mathbf{v}_i) + b_i(\mathbf{v}_i, p_i^*(\lambda_n)) = - \sum_{\Gamma_{ij} \subset \Gamma_{fp} \cup \Gamma_{pp}} \int_{\Gamma_{ij}} \lambda_n \mathbf{v}_i \cdot \mathbf{n}_i \, ds, \quad \forall \mathbf{v}_i \in X_i^h, \tag{3.14}$$

$$b_i(\mathbf{u}_i^*(\lambda_n), q_i) = 0, \quad \forall q_i \in Q_i^h, \tag{3.15}$$

and the set of Stokes subdomain problems on Ω_i , $1 \leq i \leq N_f$, with specified normal stress λ_n and tangential stress λ_τ (when applicable), $\boldsymbol{\lambda} = (\lambda_n, \lambda_\tau)$, on Γ_{ij} : find $(\mathbf{u}_i^*(\boldsymbol{\lambda}), p_i^*(\boldsymbol{\lambda})) \in X_i^h \times Q_i^h$ such that

$$\begin{aligned} a_i(\mathbf{u}_i^*(\boldsymbol{\lambda}), \mathbf{v}_i) + b_i(\mathbf{v}_i, p_i^*(\boldsymbol{\lambda})) = & - \sum_{\Gamma_{ij} \subset \Gamma_{fp} \cup \Gamma_{ff}} \int_{\Gamma_{ij}} \lambda_n \mathbf{v}_i \cdot \mathbf{n}_i ds, \\ & - \sum_{\Gamma_{ij} \subset \Gamma_{ff}} \int_{\Gamma_{ij}} \lambda_\tau \mathbf{v}_i \cdot \boldsymbol{\tau}_i ds, \quad \forall \mathbf{v}_i \in X_i^h, \end{aligned} \quad (3.16)$$

$$b_i(\mathbf{u}_i^*(\boldsymbol{\lambda}), q_i) = 0, \quad \forall q_i \in Q_i^h. \quad (3.17)$$

Consider also the set of complementary Darcy subdomain problems on Ω_i , $N_f + 1 \leq i \leq N$: find $(\bar{\mathbf{u}}_i, \bar{p}_i) \in X_i^h \times Q_i^h$ such that

$$a_i(\bar{\mathbf{u}}_i, \mathbf{v}_i) + b_i(\mathbf{v}_i, \bar{p}_i) = 0, \quad \forall \mathbf{v}_i \in X_i^h, \quad (3.18)$$

$$b_i(\bar{\mathbf{u}}_i, q_i) = - \int_{\Omega_i} f_i q_i dx, \quad \forall q_i \in Q_i^h, \quad (3.19)$$

and the set of complementary Stokes subdomain problems on Ω_i , $1 \leq i \leq N_f$: find $(\tilde{\mathbf{u}}_i, \tilde{p}_i) \in X_i^h \times Q_i^h$ such that

$$a_i(\tilde{\mathbf{u}}_i, \mathbf{v}_i) + b_i(\mathbf{v}_i, \tilde{p}_i) = \int_{\Omega_i} \mathbf{f}_i \cdot \mathbf{v}_i dx, \quad \forall \mathbf{v}_i \in X_i^h, \quad (3.20)$$

$$b_i(\tilde{\mathbf{u}}_i, q_i) = 0, \quad \forall q_i \in Q_i^h. \quad (3.21)$$

It is straightforward to see that solving (3.13) is equivalent to solving the interface problem: find $\tilde{\boldsymbol{\lambda}} = (\lambda_{fp}, \lambda_{pp}, \lambda_{ff}) \in \tilde{\Lambda}_h$ such that

$$s_h(\tilde{\boldsymbol{\lambda}}, \tilde{\boldsymbol{\mu}}) \equiv -b_I(\mathbf{u}^*(\tilde{\boldsymbol{\lambda}}), \tilde{\boldsymbol{\mu}}) = b_I(\bar{\mathbf{u}}, \tilde{\boldsymbol{\mu}}), \quad \tilde{\boldsymbol{\mu}} \in \tilde{\Lambda}^h \quad (3.22)$$

and recovering global velocity and pressure: $\mathbf{u}^h = \mathbf{u}^*(\tilde{\boldsymbol{\lambda}}) + \bar{\mathbf{u}}$, $p^h = p^*(\tilde{\boldsymbol{\lambda}}) + \bar{p}$.

Remark 3.3.1 *The subdomain problems (3.14)–(3.17) and (3.18)–(3.21) are well posed due to the local discrete inf-sup conditions (3.6) and (3.3). The boundary conditions on the interfaces in the Darcy region are of Dirichlet type:*

$$p_i = \lambda_n, \quad N_f + 1 \leq i \leq N \quad \text{on } \Gamma_{fp} \cup \Gamma_{pp}.$$

The boundary conditions on the interfaces for the local Stokes problems are of Neumann type:

$$-\mathbf{n}_i \cdot \mathbf{T} \cdot \mathbf{n}_i = \lambda_n, \quad -\mathbf{n}_i \cdot \mathbf{T} \cdot \boldsymbol{\tau}_i = \lambda_\tau, \quad 1 \leq i \leq N_f \quad \text{on } \Gamma_{ff},$$

and of Neumann-Robin type:

$$-\mathbf{n}_i \cdot \mathbf{T} \cdot \mathbf{n}_i = \lambda_n, \quad -\mathbf{n}_i \cdot \mathbf{T} \cdot \boldsymbol{\tau}_i - \frac{\mu_f}{G_i} \mathbf{u}_i \cdot \boldsymbol{\tau}_i = 0, \quad 1 \leq i \leq N_f \quad \text{on } \Gamma_{fp}.$$

In the case of two subdomains the Neumann data on the interfaces for the local Stokes problems is balanced with the Dirichlet conditions on the exterior boundary Γ_f . The situation with multiple subdomains, however, may lead to local Stokes problems that are ill-posed due to the pure Neumann boundary conditions. This can be resolved by introducing auxiliary coarse problems, which are discussed in the Section 3.3.2.

Remark 3.3.2 *Introducing the Steklov–Poincaré type operator $S_h : \tilde{\Lambda}^h \rightarrow (\tilde{\Lambda}^h)'$,*

$$(S_h \tilde{\boldsymbol{\lambda}}, \tilde{\boldsymbol{\mu}}) = s_h(\tilde{\boldsymbol{\lambda}}, \tilde{\boldsymbol{\mu}}), \quad \forall \tilde{\boldsymbol{\lambda}}, \tilde{\boldsymbol{\mu}} \in \tilde{\Lambda}^h,$$

the interface problem (3.22) can be written as: find $\tilde{\boldsymbol{\lambda}} \in \tilde{\Lambda}^h$ such that

$$S_h \tilde{\boldsymbol{\lambda}} = g_h, \tag{3.23}$$

where $g_h : \tilde{\Lambda}^h \rightarrow \mathbb{R}$, $g_h(\tilde{\boldsymbol{\mu}}) = b_I(\bar{\mathbf{u}}_h, \tilde{\boldsymbol{\mu}})$, $\forall \tilde{\boldsymbol{\mu}} \in \tilde{\Lambda}^h$.

The algebraic interpretation of the above method is as follows. Slightly abusing the notations, let u , p , and λ represent the degrees of freedom for velocity, pressure, and Lagrange multipliers, respectively. The discrete analogues of the right hand side functions in the coupled system are denoted by F_f and F_p . The linear system arising in (3.13) is of the form

$$\begin{pmatrix} A & B^T & C^T \\ B & 0 & 0 \\ C & 0 & 0 \end{pmatrix} \begin{pmatrix} u \\ p \\ \lambda \end{pmatrix} = \begin{pmatrix} F_f \\ F_p \\ 0 \end{pmatrix} \Leftrightarrow \begin{pmatrix} M & L^T \\ L & 0 \end{pmatrix} \begin{pmatrix} \xi \\ \lambda \end{pmatrix} = \begin{pmatrix} F \\ 0 \end{pmatrix},$$

where $\xi = (u, p)^T$ is the vector of subdomain unknowns and $F = (F_f, F_p)^T$. The interface problem (3.23) corresponds to the Shur complement system

$$LM^{-1}L^T\lambda = LM^{-1}F. \quad (3.24)$$

If an iterative method is employed for solving (3.24), each iteration will require evaluation the action of

$$M^{-1} = \begin{pmatrix} M_1^{-1} & & \\ & \ddots & \\ & & M_N^{-1} \end{pmatrix},$$

i.e., solving local subdomain problems.

3.3.2 Floating Stokes subdomains

The objective of domain decomposition algorithm is to solve efficiently in parallel the subdomain problems (3.14)–(3.17) and (3.18)–(3.21). It is desirable therefore to employ multiple subdomains, each assigned to an individual processor. This may lead to the occurrence of floating subdomains, i.e. Stokes subdomains that are entirely surrounded by other Stokes subdomains, whose corresponding local problems are singular due to the pure Neumann boundary conditions. In this section we present an approach to handle such floating subdomains based on the FETI methods introduced by Farhat and Roux [48]. The one-level FETI method can be viewed as a preconditioned conjugate gradient (PCG) algorithm incorporating a coarse auxiliary problem; see [90] for implementation details.

In the formulation of the FETI methods the pseudoinverses M_i^+ of the local Stokes matrices $M_i, i = 1, \dots, N_f$, are used if the corresponding subdomain problems are singular. In our approach we avoid computing M_i^+ by choosing the right hand side vector to be in the range of M_i and modifying two of the rows of M_i . To make the right hand sides in problems (3.20)–(3.21) we replace the functions $\mathbf{f}_{f,i}$ with $\mathbf{f}_{f,i} - \bar{\mathbf{f}}_{f,i}, i = 1, \dots, N_f$, where $\bar{\mathbf{f}}_{f,i} = \frac{1}{|\Omega_i|} \int_{\Omega_i} \mathbf{f}_{f,i} dx$. Let $F_{f,i}$ and $\bar{F}_{f,i}$ denote the vectors arising from the discretization of $\mathbf{f}_{f,i}$ and $\bar{\mathbf{f}}_{f,i}$, respectively. Let $F_f = (F_{f,1}, F_{f,2}, \dots, F_{f,N_f})^T$ and $\bar{F}_f = (\bar{F}_{f,1}, \bar{F}_{f,2}, \dots, \bar{F}_{f,N_f})^T$. Setting $M_f = \text{diag}\{M_1, M_2, \dots, M_f\}$ the global Stokes problem can be written as

$$M_f \xi_f + L^T \lambda = F_f, \quad (3.25)$$

subject to the constraint

$$L \xi_f = 0. \quad (3.26)$$

The solution to (3.25)–(3.26) is of the form

$$\xi_f = \bar{\xi}_f + \xi_f^*(\lambda),$$

where $\bar{\xi}_f$ solves the local Stokes problems with zero stress boundary conditions:

$$M_f \bar{\xi}_f = F_f - \bar{F}_f, \quad (3.27)$$

and $\xi_f^*(\lambda)$ satisfies the following equations

$$M_f \xi_f^*(\lambda) + L^T \lambda = \bar{F}_f, \quad (3.28)$$

$$L \xi_f^*(\lambda) = -L \bar{\xi}_f. \quad (3.29)$$

For the solvability of the above we need

$$(\bar{F}_f - L^T \lambda) \in \text{range}(M_f),$$

which is equivalent to

$$R^T (\bar{F}_f - L^T \lambda) = 0, \quad (3.30)$$

where R is a matrix whose columns form a basis for $\ker(M_f)$. Then

$$\xi_f^*(\lambda) = M_f^+(\bar{F}_f - L^T \lambda) + R\eta. \quad (3.31)$$

Here M_f^+ , as it was mentioned, does not have to be the pseudoinverse of M_f ; the notation is used purely to express the solution in terms of the known data. The components of the vector η can be understood as amplitudes measuring the contributions of the basis vectors in $\ker(M_f)$ to the solution $\xi^*(\lambda)$. Define

$$G = LR.$$

Substituting (3.31) into (3.29), and using (3.27) and the solvability condition (3.30) transforms problem (3.28)–(3.29) into

$$LM^+(\bar{F}_f - L^T \lambda) + G\eta = -L\bar{\xi}_f, \quad (3.32)$$

$$G^T \lambda = R^T \bar{F}_f. \quad (3.33)$$

We can write

$$\lambda = \lambda_0 + \lambda_1, \quad (3.34)$$

where $\lambda_0 = G(G^T G)^{-1} R^T \bar{F}_f$, and $\lambda_1 \in \ker(G^T)$. Next, we introduce the operator

$$P = I - G(G^T G)^{-1} G^T,$$

which is the orthogonal projector onto $\ker(G^T)$. Applying P^T on both sides of equation (3.32) and using the splitting (3.34) with $\lambda_1 = P\nu$ leads us to the interface problem

$$P^T L M^+ L^T P \nu = P^T L (M^+(\bar{F}_f - L^T \lambda_0) + \bar{\xi}_f), \quad (3.35)$$

which can be solved with the conjugate gradient method since the matrix $P^T L M^+ L^T P$ is symmetric and positive semi-definite. Evaluation of $M^+(\bar{F}_f - L^T \lambda_0)$ in the right hand side of (3.35) means solving once

$$M_f \xi_0 = \bar{f}_S - L^T \lambda_0,$$

which is a set of compatible Neumann problems since λ_0 satisfies (3.33). Applying at each iterative step the matrix $P^T L M^+ L^T P$ also involves solving compatible Neumann problems, because $P\nu \in \ker(G^T)$, which is equivalent to $R^T L^T P\nu = 0$ implying that

$$L^T P\nu \perp \ker(M_f)$$

for all vectors ν . Because for each local Stokes problem $\dim \ker(M_i) = 2$, $i = 1, \dots, N_f$, the matrix $G^T G$ is of size $2N_f \times 2N_f$. Computing $(G^T G)^{-1}$ requires solving coarse problems, which are local due to the block-diagonal structure of $G^T G$. The set of coarse problems resembles the balancing preconditioner introduced by Mandel [71].

3.4 ANALYSIS OF THE INTERFACE OPERATOR

Here we derive estimates for the condition number of the interface operator that depend on the mesh size and the permeability. To simplify the notations we will assume that all the subdomains have mesh sizes of the same order. We will omit the subscript h in most places throughout this section.

The interface operator can be expressed in terms of the subdomain bilinear forms $a_i(\cdot, \cdot)$. Coercivity and continuity of these forms are essential to our analysis. Due to technical difficulties in proving coercivity of $a_i(\cdot, \cdot)$ for the Stokes region in the full H^1 norm we will assume that $\partial\Omega_i \cap (\Gamma_f \cup \Gamma_{fp}) \neq \emptyset$, for $1 \leq i \leq N_f$. To estimate the bilinear forms in the Darcy region we will assume that there exist two constants $K_{min} > 0$ and $K_{max} > 0$ such that

$$\forall \mathbf{x} \in \Omega_p, \forall \xi \in \mathbb{R}^d, \quad K_{min} |\xi|^2 \leq (\mathbf{K}(\mathbf{x})\xi, \xi) \leq K_{max} |\xi|^2. \quad (3.36)$$

Lemma 3.4.1 *Under the above assumptions there exist positive constants C_1, C_2, C_3 and C_4 , independent of h such that*

$$C_1 \|\mathbf{v}_i\|_{1, \Omega_i}^2 \leq a_i(\mathbf{v}_i, \mathbf{v}_i) \leq C_2 \|\mathbf{v}_i\|_{1, \Omega_i}^2, \quad \forall \mathbf{v} \in X_i^h, \quad 1 \leq i \leq N_f, \quad (3.37)$$

$$C_3 \|\mathbf{v}_i\|_{0, \Omega_i}^2 \leq a_i(\mathbf{v}_i, \mathbf{v}_i) \leq C_4 \|\mathbf{v}_i\|_{0, \Omega_i}^2, \quad \forall \mathbf{v} \in X_i^h, \quad N_f + 1 \leq i \leq N. \quad (3.38)$$

Proof. The upper bound of $a_i(\cdot, \cdot)$ in the Stokes region is straightforward. If $\Omega_i \cap \Gamma_{fp} \neq \emptyset$,

$$\begin{aligned} a_i(\mathbf{v}_i, \mathbf{v}_i) &\leq 2\mu_f |\mathbf{De}(\mathbf{v}_i)|_{0, \Omega_i}^2 + \frac{\mu_f \alpha_0}{\sqrt{K_{min}}} \sum_{j=1}^{d-1} \|\mathbf{v}_i \cdot \boldsymbol{\tau}_j\|_{0, \partial\Omega_i \cap \Gamma_{fp}}^2 \\ &\leq 2\mu_f |\mathbf{v}_i|_{1, \Omega_i}^2 + \frac{(d-1)\mu_f \alpha_0}{\sqrt{K_{min}}} \|\mathbf{v}_i\|_{0, \partial\Omega_i}^2 \\ &\leq 2\mu_f \|\mathbf{v}_i\|_{1, \Omega_i}^2 + \frac{C_{tr,i}(d-1)\mu_f \alpha_0}{\sqrt{K_{min}}} \|\mathbf{v}_i\|_{1, \Omega_i}^2, \end{aligned}$$

where $C_{tr,i}$ arises from applying the trace theorem for H^1 functions on Ω_i . Then we set

$$C_2 = \mu_f \max \left\{ 2, \frac{C_{tr,i}(d-1)\alpha_0}{\sqrt{K_{min}}} \right\}.$$

If $\Omega_i \cap \Gamma_{fp} = \emptyset$, $a_i(\cdot, \cdot)$ is bounded above by

$$C_2 = 2\mu_f.$$

To obtain the lower bound in the Stokes region we use the Korn's inequality (3.4). First, we consider the case, in which $\partial\Omega_i \cap \Gamma_{fp} \neq \emptyset$. Then

$$a_i(\mathbf{v}_i, \mathbf{v}_i) \geq \mu_f \min \left\{ 2C_{K,i}, \frac{\alpha_0}{\sqrt{K_{max}}} \right\} \left(|\mathbf{v}_i|_{1, \Omega_i}^2 + \Phi(\mathbf{v}_i)^2 \right), \quad (3.39)$$

where the functional $\Phi(\cdot) : (H^1(\Omega_i))^d \rightarrow \mathbb{R}$, $1 \leq i \leq N_f$ is defined by

$$\Phi(\mathbf{v}_i) = \left(\sum_{j=1}^{d-1} \int_{\partial\Omega_i \cup \Gamma_{fp}} (\mathbf{v}_i \cdot \boldsymbol{\tau}_j)^2 ds \right)^{1/2}.$$

Clearly, $\Phi(\cdot)$ defines a seminorm on $(H^1(\Omega_i))^d$. Moreover, it satisfies the following properties:

1. $0 \leq \Phi(\mathbf{v}_i) \leq C \|\mathbf{v}_i\|_{1, \Omega_i}$, $\forall \mathbf{v}_i \in (H^1(\Omega_i))^d$.
2. If $|\mathbf{v}_i|_{1, \Omega_i} = 0$, and $\Phi(\mathbf{v}_i) = 0$, then $\mathbf{v}_i = 0$.

These properties allow us to use Theorem 6.3.14 from [9] to conclude that $\left(|\mathbf{v}_i|_{1,\Omega_i}^2 + \Phi(\mathbf{v}_i)^2\right)^{1/2}$ defines a norm on $(H^1(\Omega_i))^d$, which is equivalent to $\|\mathbf{v}_i\|_{1,\Omega_i}$: there exists a positive constant c_i , depending only on Ω_i such that

$$\left(|\mathbf{v}_i|_{1,\Omega_i}^2 + \Phi(\mathbf{v}_i)^2\right)^{1/2} \geq c_i \|\mathbf{v}_i\|_{1,\Omega_i}, \quad \mathbf{v}_i \in (H^1(\Omega_i))^d. \quad (3.40)$$

Combining (3.39) and (3.40) proves that $a_i(\cdot, \cdot)$ is coercive in $(H^1(\Omega_i))^d$ with coercivity constant

$$C_1 = c_i^2 \mu_f \min \left\{ 2C_{K,i}, \frac{\alpha_0}{\sqrt{K_{max}}} \right\}.$$

If $\partial\Omega_i \cap \Gamma_{fp} = \emptyset$, then according to the assumption we made regarding the Stokes subdomains it follows that there is a boundary piece $\Gamma_{i,0} = \Omega_i \cap \Gamma_f \neq \emptyset$ with homogeneous Dirichlet data. Therefore the Poincaré-Friedrich's inequality (see e.g. [17]) applies

$$\|\mathbf{v}_i\|_{0,\Omega_i} \leq C_{PF,i} |\mathbf{v}_i|_{1,\Omega_i}, \quad \forall \mathbf{v}_i \in (H_{\Gamma_{i,0}}^1(\Omega_i))^d. \quad (3.41)$$

Then, the coercivity of $a_i(\cdot, \cdot)$ follows from (3.4) and (3.41) with a constant

$$C_1 = \frac{2\mu_f C_{K,i}}{1 + C_{PF,i}^2}.$$

The proof of (3.37) is complete.

The assumption (3.36) directly implies (3.38) with

$$C_3 = \frac{\mu_f}{K_{max}}, \quad \text{and } C_4 = \frac{\mu_f}{K_{min}}.$$

□

Lemma 3.4.2 *The bilinear form $s(\cdot, \cdot)$ is symmetric and positive semidefnite on $\tilde{\Lambda}^h \times \tilde{\Lambda}^h$. Moreover, $\text{Ker}(S_h) = \mathbb{R}$.*

Proof. Let $s_{ij}(\cdot, \cdot)$ be the restriction of $s(\cdot, \cdot)$ on the interface Γ_{ij} . The definition (3.22) of $s(\cdot, \cdot)$ gives

$$s_{ij}(\tilde{\boldsymbol{\lambda}}, \tilde{\boldsymbol{\mu}}) = s_i(\tilde{\boldsymbol{\lambda}}, \tilde{\boldsymbol{\mu}}) + s_j(\tilde{\boldsymbol{\lambda}}, \tilde{\boldsymbol{\mu}}),$$

where

$$s_i(\tilde{\boldsymbol{\lambda}}, \tilde{\boldsymbol{\mu}}) = \begin{cases} -\langle \mathbf{v}_i \cdot \mathbf{n}_i, \mu_n \rangle_{\Gamma_{ij}}, & \text{if } \Gamma_{ij} \subset \Gamma_{fp} \cup \Gamma_{pp} \\ -\langle \mathbf{v}_i \cdot \mathbf{n}_i, \mu_n \rangle_{\Gamma_{ij}} - \langle \mathbf{v}_i \cdot \boldsymbol{\tau}_i, \mu_\tau \rangle_{\Gamma_{ij}}, & \text{if } \Gamma_{ij} \subset \Gamma_{ff} \end{cases}.$$

Taking $\mathbf{v}_i = \mathbf{u}_i^*(\tilde{\boldsymbol{\mu}})$ in (3.14) and (3.16),

$$s_i(\tilde{\boldsymbol{\mu}}, \tilde{\boldsymbol{\lambda}}) = a_i(\mathbf{u}_i^*(\tilde{\boldsymbol{\lambda}}), \mathbf{u}_i^*(\tilde{\boldsymbol{\mu}})),$$

which implies the symmetry of $s(\cdot, \cdot)$. Moreover,

$$s_i(\tilde{\boldsymbol{\lambda}}, \tilde{\boldsymbol{\lambda}}) = a_i(\mathbf{u}_i^*(\tilde{\boldsymbol{\lambda}}), \mathbf{u}_i^*(\tilde{\boldsymbol{\lambda}})) \geq 0. \quad (3.42)$$

Let $s(\tilde{\boldsymbol{\lambda}}, \tilde{\boldsymbol{\lambda}}) = 0$. By Lemma 3.4.1 $\mathbf{u}_i^*(\tilde{\boldsymbol{\lambda}}) = 0$, which implies

$$\begin{aligned} -(\nabla \cdot \mathbf{v}_i, p_i^*(\lambda_n))_{\Omega_i} + \langle \lambda_n, \mathbf{v}_i \cdot \mathbf{n}_i \rangle_{\partial\Omega_i \cap (\Gamma_{fp} \cup \Gamma_{pp})} &= 0, \\ \mathbf{v}_i \in X_i^h, N_f + 1 \leq i \leq N, \end{aligned} \quad (3.43)$$

and

$$\begin{aligned} -(\nabla \cdot \mathbf{v}_i, p_i^*(\boldsymbol{\lambda}))_{\Omega_i} + \langle \lambda_n, \mathbf{v}_i \cdot \mathbf{n}_i \rangle_{\partial\Omega_i \cap (\Gamma_{fp} \cup \Gamma_{ff})} + \langle \lambda_\tau, \mathbf{v}_i \cdot \boldsymbol{\tau}_i \rangle_{\partial\Omega_i \cap \Gamma_{ff}} &= 0, \\ \mathbf{v}_i \in X_i^h, 1 \leq i \leq N_f. \end{aligned} \quad (3.44)$$

Let us suppose $\Omega_i \subset \Omega_p$ and let us use λ_n to represent the normal stress on the interfaces $\gamma_i = \partial\Omega_i \cap (\Gamma_{fp} \cup \Gamma_{pp})$. Consider the auxiliary problem

$$\nabla \cdot \boldsymbol{\psi} = 0 \text{ in } \Omega_i, \quad \boldsymbol{\psi} \cdot \mathbf{n}_i = \lambda_n - \bar{\lambda}_n \text{ on } \gamma_i, \quad \boldsymbol{\psi} \cdot \mathbf{n}_i = 0 \text{ on } \partial\Omega_i \setminus \gamma_i,$$

where

$$\bar{\lambda}_n = \frac{1}{|\gamma_i|} \int_{\gamma_i} \lambda_n ds.$$

The above problem is well posed (solutions exist), since $\int (\lambda_n - \bar{\lambda}_n) ds = 0$. Also note that the piecewise polynomial Neumann data are in $H^{1/2-\varepsilon}(\partial\Omega_i)$, so $\boldsymbol{\psi} \in (H^{1-\varepsilon}(\Omega_i))^d$; therefore $\Pi_{p,i}^h(\boldsymbol{\psi})$ is well defined. Taking $\mathbf{v}_i = \Pi_{p,i}^h(\boldsymbol{\psi})$ in (3.43) and using (3.7) and (3.8),

$$\begin{aligned} 0 &= -(\nabla \cdot \Pi_{p,i}^h(\boldsymbol{\psi}), p_i^*(\lambda_n))_{\Omega_i} + \langle \lambda_n, \Pi_{p,i}^h(\boldsymbol{\psi}) \cdot \mathbf{n}_i \rangle_{\gamma_i} \\ &= -(\nabla \cdot \boldsymbol{\psi}, p_i^*(\lambda_n))_{\Omega_i} + \langle \lambda_n, \boldsymbol{\psi} \cdot \mathbf{n}_i \rangle_{\gamma_i} = \langle \lambda_n, \lambda_n - \bar{\lambda}_n \rangle_{\gamma_i} = \|\lambda_n - \bar{\lambda}_n\|_{\gamma_i}^2, \end{aligned}$$

implying $\lambda_n = \bar{\lambda}_n$ on γ_i . If $\Omega_i \subset \Omega_f$ and $\gamma_i = \partial\Omega_i \cap \Gamma_{ff}$ we take \mathbf{v}_i to be the finite element solution to the local Stokes problem in Ω_i with the boundary conditions $\mathbf{v}_i = \boldsymbol{\lambda} - \bar{\boldsymbol{\lambda}}$ on γ_i , and $\mathbf{v}_i = \mathbf{0}$ on $\partial\Omega_i \setminus \gamma_i$, where

$$\bar{\boldsymbol{\lambda}} = \frac{1}{|\gamma_i|} \int_{\gamma_i} \boldsymbol{\lambda} ds.$$

With this choice of \mathbf{v}_i , (3.44) implies that $\boldsymbol{\lambda} = \bar{\boldsymbol{\lambda}}$ on γ_i . □

As a result of Lemma 3.4.2, the conjugate gradient (CG) method can be applied for solving (3.23). We now continue with estimating the condition number of S_h . Consider the representation of $s(\cdot, \cdot)$ in terms of subdomain contributions:

$$s(\tilde{\boldsymbol{\lambda}}, \tilde{\boldsymbol{\mu}}) = \sum_{\Gamma_{ij} \subset \Gamma_I} s_{ij}(\tilde{\boldsymbol{\lambda}}, \tilde{\boldsymbol{\mu}}) = \sum_{\Gamma_{ij} \subset \Gamma_I} (s_i(\tilde{\boldsymbol{\lambda}}, \tilde{\boldsymbol{\mu}}) + s_j(\tilde{\boldsymbol{\lambda}}, \tilde{\boldsymbol{\mu}})), \quad (3.45)$$

where the terms $s_i(\cdot, \cdot)$, $1 \leq i \leq N$, have the same meaning as in Lemma 3.4.2. In general, there are three type of interfaces to consider: Stokes-Darcy, Darcy-Darcy, and Stokes-Stokes. The next lemma provides estimates for the restriction of $s(\cdot, \cdot)$ on an interface between Stokes and Darcy subdomains.

Lemma 3.4.3 *Let $\Omega_i \subset \Omega_f$, $\Omega_j \subset \Omega_p$, and let $\Lambda_{ij} = \Lambda_{fp}^h|_{\Gamma_{ij}}$. There exist positive constants $C_{f,2}^*$, $C_{p,1}$, and $C_{p,2}$ such that for all $\lambda_n \in \Lambda_{ij}^0 = \{\mu_n \in \Lambda_{ij} : \int_{\Gamma_{ij}} \mu_n ds = 0\}$,*

$$s_i(\lambda_n, \lambda_n) \leq C_{f,2}^* \|\lambda_n\|_{\Gamma_{ij}}^2 \quad (3.46)$$

$$C_{p,1} \frac{K_{min}^2}{K_{max}} \|\lambda_n\|_{\Gamma_{ij}}^2 \leq s_j(\lambda_n, \lambda_n) \leq C_{p,2} K_{max} h^{-1} \|\lambda_n\|_{\Gamma_{ij}}^2. \quad (3.47)$$

Proof: To prove the bound for $s_i(\cdot, \cdot)$ we write

$$\begin{aligned} s_i(\lambda_n, \lambda_n) &= -\langle \mathbf{u}_i^*(\lambda_n) \cdot \mathbf{n}_i, \lambda_n \rangle_{\Gamma_{ij}} \leq \|\mathbf{u}_i^*(\lambda_n) \cdot \mathbf{n}_i\|_{\Gamma_{ij}} \|\lambda_n\|_{\Gamma_{ij}} \\ &\leq \|\mathbf{u}_i^*(\lambda_n)\|_{\partial\Omega_i} \|\lambda_n\|_{\Gamma_{ij}} \\ &\leq C_{tr,i} \|\mathbf{u}_i^*(\lambda_n)\|_{1,\Omega_i} \|\lambda_n\|_{\Gamma_{ij}}, \end{aligned}$$

where we have used the trace theorem for functions in $(H^1(\Omega_i))^d$. Combining the above bound with the left inequality in (3.37) and (3.42) yields (3.46).

Let us consider the Darcy subdomain Ω_j . We have

$$\begin{aligned} s_j(\lambda_n, \lambda_n) &= -\langle \mathbf{u}_j^*(\lambda_n) \cdot \mathbf{n}_j, \lambda_n \rangle_{\Gamma_{ij}} \leq \|\mathbf{u}_j^*(\lambda_n) \cdot \mathbf{n}_j\|_{\Gamma_{ij}} \|\lambda_n\|_{\Gamma_{ij}} \\ &\leq Ch^{-1/2} \|\mathbf{u}_j^*(\lambda_n)\|_{\Omega_j} \|\lambda_n\|_{\Gamma_{ij}}, \end{aligned}$$

where we have used Lemma 4.1 in [4]. The above inequality, combined with (3.38) and (3.42), implies that

$$s_j(\lambda_n, \lambda_n) \leq C_{p,2} K_{max} h^{-1} \|\lambda_n\|_{\Gamma_{ij}}^2.$$

To prove the lower bound, let $\boldsymbol{\psi}$ solve

$$\nabla \cdot \boldsymbol{\psi} = 0 \text{ in } \Omega_j, \quad \boldsymbol{\psi} \cdot \mathbf{n}_j = \lambda_n \text{ on } \Gamma_{ij}, \quad \boldsymbol{\psi} \cdot \mathbf{n}_j = 0 \text{ on } \partial\Omega_j \setminus \Gamma_{ij}.$$

Such vectors exist, since $\lambda_n \in \Lambda_{ij}^0$. By elliptic regularity [56, 66],

$$\|\boldsymbol{\psi}\|_{1/2,\Omega_j} \leq C \|\lambda_n\|_{\Gamma_{ij}}. \quad (3.48)$$

Taking $\mathbf{v}_j = \Pi_{p,j}^h(\boldsymbol{\psi})$ in (3.14),

$$\begin{aligned} \|\lambda_n\|_{\Gamma_{ij}}^2 &= \langle \lambda_n, \boldsymbol{\psi} \cdot \mathbf{n}_j \rangle_{\Gamma_{ij}} = \langle \lambda_n, \Pi_{p,j}^h(\boldsymbol{\psi}) \cdot \mathbf{n}_j \rangle_{\Gamma_{ij}} \\ &= -a_j(\mathbf{u}_j^*(\lambda_n), \Pi_{p,j}^h(\boldsymbol{\psi})) \leq CK_{min}^{-1} \|\mathbf{u}_j^*(\lambda_n)\|_{\Omega_j} \|\boldsymbol{\psi}\|_{1/2,\Omega_j}. \end{aligned}$$

where we used (3.8), Cauchy-Schwarz inequality and (3.9) and (3.7). Therefore, with (3.48), the left inequality in (3.38) and (3.42),

$$C_{p,1} \frac{K_{min}^2}{K_{max}} \|\lambda_n\|_{\Gamma_{ij}}^2 \leq s_j(\lambda_n, \lambda_n),$$

completing the proof of (3.47). □

Remark 3.4.1 In the above lemma there is no need in bounding from below the Stokes piece $s_i(\lambda_n, \lambda_n)$ because the lower bound for the Darcy piece $s_j(\lambda_n, \lambda_n)$ is sufficient to control the condition number on the Stokes-Darcy interface. We note that according to Lemma 3.4.1 for large enough permeability values the upper bound for the Stokes piece is $C_{f,2}^* = O(K_{max}^{1/2})$.

To estimate the condition number on the Darcy-Darcy interface the inequalities (3.47) are still valid. Next, we consider an interface between two Stokes subdomains.

Lemma 3.4.4 Let $\Omega_i \subset \Omega_f$, $\Omega_j \subset \Omega_f$, and let $\Lambda_{ij} = \Lambda_{ff}^h|_{\Gamma_{ij}}$. There exist positive constants $C_{f,1}$ and $C_{f,2}$ such that for all $\boldsymbol{\lambda} \in \Lambda_{ij}^0 = \{\boldsymbol{\mu} \in \Lambda_{ij} : \int_{\Gamma_{ij}} \boldsymbol{\mu} ds = \mathbf{0}\}$,

$$C_{f,1}h\|\boldsymbol{\lambda}\|_{\Gamma_{ij}}^2 \leq s_i(\boldsymbol{\lambda}, \boldsymbol{\lambda}) \leq C_{f,2}\|\boldsymbol{\lambda}\|_{\Gamma_{ij}}^2 \quad (3.49)$$

Proof. Let $\mathbf{g} \in (H^{1/2}(\Gamma_{ij}))^d$ with $\int_{\Gamma_{ij}} \mathbf{g} ds = \mathbf{0}$, and let $\boldsymbol{\psi}$ solve

$$\nabla \cdot \boldsymbol{\psi} = 0 \text{ in } \Omega_i, \quad \boldsymbol{\psi} = \mathbf{g} \text{ on } \Gamma_{ij}, \quad \boldsymbol{\psi} = 0 \text{ on } \partial\Omega_i \setminus \Gamma_{ij}.$$

The above problem is well posed because of the choice of \mathbf{g} . We need an operator

$$\mathcal{P}_f^h : (H^{1/2}(\Gamma_{ij}))^d \rightarrow \Lambda_{ij}$$

satisfying for all $\boldsymbol{\phi} \in (H^{1/2}(\Gamma_{ij}))^d$

$$\langle \mathcal{P}_f^h(\boldsymbol{\phi}) - \boldsymbol{\phi}, \boldsymbol{\mu} \rangle_{\Gamma_{ij}} = 0, \quad \forall \boldsymbol{\mu} \in \Lambda_{ij}^0, \quad (3.50)$$

$$\|\mathcal{P}_f^h(\boldsymbol{\phi})\|_{1/2, \Gamma_{ij}} \leq C\|\boldsymbol{\phi}\|_{1/2, \Gamma_{ij}}. \quad (3.51)$$

Since we consider matching grids on Γ_{ff} , the operator \mathcal{P}_f^h is exactly the L^2 projection on Λ_{ij} and (3.51) follows from theorem 3.1.4 in [31]. We can write

$$\begin{aligned} \langle \boldsymbol{\lambda}, \mathbf{g} \rangle_{\Gamma_{ij}} &= \langle \boldsymbol{\lambda}, \boldsymbol{\psi} \rangle_{\Gamma_{ij}} = \langle \boldsymbol{\lambda}, \mathcal{P}_f^h(\boldsymbol{\psi}) \rangle_{\Gamma_{ij}} = -a_i(\mathbf{u}_i^*(\boldsymbol{\lambda}), \mathbf{u}_i^*(\mathcal{P}_f^h(\boldsymbol{\psi}))) \\ &\leq C\|\mathbf{u}_i^*(\boldsymbol{\lambda})\|_{1, \Omega_i} \|\mathbf{u}_i^*(\mathcal{P}_f^h(\boldsymbol{\psi}))\|_{1, \Omega_i} \leq C\|\mathbf{u}_i^*(\boldsymbol{\lambda})\|_{1, \Omega_i} \|\mathcal{P}_f^h(\boldsymbol{\psi})\|_{1/2, \Gamma_{ij}} \\ &\leq C\|\mathbf{u}_i^*(\boldsymbol{\lambda})\|_{1, \Omega_i} \|\boldsymbol{\psi}\|_{1/2, \Gamma_{ij}} = C\|\mathbf{u}_i^*(\boldsymbol{\lambda})\|_{1, \Omega_i} \|\mathbf{g}\|_{1/2, \Gamma_{ij}}, \end{aligned} \quad (3.52)$$

where we used (3.16), the continuity of $a_i(\cdot, \cdot)$, trace inequality, and (3.51). From (3.52) and the definition of dual norm we find

$$\|\boldsymbol{\lambda}\|_{-1/2, \Gamma_{ij}} \leq \|\mathbf{u}_i^*(\boldsymbol{\lambda})\|_{1, \Omega_i}. \quad (3.53)$$

With (3.53) and the inverse inequality

$$\|\boldsymbol{\lambda}\|_{L^2(\Gamma_{ij})} \leq Ch^{-1/2} \|\boldsymbol{\lambda}\|_{H^{-1/2}(\Gamma_{ij})},$$

we obtain

$$\|\boldsymbol{\lambda}\|_{\Gamma_{ij}} \leq Ch^{-1/2} \|\mathbf{u}_i^*(\boldsymbol{\lambda})\|_{1,\Omega_i}.$$

The last inequality combined with (3.37) and (3.42) yields the lower bound for $s_i(\boldsymbol{\lambda}, \boldsymbol{\lambda})$:

$$C_{f,1}h \|\boldsymbol{\lambda}\|_{\Gamma_{ij}}^2 \leq s_i(\boldsymbol{\lambda}, \boldsymbol{\lambda}).$$

To show the upper bound in (3.49) we write

$$s_i(\boldsymbol{\lambda}, \boldsymbol{\lambda}) = -\langle \mathbf{u}_i^*(\boldsymbol{\lambda}), \boldsymbol{\lambda} \rangle_{\Gamma_{ij}} \leq \|\mathbf{u}_i^*(\boldsymbol{\lambda})\|_{1/2,\Gamma_{ij}} \|\boldsymbol{\lambda}\|_{-1/2,\Gamma_{ij}} \leq C \|\mathbf{u}_i^*(\boldsymbol{\lambda})\|_{1,\Omega_i} \|\boldsymbol{\lambda}\|_{\Gamma_{ij}},$$

which combined with (3.37) and (3.42) implies

$$s_i(\boldsymbol{\lambda}, \boldsymbol{\lambda}) \leq C_{f,2} \|\boldsymbol{\lambda}\|_{\Gamma_{ij}}^2.$$

□

Theorem 3.4.1 *Assuming that h is smaller compared to the lengths characterizing the permeability in the porous medium, the condition number for the algebraic system associated with the coupled Stokes-Darcy flow problem is asymptotically*

$$\text{cond}(S_h) = O(h^{-1}), \quad \text{if there is a single Stokes subdomain}, \quad (3.54)$$

$$\text{cond}(S_h) = O(h^{-2}), \quad \text{if there are several Stokes subdomains}. \quad (3.55)$$

Proof. From Lemma 3.4.3 and Lemma 3.4.4 we conclude that there exist positive constants C_5, C_6, C_7, C_8, C_9 and C_{10} such that

$$C_5 h \|\boldsymbol{\lambda}\|_{\Gamma_{ff}}^2 + C_6 \frac{K_{min}^2}{K_{max}} \|\lambda_n\|_{\Gamma_{fp} \cup \Gamma_{pp}}^2 \leq s(\tilde{\boldsymbol{\lambda}}, \tilde{\boldsymbol{\lambda}}) \leq C_7 \|\boldsymbol{\lambda}\|_{\Gamma_{ff}}^2 + \max\{C_8, C_9 K_{max}^{1/2}\} \|\lambda_n\|_{\Gamma_{fp}}^2 + C_{10} \frac{K_{max}}{h} \|\lambda_n\|_{\Gamma_{fp} \cup \Gamma_{pp}}^2, \quad \forall \tilde{\boldsymbol{\lambda}} \in \tilde{\Lambda}^h.$$

If there are no Stokes-Stokes interfaces, the bounds on the Rayleigh quotient

$$C_6 \frac{K_{min}^2}{K_{max}} \leq \frac{s(\tilde{\boldsymbol{\lambda}}, \tilde{\boldsymbol{\lambda}})}{\|\tilde{\boldsymbol{\lambda}}\|_{\Gamma_I}^2} \leq \max \left\{ C_8, C_9 K_{max}^{1/2}, C_{10} \frac{K_{max}}{h} \right\}, \quad \forall \tilde{\boldsymbol{\lambda}} \in \tilde{\Lambda}^h \quad (3.56)$$

imply (3.54).

In the presence of Stokes-Stokes interfaces we have

$$\min \left\{ C_5 h, C_6 \frac{K_{min}^2}{K_{max}} \right\} \leq \frac{s(\tilde{\boldsymbol{\lambda}}, \tilde{\boldsymbol{\lambda}})}{\|\tilde{\boldsymbol{\lambda}}\|_{\Gamma_I}^2} \leq \max \left\{ C_7, C_8, C_9 K_{max}^{1/2}, C_{10} \frac{K_{max}}{h} \right\}, \quad \forall \tilde{\boldsymbol{\lambda}} \in \tilde{\Lambda}^h, \quad (3.57)$$

which proves (3.55). □

Remark 3.4.2 *It is easy to see that the analysis presented here is also valid if there are floating Stokes subdomains and the approach from Section 3.3.2 needs to be used to solve the associated pure Neumann problems.*

3.5 NUMERICAL RESULTS

We carried out several numerical experiments to study the behavior of the method. The computational domain was taken to be $\Omega = \Omega_f \cup \Omega_p$, where $\Omega_f = [0, 1] \times [\frac{1}{2}, 1]$ and $\Omega_p = [0, 1] \times [0, \frac{1}{2}]$. To discretize the system of equations we used the Taylor-Hood triangular finite elements in Ω_f and the lowest order Raviart Thomas (RT0) rectangular finite elements in Ω_p . The grid for the discretization in Ω_f is obtained by first partitioning the domain into rectangles and then dividing each rectangle along its diagonal into two triangles. The grids in Ω_f and Ω_p match on the interface Γ_{12} .

First, using two subdomains we solved the coupled Stokes-Darcy flow problem with the analytical solution in *Test 1* from Section 2.6.1 on different meshes and then we computed the associated error to verify convergence of the discretization scheme. The computed velocity field in *Test 1* is shown in Figure 3.1. Note that the flow domain decomposition scheme correctly imposes continuity of the normal velocity, but allows for discontinuous tangential velocity across the interface. The results reported in Table 3.1 confirm the expected convergence rates. In the Stokes subdomain the polynomial degrees for the Taylor-Hood elements give an approximation of second order for the velocity in the H^1 -norm and the pressure in the L^2 -norm. Convergence of second order is observed in the Darcy subdomain for the RT0 elements in the L^2 -norm for both the variables due to the superconvergence of the mixed finite elements on rectangular grids (see Section 2.6.1).

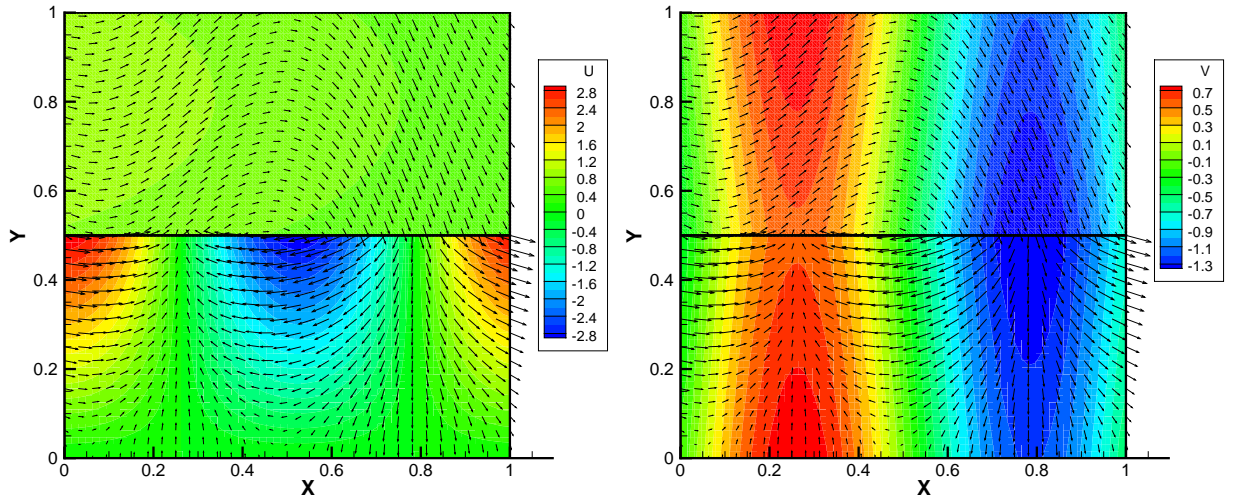


Figure 3.1: Computed velocity field in Test 1: horizontal velocity (left); vertical velocity (right).

In the other tests, for different permeabilities we varied either the mesh size or the number of subdomains to examine the convergence of the iterative method.

In Table 3.3 and Table 3.4 we see that when the coupled problem is solved on two subdomains and h is sufficiently smaller than K , the minimal eigenvalue of the interface operator does not change much as we refine the mesh, while the maximal eigenvalue changes as $O(h^{-1})$, according to (3.56), which results in condition number of order $O(h^{-1})$. In this case we also see that changing the permeability for a fixed h has no effect on the condition number, which can be explained by the fact that the permeability constants K_{min} and K_{max} appearing in the estimates of the Rayleigh quotient (3.56) cancel one another when we divide the upper bound by the lower bound. Table 3.2 shows the behavior of the method when $K < h$, in which case both the minimal and the maximal eigenvalues of the interface operator are dominated by constants independent of h , and consequently the condition number does not change significantly as the mesh is refined.

In the presence of Stokes-Stokes interfaces if h is small in comparison to K the bounds in (3.57) imply that the maximal eigenvalue of the interface operator is $O(h^{-1})$ while the minimal is $O(h)$, which means that the condition number is $O(h^{-2})$. This estimate is supported by the results

Table 3.1: Convergence of the Taylor-Hood and RT0 finite elements for Test 1.

Stokes region:					
<i>elements</i>	<i>h</i>	$\ \mathbf{u}_f - \mathbf{u}_f^h\ _{1,\Omega_f}$	<i>rate</i>	$\ p_f - p_f^h\ _{0,\Omega_f}$	<i>rate</i>
16	1/4	3.54e-01		3.00e-02	
64	1/8	8.60e-02	2.04	7.09e-03	2.08
256	1/16	2.15e-02	2.00	1.76e-03	2.01
1024	1/32	5.47e-03	1.97	4.44e-04	1.99
4096	1/64	1.40e-03	1.97	1.12e-04	1.99
16384	1/128	3.59e-04	1.96	2.84e-05	1.98
Darcy region:					
<i>elements</i>	<i>h</i>	$\ \mathbf{u}_p - \mathbf{u}_p^h\ _{0,\Omega_p}$	<i>rate</i>	$\ p_p - p_p^h\ _{0,\Omega_p}$	<i>rate</i>
8	1/4	2.16e-01		1.18e-01	
32	1/8	5.79e-02	1.90	2.87e-02	2.04
128	1/16	1.47e-02	1.98	7.13e-03	2.01
512	1/32	3.70e-03	1.99	1.78e-03	2.00
2048	1/64	9.27e-04	2.00	4.45e-04	2.00
8192	1/128	2.32e-04	2.00	1.11e-04	2.00

reported in Table 3.6 and Table 3.7. In this case the permeability appears only in the upper bound of the Rayleigh quotient (3.57), which makes the condition number proportional to K for a fixed h . For h much larger than K , the eigenvalues of the interface operator are bounded by constants that are independent of h and the condition number remains close to a constant, which is exactly what we see in the first three rows of Table 3.5.

Table 3.2: Convergence of CG iterations: $K=0.01$, varying the mesh size for 2 subdomains.

h	$eig.min.$	$eig.max.$	$cond(S_h)$	$iter.num.$
1/4	0.403	1.417	3.5	4
1/8	0.291	1.484	5.1	8
1/16	0.255	1.502	5.9	10
1/32	0.260	1.506	5.8	9
1/64	0.266	1.507	5.7	9

Table 3.3: Convergence of CG iterations: $K=1.0$, varying the mesh size for 2 subdomains.

h	$eig.min.$	$eig.max.$	$cond(S_h)$	$iter.num.$
1/4	3.161	6.051	1.9	4
1/8	3.224	11.480	3.6	8
1/16	3.240	22.447	6.9	16
1/32	3.245	44.991	13.9	17
1/64	3.246	90.169	27.8	24

Table 3.4: Convergence of CG iterations: $K=2.0$, varying the mesh size for 2 subdomains.

h	$eig.min.$	$eig.max.$	$cond(S_h)$	$iter.num.$
1/4	5.774	11.590	2.0	4
1/8	5.882	22.729	3.9	8
1/16	5.910	44.774	7.6	11
1/32	5.917	89.815	15.2	16
1/64	5.919	180.308	30.5	24

Table 3.5: Convergence of CG iterations: $K=0.01$, varying the mesh size for 4 subdomains.

h	$eig.min.$	$eig.max.$	$cond(S_h)$	$iter.num.$
1/4	0.093	4.256	45.8	12
1/8	0.114	4.601	40.4	19
1/16	0.122	4.686	38.4	23
1/32	0.061	4.714	77.3	29
1/64	0.030	4.730	157.7	46

Table 3.6: Convergence of CG iterations: $K=1.0$, varying the mesh size for 4 subdomains.

h	$eig.min.$	$eig.max.$	$cond(S_h)$	$iter.num.$
1/4	0.569	13.085	23.0	10
1/8	0.247	25.586	103.6	24
1/16	0.122	50.782	416.3	46
1/32	0.062	101.309	1634.0	95
1/64	0.032	241.302	7540.7	182

Table 3.7: Convergence of CG iterations: $K=2.0$, varying the mesh size for 4 subdomains.

h	$eig.min.$	$eig.max.$	$cond(S_h)$	$iter.num.$
1/4	0.570	25.756	45.2	11
1/8	0.247	50.904	206.1	23
1/16	0.122	101.393	831.1	56
1/32	0.064	202.509	3164.2	105
1/64	0.038	482.002	12684.0	207

4.0 COUPLING THE STOKES-DARCY FLOW WITH TRANSPORT

We employ the LDG method to approximate numerically the transport equation. The method is locally mass conservative and due to a built-in upwinding mechanism it accurately approximates sharp fronts. The LDG method can be formulated on general unstructured grids and allows one to vary the degree of the approximating polynomials from element to element. The LDG method combines ideas from the DG and the MFE methods, since it approximates both the concentration and the diffusive flux using functions, which are discontinuous across the inter-element boundaries.

Here we develop stability and convergence analysis for the concentration and the diffusive flux in the transport equation. The numerical error is a combination of the LDG discretization error and the error from the discretization of the Stokes-Darcy velocity. The former is shown to be of the order $O(h^k)$, where k is the polynomial degree in the LDG approximating space, and h is the size of the mesh for the discretization of the transport equation. This is similar to existing bounds in the literature for stand-alone LDG discretizations [34, 32, 29]. The error terms coming from the Stokes-Darcy flow discretization are of optimal order, similar to the bounds obtained in [65, 81]. This is an improvement of $O(h)$ from the result in [39], where the Darcy velocity discretization error is incorporated into the error analysis of a LDG method for the transport equation. We also extend previous LDG transport analysis [34, 39, 29, 32] to non-divergence free velocity. We will include in our analysis the possibility of non-homogeneous boundary conditions for the flow problem: for $\mathbf{g}_f \in (H^{1/2}(\Gamma_f))^d$ and $g_p \in L^2(\Gamma_p)$ we let

$$\mathbf{u}_f = \mathbf{g}_f \text{ on } \Gamma_f, \quad \text{and } \mathbf{u}_p \cdot \mathbf{n}_p = g_p \text{ on } \Gamma_p$$

in (1.12) and (1.13), respectively.

To save space we will only present a discretization of the coupled flow-transport problem based on the approach in Section 3.2.

We will use the following standard notation. For a domain $G \subset \mathbb{R}^d$, the $L^2(G)$ inner product and norm for scalar and vector valued functions are denoted $(\cdot, \cdot)_G$ and $\|\cdot\|_G$, respectively. The norms and seminorms of the Sobolev spaces $W^{k,p}(G)$, $k \in \mathbb{R}$, $p > 0$ are denoted by $\|\cdot\|_{k,p,G}$ and $|\cdot|_{k,p,G}$, respectively. The norms and seminorms of the Hilbert spaces $H^k(G)$ are denoted by $\|\cdot\|_{k,G}$ and $|\cdot|_{k,G}$, respectively. We omit G in the subscript if $G = \Omega$. For a section of the domain or element boundary $S \subset \mathbb{R}^{d-1}$ we write $\langle \cdot, \cdot \rangle_S$ and $\|\cdot\|_S$ for the $L^2(S)$ inner product (or duality pairing) and norm, respectively. In order to avoid extensive usage of the superscript h in this chapter we will denote all the numerically computed quantities by capital letters. In the analysis of the LDG scheme we will use K to represent a generic constant independent of the discretization parameters h_f , h_p , and h .

Let $\mathbf{u}_g \in H(\text{div}; \Omega)$ be such that $\mathbf{u}_g|_{\Omega_f} \in (H^1(\Omega_f))^d$, $\mathbf{u}_g = \mathbf{g}_f$ on Γ_f and $\mathbf{u}_g \cdot \mathbf{n}_p = g_p$ on Γ_p . Let V^h and Q^h be the discrete spaces introduced in Section 3.2. Let $\mathbf{U}_g \in V^h$ be a suitable approximation to \mathbf{u}_g . The numerical scheme for the Stokes-Darcy flow problem is: find $\mathbf{U} \in V^h + \mathbf{U}_g$ and $P \in Q^h$ satisfying (3.10)–(3.11).

We take \mathbf{U}_g to be any function in V^h such that $\mathbf{U}_g = O_f^h \mathbf{g}_f$ on Γ_f and $\mathbf{U}_g \cdot \mathbf{n}_p = O_p^h g_p$ on Γ_p , where O_f^h is the $L^2(\Gamma_f)$ -projection onto $X_f^h|_{\Gamma_f}$ and O_p^h is the $L^2(\Gamma_p)$ -projection onto $X_p^h \cdot \mathbf{n}_p|_{\Gamma_p}$. The computed flow solution is independent of the choice of \mathbf{U}_g and depends only on $O_f^h \mathbf{g}_f$ and $O_p^h g_p$. For the homogeneous boundary conditions case, it was shown in [65] that the above method has a unique solution satisfying (3.12). The results easily extend to the non-homogeneous case considered here. We show later that the error in the transport equations depends on the error in the approximation of the velocity on Γ . The approximation properties of O_f^h and O_p^h imply that

$$\|(\mathbf{u} - \mathbf{U}) \cdot \mathbf{n}\|_{\Gamma} \leq K \left(h_f^{k_f+1} + h_p^{k_p+1} \right). \quad (4.1)$$

Usually no flow boundary conditions $\mathbf{u}_p \cdot \mathbf{n}_p = 0$ are specified on Γ_p , which corresponds to an impermeable rock surrounding the aquifer. In that case the second term on the right in the above bound vanishes.

4.1 FORMULATION OF THE LDG METHOD FOR TRANSPORT

We rewrite the transport equation in a mixed form by introducing the diffusive flux

$$\mathbf{z} = -\mathbf{D}\nabla c. \quad (4.2)$$

The system (1.16)-(1.19) is equivalent to

$$\phi c_t + \nabla \cdot (c\mathbf{u} + \mathbf{z}) = \phi f_c, \quad (4.3)$$

$$(c\mathbf{u} + \mathbf{z}) \cdot \mathbf{n} = c_{in}\mathbf{u} \cdot \mathbf{n} \quad \text{on } \Gamma_{in}, \quad (4.4)$$

$$\mathbf{z} \cdot \mathbf{n} = 0 \quad \text{on } \Gamma_{out}. \quad (4.5)$$

Let \mathcal{T}^h be a shape-regular finite element partition of Ω . Let \mathcal{E}^h be the set of interior faces of \mathcal{T}^h . Again, the term *face* means a face in 3D and an edge in 2D. We denote by h_E the diameter of an element E and set h to be the maximum element diameter. We assume that no element E overlaps with both Γ_{in} and Γ_{out} and that each element E has a Lipschitz boundary ∂E . The partition \mathcal{T}^h may be different from $\Omega_f^h = \bigcup_{i=1}^{N_f} \Omega_i^h$ and $\Omega_p^h = \bigcup_{i=N_f+1}^N \Omega_i^h$.

Let $W_E = H^1(E)$, $\mathbf{V}_E = (W_E)^d$, and let \mathbf{n}_E be the outward unit normal on ∂E . Let

$$W = \{w \in L^2(\Omega) : \text{on each } E \in \mathcal{T}^h, w \in W_E\},$$

$$\mathbf{V} = \{\mathbf{v} \in (L^2(\Omega))^d : \text{on each } E \in \mathcal{T}^h, \mathbf{v} \in \mathbf{V}_E\}.$$

Let $w \in W$. For any $E \in \mathcal{T}^h$ and any $\mathbf{x} \in \partial E$ we define

$$w^-(\mathbf{x}) = \lim_{s \rightarrow 0^-} w(\mathbf{x} + s\mathbf{n}_E), \quad w^+(\mathbf{x}) = \lim_{s \rightarrow 0^+} w(\mathbf{x} + s\mathbf{n}_E), \quad (4.6)$$

$$\bar{w}(\mathbf{x}) = \frac{1}{2}(w^+(\mathbf{x}) + w^-(\mathbf{x})), \quad \text{and} \quad w^u(\mathbf{x}) = \begin{cases} w^-(\mathbf{x}) & \text{if } \mathbf{U} \cdot \mathbf{n}_E \geq 0 \\ w^+(\mathbf{x}) & \text{if } \mathbf{U} \cdot \mathbf{n}_E < 0 \end{cases}. \quad (4.7)$$

For a vector function $\mathbf{v} \in \mathbf{V}$, \mathbf{v}^- , \mathbf{v}^+ , and $\bar{\mathbf{v}}$ are defined in a similar way. Note that the upwinding is based on the computed velocity \mathbf{U} .

Assuming that the solution to (4.3)–(4.5) is smooth enough, multiplying by appropriate test functions on every element E and integrating by parts, we obtain the following weak formulation. For every $E \in \mathcal{T}^h$, $c \in W_E$ and $\mathbf{z} \in \mathbf{V}_E$ satisfy

$$(\mathbf{D}^{-1}\mathbf{z}, \mathbf{v})_E - (c, \nabla \cdot \mathbf{v})_E + \langle c, \mathbf{v}^- \cdot \mathbf{n}_E \rangle_{\partial E} = 0, \quad \forall \mathbf{v} \in \mathbf{V}_E, \quad (4.8)$$

$$\begin{aligned} & (\phi c_t, w)_E - (c\mathbf{u} + \mathbf{z}, \nabla w)_E + \langle (c\mathbf{u} + \mathbf{z}) \cdot \mathbf{n}_E, w^- \rangle_{\partial E \setminus \Gamma} + \langle c\mathbf{u} \cdot \mathbf{n}_E, w^- \rangle_{\partial E \cap \Gamma_{out}} \\ & = (\phi s, w)_E - \langle c_{in} \mathbf{u} \cdot \mathbf{n}_E, w^- \rangle_{\partial E \cap \Gamma_{in}}, \quad \forall w \in W_E. \end{aligned} \quad (4.9)$$

Let $W_E^h \subset W_E$ denote the space of all polynomials on E of degree $\leq k_E$, $k_E \geq 1$, and let $\mathbf{V}_E^h = (W_E^h)^d$. Let $k = \min_E k_E$. On each element E , $c(\cdot, t)$ and $\mathbf{z}(\cdot, t)$ are approximated by $C(\cdot, t) \in W_E^h$ and $\mathbf{Z}(\cdot, t) \in \mathbf{V}_E^h$ respectively. Let

$$W^h := \{w \in L^2(\Omega) : \text{on each } E \in \mathcal{T}_h, w \in W_E^h\},$$

$$\mathbf{V}^h := \{\mathbf{v} \in (L^2(\Omega))^d : \text{on each } E \in \mathcal{T}_h, \mathbf{v} \in \mathbf{V}_E^h\}.$$

Let $C^0 \in W^h$ be the L^2 -projection of c^0 :

$$\forall E \in \mathcal{T}^h, \quad (C^0 - c^0, w)_E = 0, \quad \forall w \in W_E^h. \quad (4.10)$$

The semi-discrete LDG method is defined as follows: for each $t \in [0, T]$ find $C(\cdot, t) \in W^h$ and $\mathbf{Z}(\cdot, t) \in \mathbf{V}^h$ such that on each $E \in \mathcal{T}^h$

$$\begin{aligned} & (\mathbf{D}^{-1}\mathbf{Z}, \mathbf{v})_E - (C, \nabla \cdot \mathbf{v})_E + \langle \bar{C}, \mathbf{v}^- \cdot \mathbf{n}_E \rangle_{\partial E \setminus \Gamma} \\ & + \langle C^-, \mathbf{v}^- \cdot \mathbf{n}_E \rangle_{\partial E \cap \Gamma} = 0, \quad \forall \mathbf{v} \in \mathbf{V}_E^h, \quad t \in [0, T], \end{aligned} \quad (4.11)$$

$$\begin{aligned} & (\phi C_t, w)_E - (C\mathbf{U} + \mathbf{Z}, \nabla w)_E + \langle (C^u \mathbf{U} + \bar{\mathbf{Z}}) \cdot \mathbf{n}_E, w^- \rangle_{\partial E \setminus \Gamma} \\ & + \langle C^- \mathbf{U} \cdot \mathbf{n}_E, w^- \rangle_{\partial E \cap \Gamma_{out}} + \frac{1}{2} (C \nabla \cdot (\mathbf{u} - \mathbf{U}), w)_E \\ & + \frac{1}{2} \langle C^- (\mathbf{u} - \mathbf{U}) \cdot \mathbf{n}_E, w^- \rangle_{\partial E \cap \Gamma_{out}} - \frac{1}{2} \langle C^- (\mathbf{u} - \mathbf{U}) \cdot \mathbf{n}_E, w^- \rangle_{\partial E \cap \Gamma_{in}} \\ & = (\phi f_c, w)_E - \langle c_{in} \mathbf{u} \cdot \mathbf{n}_E, w^- \rangle_{\partial E \cap \Gamma_{in}}, \quad \forall w \in W_E^h, \quad t \in (0, T), \end{aligned} \quad (4.12)$$

$$C(\cdot, 0) = C^0. \quad (4.13)$$

The method is based on the weak formulation (4.8)–(4.9) with several modifications. The terms $\frac{1}{2}(C\nabla \cdot (\mathbf{u} - \mathbf{U}), w)_E$, $\frac{1}{2}\langle C^-(\mathbf{u} - \mathbf{U}) \cdot \mathbf{n}_E, w^- \rangle_{\partial E \cap \Gamma_{out}}$, and $-\frac{1}{2}\langle C^-(\mathbf{u} - \mathbf{U}) \cdot \mathbf{n}_E, w^- \rangle_{\partial E \cap \Gamma_{in}}$ have been added to the mass conservation equation. A term similar to the first one, but with a different scaling has been used in [39]. These terms can be viewed as corrections for the error in approximating $\nabla \cdot \mathbf{u}$ and $\mathbf{u} \cdot \mathbf{n}$ on Γ . As we show later, they provide better stability properties of the method without affecting the accuracy. Note also that the true normal velocity $\mathbf{u} \cdot \mathbf{n}$ is used on the right hand side in the Γ_{in} -term. Furthermore, the average concentration value is used on the interior faces in the diffusive flux equation, while upwinding is used in the conservation equation.

In the above scheme we assume that high enough quadrature rules are used, so that the numerical integration error is dominated by the discretization error. Note that the computed velocity \mathbf{U} is needed to evaluate element and edge integrals in (4.12). As a result \mathbf{U} has to be evaluated at any quadrature point in E or on ∂E . Since we allow for the flow and transport grids to differ and the velocity approximation could be discontinuous, \mathbf{U} may not be well defined at a given quadrature point. This problem is handled by decomposing E into sub-elements according to its intersection with the flow grid. More precisely, let $E_{X^h}^i$, $i = 1, \dots, m_E$ be the elements of the flow grid that overlap with E . Then we have

$$\int_E \varphi dx = \sum_{i=1}^{m_E} \int_{E \cap E_{X^h}^i} \varphi dx, \quad \int_{\partial E} \varphi d\sigma = \sum_{i=1}^{m_E} \int_{\partial E \cap E_{X^h}^i} \varphi d\sigma.$$

The computed velocity \mathbf{U} is well defined on all sub-elements and sub-edges.

We restrict our attention to the semi-discrete formulation. Standard methods such as Euler or Runge-Kutta can be employed for the time discretization, see, e.g. [35].

4.2 STABILITY OF THE LDG SCHEME

The stability argument is based on the analysis in [32]. The main difference here is that we allow for velocity with non-zero divergence, as well as account for the use of an approximate velocity in the transport equation.

By adding equations (4.11) and (4.12), summing over all the elements and integrating over t , we obtain the equivalent formulation

$$B_{\mathbf{U}}(C, \mathbf{Z}; w, \mathbf{v}) = - \int_0^T \langle c_{in} \mathbf{u} \cdot \mathbf{n}, w^- \rangle_{\Gamma_{in}} dt + \int_0^T (\phi f_c, w) dt, \quad (4.14)$$

$$\forall (w, \mathbf{v}) \in \mathcal{C}^0(0, T; W^h \times \mathbf{V}^h),$$

where

$$B_{\mathbf{U}}(C, \mathbf{Z}; w, \mathbf{v}) := \int_0^T \sum_E \left\{ (\phi C_t, w)_E - (C\mathbf{U} + \mathbf{Z}, \nabla w)_E \right. \\ \left. + \langle C^- \mathbf{U} \cdot \mathbf{n}_E, w^- \rangle_{\partial E \cap \Gamma_{out}} + \langle (C^u \mathbf{U} + \bar{\mathbf{Z}}) \cdot \mathbf{n}_E, w^- \rangle_{\partial E \setminus \Gamma} + (\mathbf{D}^{-1} \mathbf{Z}, \mathbf{v})_E \right. \\ \left. - (C, \nabla \cdot \mathbf{v})_E + \langle \bar{C}, \mathbf{v}^- \cdot \mathbf{n}_E \rangle_{\partial E \setminus \Gamma} + \langle C^-, \mathbf{v}^- \cdot \mathbf{n}_E \rangle_{\partial E \cap \Gamma} \right. \\ \left. + \frac{1}{2} (\nabla \cdot (\mathbf{u} - \mathbf{U}) C, w)_E + \frac{1}{2} \langle C^- (\mathbf{u} - \mathbf{U}) \cdot \mathbf{n}_E, w^- \rangle_{\partial E \cap \Gamma_{out}} \right. \\ \left. - \frac{1}{2} \langle C^- (\mathbf{u} - \mathbf{U}) \cdot \mathbf{n}_E, w^- \rangle_{\partial E \cap \Gamma_{in}} \right\} dt. \quad (4.15)$$

Taking $w = C$ and $\mathbf{v} = \mathbf{Z}$, we have

$$B_{\mathbf{U}}(C, \mathbf{Z}; C, \mathbf{Z}) = \Theta_1 + \Theta_2 + \Theta_3, \quad (4.16)$$

where

$$\Theta_1 = \int_0^T \sum_E \left\{ (\phi C_t, C)_E + (\mathbf{D}^{-1} \mathbf{Z}, \mathbf{Z})_E \right\} dt, \\ \Theta_2 = \int_0^T \sum_E \left\{ - (C\mathbf{U}, \nabla C)_E + \langle C^u \mathbf{U} \cdot \mathbf{n}_E, C^- \rangle_{\partial E \setminus \Gamma} + \langle C^- \mathbf{U} \cdot \mathbf{n}_E, C^- \rangle_{\partial E \cap \Gamma_{out}} \right. \\ \left. + \frac{1}{2} (C \nabla \cdot (\mathbf{u} - \mathbf{U}), C)_E + \frac{1}{2} \langle C^- (\mathbf{u} - \mathbf{U}) \cdot \mathbf{n}_E, C^- \rangle_{\partial E \cap \Gamma_{out}} \right. \\ \left. - \frac{1}{2} \langle C^- (\mathbf{u} - \mathbf{U}) \cdot \mathbf{n}_E, C^- \rangle_{\partial E \cap \Gamma_{in}} \right\} dt, \quad (4.17) \\ \Theta_3 = \int_0^T \sum_E \left\{ - (\mathbf{Z}, \nabla C)_E + \langle \bar{\mathbf{Z}} \cdot \mathbf{n}_E, C^- \rangle_{\partial E \setminus \Gamma} - (C, \nabla \cdot \mathbf{Z})_E \right. \\ \left. + \langle \bar{C}, \mathbf{Z}^- \cdot \mathbf{n}_E \rangle_{\partial E \setminus \Gamma} + \langle C^-, \mathbf{Z}^- \cdot \mathbf{n}_E \rangle_{\partial E \cap \Gamma} \right\} dt.$$

Since

$$(\phi C_t, C)_E = \frac{1}{2} \frac{d}{dt} (\phi^{1/2} C, \phi^{1/2} C)_E$$

we can write

$$\Theta_1 = \frac{1}{2} \|\phi^{1/2} C(T)\|^2 - \frac{1}{2} \|\phi^{1/2} C(0)\|^2 + \int_0^T \|\mathbf{D}^{-1/2} \mathbf{Z}\|^2 dt. \quad (4.18)$$

We continue with the bound on Θ_2 . Integration by parts gives

$$(C\mathbf{U}, \nabla C)_E = \frac{1}{2} \int_{\partial E} (C^-)^2 \mathbf{U} \cdot \mathbf{n}_E d\sigma - \frac{1}{2} \int_E C^2 \nabla \cdot \mathbf{U} dx.$$

Then we have

$$\begin{aligned} \Theta_2 &= \int_0^T \sum_E \left\{ -\frac{1}{2} \langle C^- \mathbf{U} \cdot \mathbf{n}_E, C^- \rangle_{\partial E \setminus \Gamma} - \frac{1}{2} \langle C^- \mathbf{u} \cdot \mathbf{n}_E, C^- \rangle_{\partial E \cap \Gamma_{in}} \right. \\ &\quad \left. + \frac{1}{2} \langle C^- \mathbf{u} \cdot \mathbf{n}_E, C^- \rangle_{\partial E \cap \Gamma_{out}} + \frac{1}{2} (C^2, \nabla \cdot \mathbf{u})_E + \langle C^u \mathbf{U} \cdot \mathbf{n}_E, C^- \rangle_{\partial E \setminus \Gamma} \right\} dt \\ &= \int_0^T \left\{ \frac{1}{2} (C^2, \nabla \cdot \mathbf{u}) + \frac{1}{2} \langle |\mathbf{u} \cdot \mathbf{n}|, (C^-)^2 \rangle_\Gamma \right. \\ &\quad \left. + \sum_E \langle (C^u - \frac{1}{2} C^-) \mathbf{U} \cdot \mathbf{n}_E, C^- \rangle_{\partial E \setminus \Gamma} \right\} dt. \end{aligned} \quad (4.19)$$

It is convenient to express the sum over the elements in the last term in (4.19) as a sum over all faces in the set \mathcal{E}^h . Let $e \in \partial E$ be an interior face of the element E . For $w \in W^h$ and $\mathbf{v} \in \mathbf{V}^h$ we set on e

$$[w] = (w^- - w^+) \mathbf{n}_E, \quad [\mathbf{v}] = (\mathbf{v}^- - \mathbf{v}^+) \cdot \mathbf{n}_E.$$

Note that these definitions do not depend on which element E is taken as a reference. Let us also fix arbitrarily a unit normal vector on e , denoted by \mathbf{n}_e . Since

$$\frac{1}{2} [C^2] = \frac{1}{2} ((C^-)^2 - (C^+)^2) \mathbf{n}_E = \frac{1}{2} (C^- + C^+) (C^- - C^+) \mathbf{n}_E = \overline{C} [C],$$

we can write

$$\begin{aligned}
\sum_E \langle (C^u - \frac{1}{2}C^-) \mathbf{U} \cdot \mathbf{n}_E, C^- \rangle_{\partial E \setminus \Gamma} &= \sum_e \langle \mathbf{U} \cdot (C^u [C] - \frac{1}{2}[C^2]), 1 \rangle_e \\
&= \sum_e \langle \mathbf{U} \cdot (C^u [C] - \bar{C}[C]), 1 \rangle_e \\
&= \sum_e \langle \mathbf{U} \cdot [C] (C^u - \bar{C}), 1 \rangle_e \\
&= \frac{1}{2} \sum_e \langle |\mathbf{U} \cdot \mathbf{n}_e|, [C] \cdot [C] \rangle_e,
\end{aligned} \tag{4.20}$$

where we used in the last equality that on any $e \in \partial E$

$$\begin{aligned}
\mathbf{U} \cdot [C] (C^u - \bar{C}) &= \mathbf{U} \cdot \mathbf{n}_E (C^- - C^+) \left(\left\{ \begin{array}{l} C^-, \mathbf{U} \cdot \mathbf{n}_E \geq 0 \\ C^+, \mathbf{U} \cdot \mathbf{n}_E < 0 \end{array} \right\} - \frac{C^- + C^+}{2} \right) \\
&= \mathbf{U} \cdot \mathbf{n}_E (C^- - C^+) \frac{(C^- - C^+)}{2} \text{sign}(\mathbf{U} \cdot \mathbf{n}_E) = \frac{1}{2} |\mathbf{U} \cdot \mathbf{n}_e| [C] \cdot [C].
\end{aligned}$$

Substituting (4.20) into (4.19) we obtain

$$\Theta_2 = \frac{1}{2} \int_0^T \left\{ (C^2, \nabla \cdot \mathbf{u}) + \langle |\mathbf{u} \cdot \mathbf{n}|, (C^-)^2 \rangle_\Gamma + \sum_e \langle |\mathbf{U} \cdot \mathbf{n}_e|, [C] \cdot [C] \rangle_e \right\} dt. \tag{4.21}$$

To estimate Θ_3 we use the Green's formula to obtain

$$\begin{aligned}
\Theta_3 &= \int_0^T \sum_E \left\{ -\langle \mathbf{Z}^- \cdot \mathbf{n}_E, C^- \rangle_{\partial E \setminus \Gamma} + \frac{1}{2} \langle (\mathbf{Z}^+ + \mathbf{Z}^-) \cdot \mathbf{n}_E, C^- \rangle_{\partial E \setminus \Gamma} \right. \\
&\quad \left. + \frac{1}{2} \langle C^+ + C^-, \mathbf{Z}^- \cdot \mathbf{n}_E \rangle_{\partial E \setminus \Gamma} \right\} dt \\
&= \int_0^T \sum_E \left\{ \frac{1}{2} \langle C^+, \mathbf{Z}^- \cdot \mathbf{n}_E \rangle_{\partial E \setminus \Gamma} + \frac{1}{2} \langle \mathbf{Z}^+ \cdot \mathbf{n}_E, C^- \rangle_{\partial E \setminus \Gamma} \right\} dt = 0,
\end{aligned} \tag{4.22}$$

where the last equality follows from the fact that on each interior face the contributions from the two adjacent elements cancel, due to the opposite directions of the outward normal vectors. A combination of (4.16), (4.18), (4.21), and (4.22) gives

$$\begin{aligned}
B_{\mathbf{U}}(C, \mathbf{Z}; C, \mathbf{Z}) &= \frac{1}{2} \|\phi^{1/2} C(T)\|^2 - \frac{1}{2} \|\phi^{1/2} C(0)\|^2 + \int_0^T \|\mathbf{D}^{-1/2} \mathbf{Z}\|^2 dt \\
&\quad + \frac{1}{2} \int_0^T \left\{ (C^2, \nabla \cdot \mathbf{u}) + \langle |\mathbf{u} \cdot \mathbf{n}|, (C^-)^2 \rangle_\Gamma + \sum_e \langle |\mathbf{U} \cdot \mathbf{n}_e|, [C] \cdot [C] \rangle_e \right\} dt.
\end{aligned} \tag{4.23}$$

Combining (4.14) and (4.23), and using Young's inequality

$$ab \leq \frac{\epsilon}{2}a^2 + \frac{1}{2\epsilon}b^2, \quad a, b \in \mathbb{R}, \epsilon > 0 \quad (4.24)$$

with $\epsilon = 1$, we obtain

$$\begin{aligned} & \frac{1}{2}\|\phi^{1/2}C(T)\|^2 + \int_0^T \|\mathbf{D}^{-1/2}\mathbf{Z}\|^2 dt \\ & \leq \frac{1}{2}\|\phi^{1/2}C(0)\|^2 + \frac{1}{2}\int_0^T (C^2, (\nabla \cdot \mathbf{u})_-) dt \\ & \quad + \frac{1}{2}\int_0^T \langle |\mathbf{u} \cdot \mathbf{n}|, (c_{in})^2 \rangle_{\Gamma_{in}} dt + \int_0^T \|\phi^{1/2}s\| \|\phi^{1/2}C\| dt, \end{aligned} \quad (4.25)$$

where

$$(\nabla \cdot \mathbf{u})_- := \begin{cases} 0, & \nabla \cdot \mathbf{u} \geq 0, \\ -\nabla \cdot \mathbf{u}, & \nabla \cdot \mathbf{u} < 0. \end{cases}$$

For the second term on the right in (4.25) we have

$$\frac{1}{2}\int_0^T (C^2, (\nabla \cdot \mathbf{u})_-) dt \leq \frac{1}{2}\|\phi^{-1}(\nabla \cdot \mathbf{u})_-\|_{0,\infty} \int_0^T \|\phi^{1/2}C(t)\|^2 dt,$$

and the use of Gronwall's inequality implies

$$\begin{aligned} & \|\phi^{1/2}C(T)\|^2 + 2\int_0^T \|\mathbf{D}^{-1/2}\mathbf{Z}\|^2 dt \\ & \leq e^{LT} \left(\|\phi^{1/2}C(0)\|^2 + \int_0^T \langle |\mathbf{u} \cdot \mathbf{n}|, (c_{in})^2 \rangle_{\Gamma_{in}} dt + 2\int_0^T \|\phi^{1/2}s\| \|\phi^{1/2}C\| dt \right), \end{aligned} \quad (4.26)$$

where $L := \|\phi^{-1}(\nabla \cdot \mathbf{u})_-\|_{0,\infty}$. Using (4.10),

$$\|\phi^{1/2}C(0)\| \leq (\phi^*)^{1/2}\|c^0\|. \quad (4.27)$$

To complete the stability analysis we need the following result shown in [32].

Lemma 4.2.1 *Suppose that for all $T > 0$*

$$\chi^2(T) + R(T) \leq A(T) + 2 \int_0^T B(t) \chi(t) dt,$$

where R , A and B are non-negative functions. Then

$$\sqrt{\chi^2 + R(T)} \leq \sup_{0 \leq t \leq T} A^{1/2}(t) + \int_0^T B(t) dt.$$

Let us define the norm $|||(C, \mathbf{Z})|||$ by

$$|||(C, \mathbf{Z})|||^2 := \|\phi^{1/2}C(T)\|^2 + 2 \int_0^T \|\mathbf{D}^{-1/2}\mathbf{Z}\|^2 dt. \quad (4.28)$$

Then, using (4.26), (4.27), and Lemma 4.2.1, we obtain the following stability result.

Theorem 4.2.1 *The solution to the semi-discrete LDG method (4.11)–(4.13) satisfies*

$$|||(C, \mathbf{Z})||| \leq e^{\frac{LT}{2}} \left(\phi^* \|c^0\|^2 + \int_0^T \langle |\mathbf{u} \cdot \mathbf{n}|, (c_{in})^2 \rangle_{\Gamma_{in}} dt \right)^{1/2} + e^{LT} \int_0^T \|\phi^{1/2}s\| dt, \quad (4.29)$$

where L is defined in (4.26).

Remark 4.2.1 *Note that, due to including the additional terms in the scheme, the stability estimate depends on the true velocity, $\nabla \cdot \mathbf{u}$ and $\mathbf{u} \cdot \mathbf{n}$ on Γ_{in} , rather than on the computed velocity \mathbf{U} .*

4.3 ERROR ANALYSIS OF THE LDG SCHEME

Let $\Pi c \in W^h$, $\Pi \mathbf{z} \in \mathbf{V}^h$, and $\Pi \mathbf{u} \in \mathbf{V}^h$ denote the L^2 -projections of c , \mathbf{z} , and \mathbf{u} , respectively:

$$\forall E \in \mathcal{T}^h, \quad (c - \Pi c, w)_E = 0, \quad \forall w \in W_E^h, \quad (4.30)$$

$$\forall E \in \mathcal{T}^h, \quad (\mathbf{z} - \Pi \mathbf{z}, \mathbf{v})_E = 0, \quad \forall \mathbf{v} \in \mathbf{V}_E^h, \quad (4.31)$$

$$\forall E \in \mathcal{T}^h, \quad (\mathbf{u} - \Pi \mathbf{u}, \mathbf{v})_E = 0, \quad \forall \mathbf{v} \in \mathbf{V}_E^h. \quad (4.32)$$

The L^2 -projection has the approximation property [31]

$$\|q - \Pi q\|_{m,p,E} \leq K h_E^{l-m} \|q\|_{l,p,E}, \quad 0 \leq m \leq l \leq k_E + 1, \quad 1 \leq p \leq \infty, \quad (4.33)$$

where q is either a scalar or a vector function. We will also make use of the trace inequality [6]

$$\forall e \in \partial E, \quad \|\chi\|_e \leq K \left(h_E^{-1/2} \|\chi\|_E + h_E^{1/2} |\chi|_{1,E} \right) \quad \forall \chi \in H^1(E). \quad (4.34)$$

Using (4.33) and (4.34),

$$\|q - \Pi q\|_e \leq K h_E^{l-1/2} \|q\|_{l,E}, \quad 1 \leq l \leq k_E + 1. \quad (4.35)$$

For polynomial functions, (4.34) and the inverse inequality [31]

$$\|w\|_{1,E} \leq K h_E^{-1} \|w\|_E. \quad (4.36)$$

imply

$$\|w\|_e \leq K h_E^{-1/2} \|w\|_E. \quad (4.37)$$

Similarly to the discrete variational formulation (4.14), the weak solution of (4.8)–(4.9) satisfies

$$B_{\mathbf{u}}(c, \mathbf{z}; w, \mathbf{v}) = - \int_0^T \langle c_{in} \mathbf{u} \cdot \mathbf{n}, w^- \rangle_{\Gamma_{in}} dt + \int_0^T (\phi_S, w) dt, \quad (4.38)$$

$$\forall (w, \mathbf{v}) \in \mathcal{C}^0(0, T; W \times \mathbf{V}),$$

where

$$\begin{aligned}
B_{\mathbf{u}}(c, \mathbf{z}; w, \mathbf{v}) &:= \int_0^T \sum_E \{ (\phi c_t, w)_E - (c\mathbf{u} + \mathbf{z}, \nabla w)_E \\
&+ \langle c^- \mathbf{u} \cdot \mathbf{n}_E, w^- \rangle_{\partial E \cap \Gamma_{out}} + \langle (c^u \mathbf{u} + \bar{\mathbf{z}}) \cdot \mathbf{n}_E, w^- \rangle_{\partial E \setminus \Gamma} + (\mathbf{D}^{-1} \mathbf{z}, \mathbf{v})_E \\
&- (c, \nabla \cdot \mathbf{v})_E + \langle \bar{c}, \mathbf{v}^- \cdot \mathbf{n}_E \rangle_{\partial E \setminus \Gamma} + \langle c^-, \mathbf{v}^- \cdot \mathbf{n}_E \rangle_{\partial E \cap \Gamma} \} dt.
\end{aligned} \tag{4.39}$$

Subtracting (4.14) from (4.38) gives

$$B_{\mathbf{u}}(c, \mathbf{z}; w, \mathbf{v}) - B_{\mathbf{U}}(C, \mathbf{Z}; w, \mathbf{v}) = 0. \tag{4.40}$$

Let $\psi_c = C - \Pi c$, $\psi_{\mathbf{z}} = \mathbf{Z} - \Pi \mathbf{z}$, $\theta_c = c - \Pi c$, and $\theta_{\mathbf{z}} = \mathbf{z} - \Pi \mathbf{z}$. Setting $(w, \mathbf{v}) = (\psi_c, \psi_{\mathbf{z}})$ in (4.40), we get

$$B_{\mathbf{U}}(\psi_c, \psi_{\mathbf{z}}; \psi_c, \psi_{\mathbf{z}}) = B_{\mathbf{u}}(\theta_c, \theta_{\mathbf{z}}; \psi_c, \psi_{\mathbf{z}}) + B_{\mathbf{u}}(\Pi c, \Pi \mathbf{z}; \psi_c, \psi_{\mathbf{z}}) - B_{\mathbf{U}}(\Pi c, \Pi \mathbf{z}; \psi_c, \psi_{\mathbf{z}}). \tag{4.41}$$

For the error due to the velocity approximation we have

$$\begin{aligned}
&B_{\mathbf{u}}(\Pi c, \Pi \mathbf{z}; \psi_c, \psi_{\mathbf{z}}) - B_{\mathbf{U}}(\Pi c, \Pi \mathbf{z}; \psi_c, \psi_{\mathbf{z}}) \\
&= \int_0^T \sum_E \{ -(\Pi c(\mathbf{u} - \mathbf{U}), \nabla \psi_c)_E + \langle (\Pi c)^u (\mathbf{u} - \mathbf{U}) \cdot \mathbf{n}_E, \psi_c^- \rangle_{\partial E \setminus \Gamma} \\
&+ \langle (\Pi c)^- (\mathbf{u} - \mathbf{U}) \cdot \mathbf{n}_E, \psi_c^- \rangle_{\partial E \cap \Gamma_{out}} - \frac{1}{2}(\Pi c \nabla \cdot (\mathbf{u} - \mathbf{U}), \psi_c)_E \\
&- \frac{1}{2} \langle (\Pi c)^- (\mathbf{u} - \mathbf{U}) \cdot \mathbf{n}_E, \psi_c^- \rangle_{\partial E \cap \Gamma_{out}} + \frac{1}{2} \langle (\Pi c)^- (\mathbf{u} - \mathbf{U}) \cdot \mathbf{n}_E, \psi_c^- \rangle_{\partial E \cap \Gamma_{in}} \} dt \\
&= \int_0^T \sum_E \{ (\nabla \cdot (\Pi c(\mathbf{u} - \mathbf{U})), \psi_c)_E + \langle ((\Pi c)^u - (\Pi c)^-) (\mathbf{u} - \mathbf{U}) \cdot \mathbf{n}_E, \psi_c^- \rangle_{\partial E \setminus \Gamma} \\
&- \frac{1}{2}(\Pi c \nabla \cdot (\mathbf{u} - \mathbf{U}), \psi_c)_E - \frac{1}{2} \langle (\Pi c)^- (\mathbf{u} - \mathbf{U}) \cdot \mathbf{n}_E, \psi_c^- \rangle_{\partial E \cap \Gamma} \} dt.
\end{aligned} \tag{4.42}$$

Substituting (4.42) into (4.41) and using the definition (4.39) for $B_{\mathbf{u}}(\theta_c, \theta_{\mathbf{z}}; \psi_c, \psi_{\mathbf{z}})$, we obtain

$$\begin{aligned}
B_{\mathbf{U}}(\psi_c, \psi_{\mathbf{z}}; \psi_c, \psi_{\mathbf{z}}) &= \int_0^T \sum_E \{(\phi(\theta_c)_t, \psi_c)_E - (\theta_c \mathbf{u}, \nabla \psi_c)_E - (\theta_{\mathbf{z}}, \nabla \psi_c)_E \\
&+ \langle \theta_c^u \mathbf{u} \cdot \mathbf{n}_E, \psi_c^- \rangle_{\partial E \setminus \Gamma} + \langle \bar{\theta}_{\mathbf{z}} \cdot \mathbf{n}_E, \psi_c^- \rangle_{\partial E \setminus \Gamma} + \langle \theta_c^- \mathbf{u} \cdot \mathbf{n}_E, \psi_c^- \rangle_{\partial E \cap \Gamma_{out}} \\
&+ (\mathbf{D}^{-1} \theta_{\mathbf{z}}, \psi_{\mathbf{z}})_E - (\theta_c, \nabla \cdot \psi_{\mathbf{z}})_E + \langle \bar{\theta}_c, \psi_{\mathbf{z}}^- \cdot \mathbf{n}_E \rangle_{\partial E \setminus \Gamma} + \langle \theta_c^-, \psi_{\mathbf{z}}^- \cdot \mathbf{n}_E \rangle_{\partial E \cap \Gamma} \\
&+ (\nabla \cdot (\Pi c(\mathbf{u} - \mathbf{U})), \psi_c)_E + \langle ((\Pi c)^u - (\Pi c)^-)(\mathbf{u} - \mathbf{U}) \cdot \mathbf{n}_E, \psi_c^- \rangle_{\partial E \setminus \Gamma} \\
&- \frac{1}{2} (\Pi c \nabla \cdot (\mathbf{u} - \mathbf{U}), \psi_c)_E - \frac{1}{2} \langle (\Pi c)^- (\mathbf{u} - \mathbf{U}) \cdot \mathbf{n}_E, \psi_c^- \rangle_{\partial E \cap \Gamma} \} dt.
\end{aligned} \tag{4.43}$$

We now rewrite the summation over the elements in (4.43) in terms of a summation over the interior faces where it is relevant:

$$\begin{aligned}
B_{\mathbf{U}}(\psi_c, \psi_{\mathbf{z}}; \psi_c, \psi_{\mathbf{z}}) &= \int_0^T \sum_E \{(\phi(\theta_c)_t, \psi_c)_E - (\theta_c \mathbf{u}, \nabla \psi_c)_E - (\theta_{\mathbf{z}}, \nabla \psi_c)_E \\
&+ (\mathbf{D}^{-1} \theta_{\mathbf{z}}, \psi_{\mathbf{z}})_E - (\theta_c, \nabla \cdot \psi_{\mathbf{z}})_E + (\nabla \cdot (\Pi c(\mathbf{u} - \mathbf{U})), \psi_c)_E \\
&- \frac{1}{2} (\Pi c \nabla \cdot (\mathbf{u} - \mathbf{U}), \psi_c)_E + \langle ((\Pi c)^u - (\Pi c)^-)(\mathbf{u} - \mathbf{U}) \cdot \mathbf{n}_E, \psi_c^- \rangle_{\partial E \setminus \Gamma} \} dt \\
&+ \int_0^T \sum_e \{ \langle \theta_c^u \mathbf{u}, [\psi_c] \rangle_e + \langle \bar{\theta}_{\mathbf{z}}, [\psi_c] \rangle_e + \langle \bar{\theta}_c, [\psi_{\mathbf{z}}] \rangle_e \} dt \\
&+ \int_0^T \{ \langle \theta_c^- \mathbf{u} \cdot \mathbf{n}, \psi_c^- \rangle_{\Gamma_{out}} + \langle \theta_c^-, \psi_{\mathbf{z}}^- \cdot \mathbf{n} \rangle_{\Gamma} \\
&- \frac{1}{2} \langle (\Pi c)^- (\mathbf{u} - \mathbf{U}) \cdot \mathbf{n}_E, \psi_c^- \rangle_{\Gamma} \} dt \equiv T_1 + T_2 + \dots + T_{14}.
\end{aligned} \tag{4.44}$$

Using (4.23) and (4.10), (4.44) implies

$$\frac{1}{2} \|\phi^{1/2} \psi_c(T)\|^2 + \int_0^T \|\mathbf{D}^{-1/2} \psi_{\mathbf{z}}\|^2 dt \leq \frac{1}{2} \int_0^T (\psi_c^2, (\nabla \cdot \mathbf{u})_-) dt + T_1 + T_2 + \dots + T_{14}. \tag{4.45}$$

For the first term on the right above we have

$$\frac{1}{2} \int_0^T (\psi_c^2, (\nabla \cdot \mathbf{u})_-) dt \leq \frac{1}{2} \|\phi^{-1} (\nabla \cdot \mathbf{u})_-\|_{0, \infty} \int_0^T \|\phi^{1/2} \psi_c(t)\|^2 dt. \tag{4.46}$$

We continue with bounds on the other terms on the right in (4.45).

From the definition of the L^2 -projections (4.30) and (4.31) it follows that

$$T_3 = T_5 = 0. \quad (4.47)$$

Applying the Cauchy-Schwarz inequality, we obtain for T_1

$$T_1 = \int_0^T (\phi^{1/2}(\theta_c)_t, \phi^{1/2}\psi_c) dt \leq (\phi^*)^{1/2} \int_0^T \|(\theta_c)_t\| \|\phi^{1/2}\psi_c\| dt. \quad (4.48)$$

For the bound of T_2 we will use the L^2 -projection of \mathbf{u} onto the space of piecewise constant vectors $\Pi_0\mathbf{u}$ satisfying

$$\forall E \in \mathcal{T}^h, \quad (\mathbf{u} - \Pi_0\mathbf{u}, \mathbf{1})_E = 0, \quad \|\mathbf{u} - \Pi_0\mathbf{u}\|_{0,p,E} \leq Kh_E \|\mathbf{u}\|_{1,p,E}, \quad 1 \leq p \leq \infty.$$

Using (4.30) we have

$$\begin{aligned} T_2 &= - \int_0^T \sum_E (\theta_c \mathbf{u}, \nabla \psi_c)_E dt = \int_0^T \sum_E (\theta_c (\Pi_0 \mathbf{u} - \mathbf{u}), \nabla \psi_c)_E dt \\ &\leq K \|\mathbf{u}\|_{1,\infty} \int_0^T \sum_E h_E \|\theta_c\|_E \|\nabla \psi_c\|_E dt \leq K \|\mathbf{u}\|_{1,\infty} \int_0^T \sum_E \|\theta_c\|_E \|\psi_c\|_E dt \\ &\leq K \|\mathbf{u}\|_{1,\infty} \phi_*^{-1/2} \int_0^T \|\theta_c\| \|\phi^{1/2}\psi_c\| dt, \end{aligned} \quad (4.49)$$

where we used (4.36) for the second inequality. Handling T_4 is straightforward, using (4.24) with $\epsilon = 1/2$:

$$T_4 = \int_0^T \sum_E (\mathbf{D}^{-1}\theta_{\mathbf{z}}, \psi_{\mathbf{z}})_E dt \leq \int_0^T \|\mathbf{D}^{-1/2}\theta_{\mathbf{z}}\|^2 dt + \frac{1}{4} \int_0^T \|\mathbf{D}^{-1/2}\psi_{\mathbf{z}}\|^2 dt. \quad (4.50)$$

Using (4.33), we have for T_6 and T_7 :

$$\begin{aligned}
T_6 + T_7 &= \int_0^T \sum_E \left\{ (\nabla \cdot (\Pi c(\mathbf{u} - \mathbf{U})), \psi_c)_E - \frac{1}{2} (\Pi c \nabla \cdot (\mathbf{u} - \mathbf{U}), \psi_c)_E \right\} dt \\
&= \int_0^T \sum_E \left\{ (\nabla \Pi c \cdot (\mathbf{u} - \mathbf{U}), \psi_c)_E + \frac{1}{2} (\Pi c \nabla \cdot (\mathbf{u} - \mathbf{U}), \psi_c)_E \right\} dt \\
&\leq \phi_*^{-1/2} \int_0^T \sum_E (\|\nabla \Pi c\|_{0,\infty,E} \|\mathbf{u} - \mathbf{U}\|_E + \|\Pi c\|_{0,\infty,E} \|\nabla \cdot (\mathbf{u} - \mathbf{U})\|_E) \|\phi^{1/2} \psi_c\|_E dt \\
&\leq K \phi_*^{-1/2} \int_0^T \|c\|_{1,\infty} \|\mathbf{u} - \mathbf{U}\|_X \|\phi^{1/2} \psi_c\| dt.
\end{aligned} \tag{4.51}$$

For T_8 we have

$$\begin{aligned}
T_8 &= \int_0^T \sum_E \langle ((\Pi c)^u - (\Pi c)^-)(\mathbf{u} - \mathbf{U}) \cdot \mathbf{n}_E, \psi_c^- \rangle_{\partial E \setminus \Gamma} dt \\
&\leq \int_0^T \sum_E \|(\Pi c)^u - (\Pi c)^-\|_{0,\infty,\partial E \setminus \Gamma} \|(\mathbf{u} - \mathbf{U}) \cdot \mathbf{n}_E\|_{\partial E \setminus \Gamma} \|\psi_c^-\|_{\partial E \setminus \Gamma} dt.
\end{aligned} \tag{4.52}$$

Note that

$$\|(\Pi c)^u - (\Pi c)^-\|_{0,\infty,\partial E} \leq \|(\Pi c)^u - c\|_{0,\infty,\partial E} + \|c - (\Pi c)^-\|_{0,\infty,\partial E} \leq \|c - \Pi c\|_{0,\infty,\delta(E)},$$

where $\delta(E)$ is the union of all elements that share an face with E . For the second term on the right in (4.52) we have

$$\begin{aligned}
\|(\mathbf{u} - \mathbf{U}) \cdot \mathbf{n}_e\|_e &\leq \|(\mathbf{u} - \Pi \mathbf{u}) \cdot \mathbf{n}_e\|_e + \|(\Pi \mathbf{u} - \mathbf{U}) \cdot \mathbf{n}_e\|_e \\
&\leq K (\|(\mathbf{u} - \Pi \mathbf{u}) \cdot \mathbf{n}_e\|_e + h_E^{-1/2} \|\Pi \mathbf{u} - \mathbf{U}\|_E) \\
&\leq K (\|(\mathbf{u} - \Pi \mathbf{u}) \cdot \mathbf{n}_e\|_e + h_E^{-1/2} \|\mathbf{u} - \Pi \mathbf{u}\|_E + h_E^{-1/2} \|\mathbf{u} - \mathbf{U}\|_E),
\end{aligned}$$

where second inequality follows from an application of (4.37). Therefore for T_8 we obtain, using (4.37) again,

$$\begin{aligned}
T_8 &\leq K \int_0^T \|\theta_c\|_{0,\infty} \sum_E (\|(\mathbf{u} - \Pi\mathbf{u}) \cdot \mathbf{n}_E\|_{\partial E \setminus \Gamma} + h_E^{-1/2} \|\mathbf{u} - \Pi\mathbf{u}\|_E \\
&\quad + h_E^{-1/2} \|\mathbf{u} - \mathbf{U}\|_E) h_E^{-1/2} \|\psi_c\|_E \\
&\leq K \phi_*^{-1/2} \int_0^T \|c\|_{1,\infty} (h^{1/2} \|(\mathbf{u} - \Pi\mathbf{u}) \cdot \mathbf{n}\|_{\mathcal{E}^h} + \|\mathbf{u} - \Pi\mathbf{u}\| + \|\mathbf{u} - \mathbf{U}\|) \|\phi^{1/2} \psi_c\|,
\end{aligned} \tag{4.53}$$

where $\|w\|_{\mathcal{E}^h} = \left(\sum_e \|w\|_e^2 \right)^{1/2}$. Similarly, for T_9 we have

$$\langle \theta_c^u \mathbf{u}, [\psi_c] \rangle_e \leq K \phi_*^{-1/2} \|\mathbf{u} \cdot \mathbf{n}_e\|_{0,\infty,e} \|\theta_c^u\|_e h_E^{-1/2} \|\phi^{1/2} \psi_c\|_E,$$

therefore

$$T_9 \leq K \|\mathbf{u}\|_{0,\infty} \phi_*^{-1/2} \int_0^T h^{-1/2} \|\theta_c^u\|_{\mathcal{E}^h} \|\phi^{1/2} \psi_c\|. \tag{4.54}$$

Similarly,

$$T_{10} \leq K \phi_*^{-1/2} \int_0^T h^{-1/2} \|\overline{\theta}_{\mathbf{z}} \cdot \mathbf{n}\|_{\mathcal{E}^h} \|\phi^{1/2} \psi_c\|, \tag{4.55}$$

and

$$\begin{aligned}
T_{11} &= \int_0^T \sum_e \langle \overline{\theta}_c, [\psi_{\mathbf{z}}] \rangle_e dt \\
&\leq K (D^*)^{1/2} \int_0^T h^{-1/2} \|\overline{\theta}_c\|_{\mathcal{E}^h} \|\mathbf{D}^{-1/2} \psi_{\mathbf{z}}\| dt \\
&\leq K^2 D^* \int_0^T h^{-1} \|\overline{\theta}_c\|_{\mathcal{E}^h}^2 dt + \frac{1}{4} \int_0^T \|\mathbf{D}^{-1/2} \psi_{\mathbf{z}}\|^2 dt,
\end{aligned} \tag{4.56}$$

using (4.24) with $\epsilon = 1/2$ for the last inequality. In a similar way we obtain

$$T_{12} \leq K \|\mathbf{u}\|_{0,\infty} \phi_*^{-1/2} \int_0^T h^{-1/2} \|\theta_c^-\|_{\Gamma_{out}} \|\phi^{1/2} \psi_c\| dt, \tag{4.57}$$

$$T_{13} \leq KD^* \int_0^T h^{-1} \|\theta_c^-\|_{\Gamma}^2 dt + \frac{1}{4} \int_0^T \|\mathbf{D}^{-1/2} \psi_{\mathbf{z}}\|^2 dt, \quad (4.58)$$

and

$$T_{14} \leq K\phi_*^{-1/2} \int_0^T \|c\|_{0,\infty,\Gamma} h^{-1/2} \|(\mathbf{u} - \mathbf{U}) \cdot \mathbf{n}\|_{\mathbf{G}} \|\phi^{1/2} \psi_c\| dt. \quad (4.59)$$

A combination of (4.45)–(4.59), the use of Gronwall’s inequality for the term in (4.46), and an application of Lemma 4.2.1 imply

$$\begin{aligned} |||(\psi_c, \psi_{\mathbf{z}})||| \leq K \int_0^T & (\|\mathbf{D}^{-1/2} \theta_{\mathbf{z}}\| + h^{-1/2} \|\bar{\theta}_c\|_{\mathcal{E}^h} + h^{-1/2} \|\theta_c^-\|_{\Gamma} \\ & + \|(\theta_c)_t\| + \|\theta_c\| + \|\mathbf{u} - \mathbf{U}\|_X + h^{1/2} \|(\mathbf{u} - \Pi\mathbf{u}) \cdot \mathbf{n}\|_{\mathcal{E}^h} \\ & + \|\mathbf{u} - \Pi\mathbf{u}\| + \|\mathbf{u} - \mathbf{U}\| + h^{-1/2} \|\theta_c^u\|_{\mathcal{E}^h} + h^{-1/2} \|\bar{\theta}_{\mathbf{z}} \cdot \mathbf{n}\|_{\mathcal{E}^h} \\ & + h^{-1/2} \|\theta_c^-\|_{\Gamma_{out}} + h^{-1/2} \|(\mathbf{u} - \mathbf{U}) \cdot \mathbf{n}\|_{\Gamma}) dt, \end{aligned} \quad (4.60)$$

where $K = K(e^{LT})$. The above bound, combined with the velocity error bounds (3.12) and (4.1) and the approximation properties (4.33) and (4.35), implies the following convergence result.

Theorem 4.3.1 *If the solution to the coupled system (1.12)–(1.19) is smooth enough, then the solution to the semi-discrete transport LDG method (4.11)–(4.13) satisfies*

$$|||(c - C, \mathbf{z} - \mathbf{Z})||| \leq K(h^k + h_f^{k_f} + h_p^{k_p+\beta} + h_p^{l_p+1}), \quad (4.61)$$

where $\beta = 1$ if $g_p = 0$ and $\beta = 1/2$ otherwise.

4.4 NUMERICAL RESULTS

In this section we present results from several computational experiments. The first three confirm the theoretical convergence rates for problems with given analytical solutions, while the last two illustrate the behavior of the method for realistic problems of coupled surface-subsurface flows with contaminant transport. In all tests the computational domain is taken to be $\Omega = \Omega_f \cup \Omega_p$, where $\Omega_f = [0, 1] \times [\frac{1}{2}, 1]$ and $\Omega_p = [0, 1] \times [0, \frac{1}{2}]$. We have used

$$\mathbf{T}(\mathbf{u}_f, p_f) = -p_f \mathbf{I} + \mu_f \nabla \mathbf{u}_f$$

in the Stokes equation. The flow equations are solved via domain decomposition using the Taylor-Hood triangular finite elements in Ω_f and the lowest order Raviart Thomas rectangular finite elements in Ω_p . In the LDG discretization of the transport equation we chose W_E^h to be the space of bilinear functions on E . With these choices,

$$k_f = 2, \quad k_p = l_p = 0, \quad \text{and} \quad k = 1.$$

The grid for the Stokes discretization in Ω_f is obtained by first partitioning the domain into rectangles and then dividing each rectangle along its diagonal into two triangles. The flow grids in Ω_f and Ω_p match on the interface. The LDG transport grid on Ω is the rectangular grid used for the flow discretization (on Ω_f this is the grid before subdividing into triangles).

The computed Stokes-Darcy velocity \mathbf{U} is used in the transport scheme by first projecting it onto the space of piecewise bilinear functions on the transport grid. In the Stokes region the computed Taylor-Hood velocity vector is quadratic on each triangle and it is simply evaluated at the vertices of each rectangle. In the Darcy region the velocity vector at each vertex is recovered by combining the Raviart-Thomas normal velocities on the two edges forming the vertex.

Remark 4.4.1 *The choice of rectangular elements in the Darcy domain was motivated by the superior accuracy and efficiency, including velocity superconvergence (see Section 2.6.1 and Section 3.5), of the MFE method on rectangles, compared to simplicial elements. There exist extensions of the MFE method to quadrilaterals and hexahedra that exhibit accuracy and efficiency similar to the rectangular case. However, since the theory in this work is presented only for affine elements, we limit the numerical results to rectangular elements in the Darcy domain.*

4.4.1 Convergence tests

In the three convergence tests we use a second order Runge-Kutta method to discretize the transport equation in time. The final time is $T = 2$ and the time step is $\Delta t = 10^{-3}$, all numbers being dimensionless. The time step is chosen small enough so that the time discretization error is smaller than the spatial discretization error even for the finest grids used. In the convergence tests with nonzero diffusion we take $\mathbf{D} = 10^{-3} \mathbf{I}$. To handle the purely hyperbolic case $\mathbf{D} = \mathbf{0}$, we introduce an auxiliary variable $\tilde{\mathbf{z}} = -\nabla c$ and set $\mathbf{z} = \mathbf{D}\tilde{\mathbf{z}}$, following an approach from [5] for mixed finite element methods for elliptic problems. The LDG analysis for this formulation has been carried out in [32]. In all convergence tests we take $\phi = 1$ and $\mathbf{K} = K\mathbf{I}$, where K is a constant.

The true solution of the transport equation for all three tests is

$$c(x, y, t) = t(\cos(\pi x) + \cos(\pi y))/\pi.$$

It is chosen to satisfy the outflow boundary condition (1.19) on $\partial\Omega$. The source function f_c is obtained by plugging into (1.16) the true solution functions for the concentration and the velocity specified below. The sign of the normal component of the true velocity determines whether the inflow or the outflow boundary condition is used for the transport equation. The initial condition function c^0 and the inflow condition function c_{in} are obtained by evaluating the true concentration at $t = 0$ and $\mathbf{x} \in \Gamma_{in}$, respectively.

The first two tests use the constructed analytical solutions in *Test 1* (discontinuous velocity across Γ_{fp}) and *Test 2* (smooth velocity across Γ_{fp}) from Section 2.6.1. Next, in *Test 3* the velocity field is continuous, but not smooth, across the interface between the two subdomains:

$$\begin{aligned} \mathbf{u}_f &= \begin{bmatrix} (2-x)(1.5-y)(y-\xi) \\ -\frac{y^3}{3} + \frac{y^2}{2}(\xi+1.5) - 1.5\xi y - 0.5 \end{bmatrix}, \\ \mathbf{u}_p &= \begin{bmatrix} (2-x)(0.5-\xi) \\ \chi(y+0.5) \end{bmatrix}, \\ p_f &= \frac{1}{K}\left(\frac{x^2}{2} - 2x\right)(0.5-\xi) - \frac{11\chi}{8K} + \mu_f(0.5-\xi) + y - 0.5, \\ p_p &= \frac{1}{K}\left(\frac{x^2}{2} - 2x\right)(0.5-\xi) + \frac{\chi}{K}\left(-\frac{y^2+y}{2} - 1\right), \end{aligned}$$

where the parameters μ_f , K , ξ , and χ are defined as in *Test 1*.

Table 4.1: Convergence of the LDG scheme for Test 1: discontinuous tangential velocity.

h	$\mathbf{D} = 10^{-3} \mathbf{I}$				$\mathbf{D} = 0$	
	$\ c - C\ _{L^\infty(L^2)}$	<i>rate</i>	$\ \mathbf{z} - \mathbf{Z}\ _{L^2(L^2)}$	<i>rate</i>	$\ c - C\ _{L^\infty(L^2)}$	<i>rate</i>
1/4	1.99e+00		8.95e-03		2.07e+00	
1/8	3.27e-01	2.60	2.71e-03	1.72	3.39e-01	2.61
1/16	8.48e-02	1.95	1.20e-03	1.18	9.04e-02	1.91
1/32	2.23e-02	1.93	5.33e-04	1.17	2.59e-02	1.80
1/64	5.60e-03	2.00	1.77e-04	1.59	7.76e-03	1.74

Convergence rates for the flow and plots of the computed velocity field in *Test 1* are presented in Section 2.6.1. The convergence rates for the transport equation are studied by solving the coupled flow-transport system with and without diffusion on several levels of grid refinement. The numerical errors and convergence rates for the three tests are reported in Tables 4.1, 4.2, and 4.3. In all three cases we observe experimental convergence of order $O(h^2)$ for the concentration error in $L^\infty(0, T; L^2(\Omega))$ and approaching $O(h)$ for the diffusive flux error in $L^2(0, T; L^2(\Omega))$. Our theoretical results predict $O(h)$ for both variables. Similar second order convergence for the concentration has been observed numerically in the literature for the stand-alone transport equation, see e.g. [3]. Higher order convergence $O(h^{k+1})$ for the $L^2(0, T; L^2(\Omega))$ error of the concentration has been obtained theoretically by adding penalty terms [40, 28]. In our case there are additional terms contributing to the transport numerical error that are coming from the discretization error in the Stokes-Darcy velocity. For our particular choice of flow discretization these terms are $O(h^2)$ from Stokes and $O(h)$ from Darcy. The observed second order convergence of the concentration may be due to the superconvergence of the Raviart-Thomas velocity at the edge midpoints, which are used to obtain the bilinear velocity for the transport scheme. Further theoretical investigation of this phenomenon will be a topic of future work.

Table 4.2: Convergence of the LDG scheme for Test 2: smooth velocity.

h	$\mathbf{D} = 10^{-3} \mathbf{I}$				$\mathbf{D} = 0$	
	$\ c - C\ _{L^\infty(L^2)}$	<i>rate</i>	$\ \mathbf{z} - \mathbf{Z}\ _{L^2(L^2)}$	<i>rate</i>	$\ c - C\ _{L^\infty(L^2)}$	<i>rate</i>
1/4	5.50e-02		5.31e-04		5.54e-02	
1/8	1.44e-02	1.93	2.39e-04	1.15	1.46e-02	1.93
1/16	3.75e-03	1.95	1.09e-04	1.13	3.81e-03	1.93
1/32	9.84e-04	1.93	5.09e-05	1.10	1.01e-03	1.92
1/64	2.60e-04	1.92	2.43e-05	1.07	2.71e-04	1.90

Table 4.3: Convergence of the LDG scheme for Test 3.

h	$\mathbf{D} = 10^{-3} \mathbf{I}$				$\mathbf{D} = 0$	
	$\ c - C\ _{L^\infty(L^2)}$	<i>rate</i>	$\ \mathbf{z} - \mathbf{Z}\ _{L^2(L^2)}$	<i>rate</i>	$\ c - C\ _{L^\infty(L^2)}$	<i>rate</i>
1/4	5.57e-02		4.33e-04		5.63e-02	
1/8	1.39e-02	2.00	2.01e-04	1.10	1.41e-02	2.00
1/16	3.48e-03	2.00	9.62e-05	1.07	3.51e-03	2.00
1/32	8.69e-04	2.00	4.70e-05	1.03	8.77e-04	2.00
1/64	2.17e-04	2.00	2.33e-05	1.01	2.19e-04	2.00

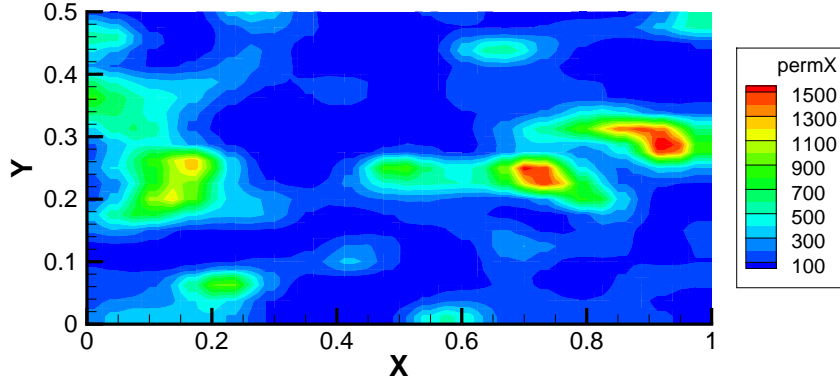


Figure 4.1: Permeability of the porous medium in the contaminant transport examples.

4.4.2 Contaminant transport examples

We present two simulations of coupled surface and subsurface flow and contaminant transport. The Stokes region Ω_f represents a lake or a river, which interacts with an aquifer occupying the Darcy region Ω_p . The porous medium is heterogeneous with permeability varying approximately two orders of magnitude, see Figure 4.1.

In both examples we use the following flow boundary conditions. In the Stokes region we set parabolic inflow on the left boundary, no normal flow and zero tangential stress on the top boundary, and zero normal and tangential stress on the right (outflow) boundary. In the Darcy region we set no flow on the left and right boundaries and specify pressure on the bottom boundary to simulate a gravity force. The computed velocity field for the two simulations is shown in Figure 4.2.

In *Example 1*, a plume of contaminant present at the initial time in the surface water region is transported into the porous media. In *Example 2*, inflow of contaminant is specified on part of the left boundary in the surface water region. The contaminant front eventually reaches and penetrates into the subsurface water region.

The diffusion tensor is chosen to be $\mathbf{D}_{\Omega_f} = 10^{-6}\mathbf{I}$ in the Stokes region, and

$$\mathbf{D}_{\Omega_p} = \phi d_m \mathbf{I} + d_l |\mathbf{u}| \mathbf{T} + d_t |\mathbf{u}| (\mathbf{I} - \mathbf{T})$$

in the Darcy region, where $\mathbf{T} = \frac{\mathbf{u}\mathbf{u}}{|\mathbf{u}|^2}$ and the parameters values are $\phi = 0.4, d_m = d_l = d_t = 10^{-5}$. Here d_m represents molecular diffusion, while d_l and d_t represent longitudinal and transverse

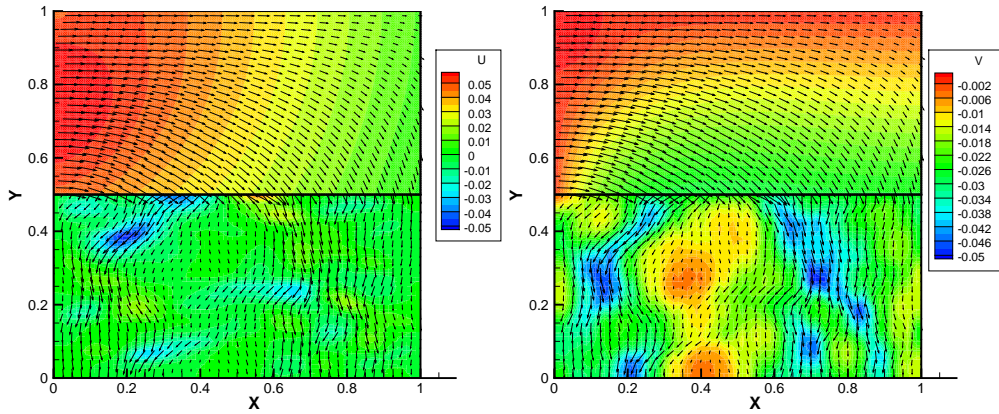


Figure 4.2: Computed velocity field in the contaminant transport examples: horizontal velocity (left); vertical velocity (right).

dispersion, respectively. The simulations were carried out using the forward Euler method for the temporal discretization with $\Delta t = 10^{-3}$ on a square 80×80 mesh.

Due to the discontinuity in the initial (*Example 1*) or boundary (*Example 2*) conditions and small diffusion/dispersion values, the simulations exhibit steep concentration gradients. In such cases a slope limiting procedure is often employed in the LDG scheme to remove oscillations [33, 3]. Our approach is based on [59]. For each element local extremum is avoided by comparing the averages of the concentration over the edges with the averages of the concentration over the neighboring elements. The concentration values at the vertices are reconstructed by imposing mass conservation on the element. The procedure is equivalent to an optimization problem with parametrized equality constraints. Tighter constraints introduce more numerical diffusion and lead to a smoother solution. More relaxed constraints allow for better approximation of propagating sharp fronts.

Plots of the contaminant concentration at various simulation times are shown in Figures 4.3–4.7 for *Example 1* and Figures 4.8–4.10 for *Example 2*. Both two and three dimensional views are included for better illustration of the steep concentration gradients. In *Example 1*, the plume stays compact while in the surface water region. When it reaches the groundwater region, it starts to

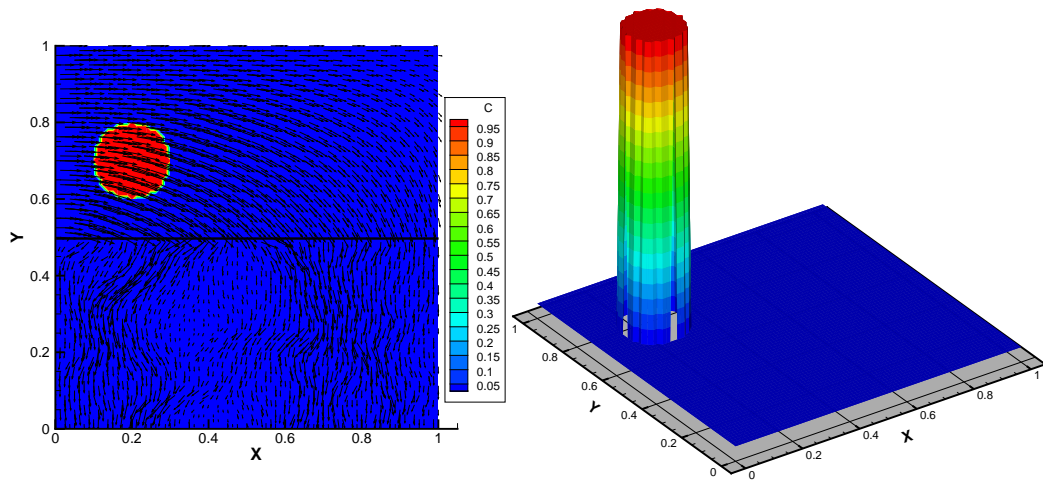


Figure 4.3: Initial plume, $t=0.0$. The arrows represent the computed Stokes-Darcy velocity.

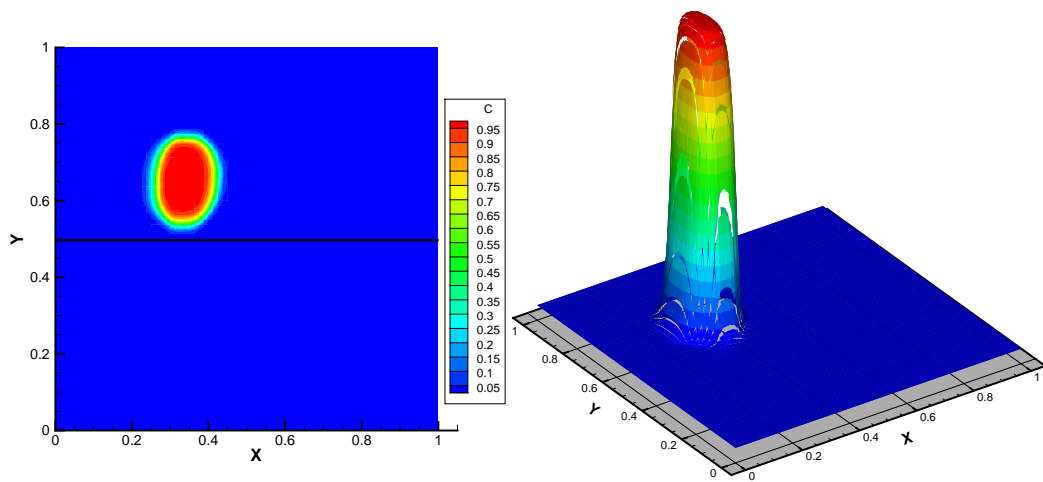


Figure 4.4: The plume at early time is confined to the surface water region, $t=3.0$.

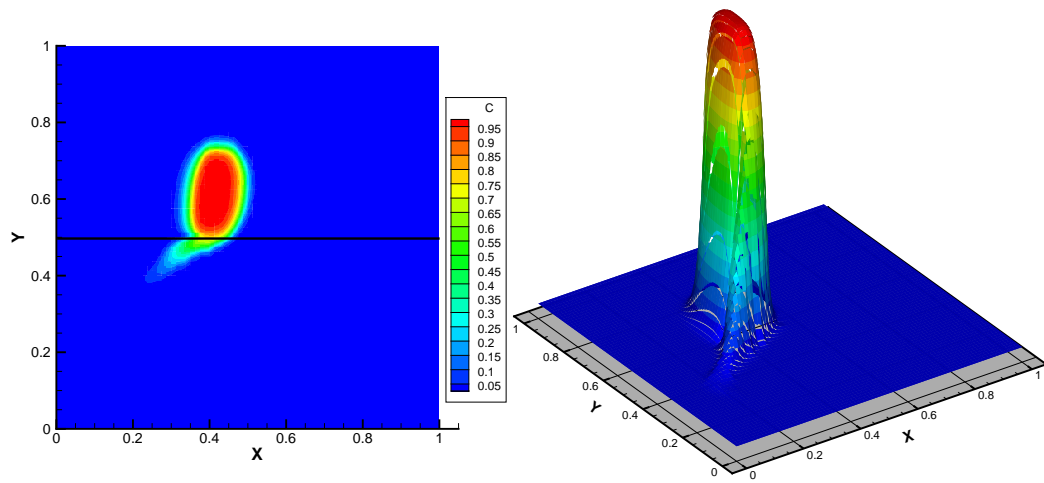


Figure 4.5: The plume penetrates the porous medium, $t=5.0$.

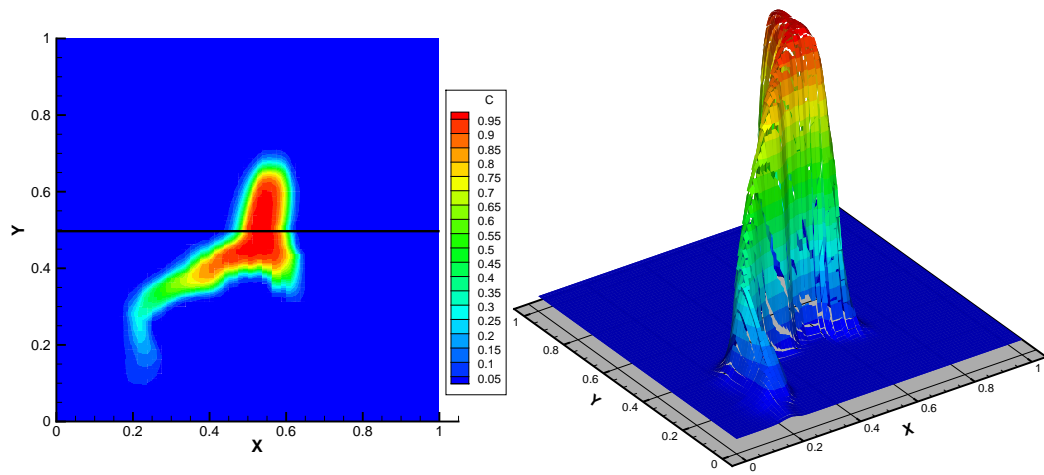


Figure 4.6: The plume spreads through the porous medium, $t=9.0$.

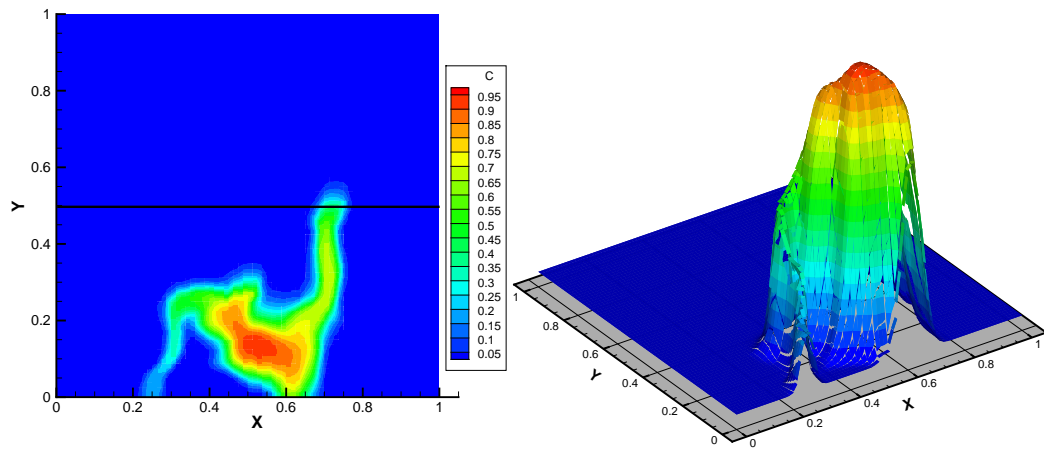


Figure 4.7: Most of the plume has been transported to the porous medium, $t=16.0$.

spread due to the heterogeneity of the porous media. The discontinuity in the tangential velocity along the interface causes some of the contaminant to lag behind and even move in the opposite direction. Similar behavior is observed in *Example 2*, where the contaminant front maintains a relatively flat interface in the surface water region and spreads non-uniformly in the porous media. In both cases, the LDG method with slope limiter preserves sharp discontinuities in the concentration without numerical oscillations.

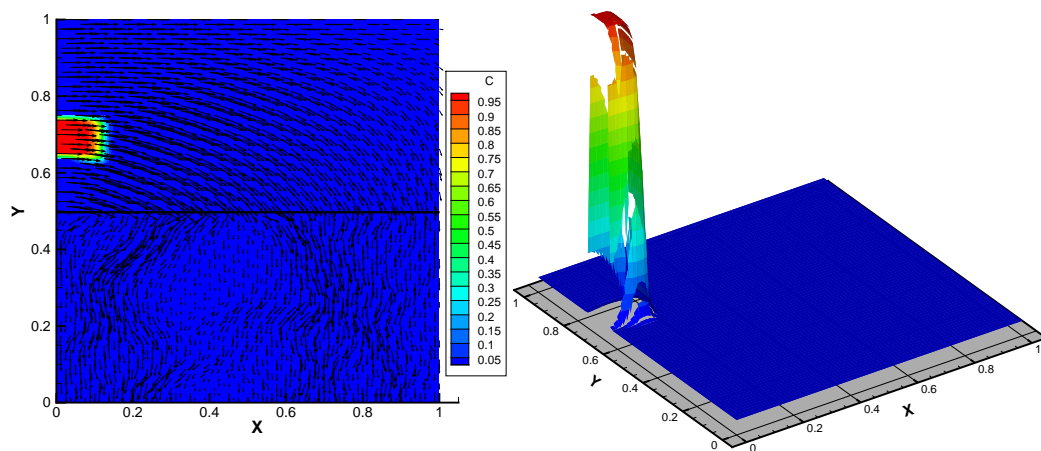


Figure 4.8: The front enters the surface water region, $t=2.0$. The arrows represent the computed Stokes-Darcy velocity.

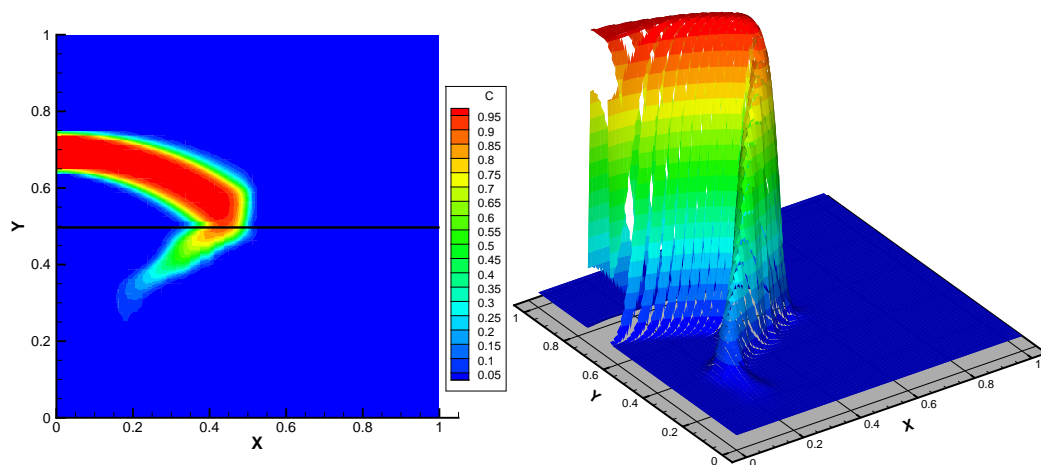


Figure 4.9: The front reaches the porous medium, $t=11.0$.

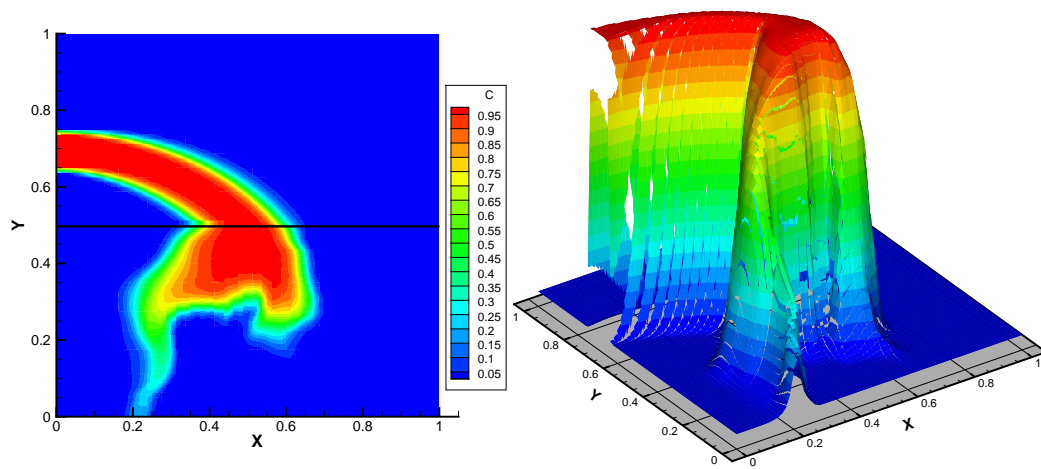


Figure 4.10: The front propagates inside the porous medium, $t=17.0$.

5.0 FUTURE WORK AND CONCLUSIONS

We presented several numerical schemes to discretize the coupled flow-transport problem (1.12)–(1.19). The properties of each scheme were analyzed and error estimates were derived. Then, numerical tests were carried out to confirm the theoretical convergence rates and to illustrate the capability of the method for practical applications. We finish by outlining possible extensions and topics of future work.

- (1) Using a preconditioned iterative method for solving the algebraic system (2.99) is very attractive from practical point of view. Block-diagonal preconditioners for saddle point problems are discussed in [63, 83]. We propose to use a preconditioner

$$\mathbf{H} = \begin{pmatrix} \mathbf{A}_f & \mathbf{0} & \mathbf{0} \\ \mathbf{0} & \mathbf{A}_p & \mathbf{0} \\ \mathbf{0} & \mathbf{0} & \mathbf{S} \end{pmatrix}, \quad (5.1)$$

where \mathbf{S} is a suitable diagonal matrix. An analysis is needed to guarantee that \mathbf{H} results in mesh independent convergence of Krylov space based iterative methods (Lanzcos, MINRES). To invert \mathbf{A}_f and \mathbf{A}_p we intend to use one V-cycle of the algebraic multigrid [87].

- (2) We mentioned several advantages of extending the method presented in Chapter 2 on general polyhedral meshes. This requires constructing operators that map from degrees of freedom to functional spaces and satisfy the properties (L1)–(L3) in Section 2.1.2. Defining such operators on general polyhedral elements is an open question.
- (3) In Chapter 3 the subdomains can be discretized locally with non-matching grids across the interfaces. A mortar grid is then introduced, from which the interface variables are projected onto the subdomain grids. This approach provides flexibility in modelling irregular geometries

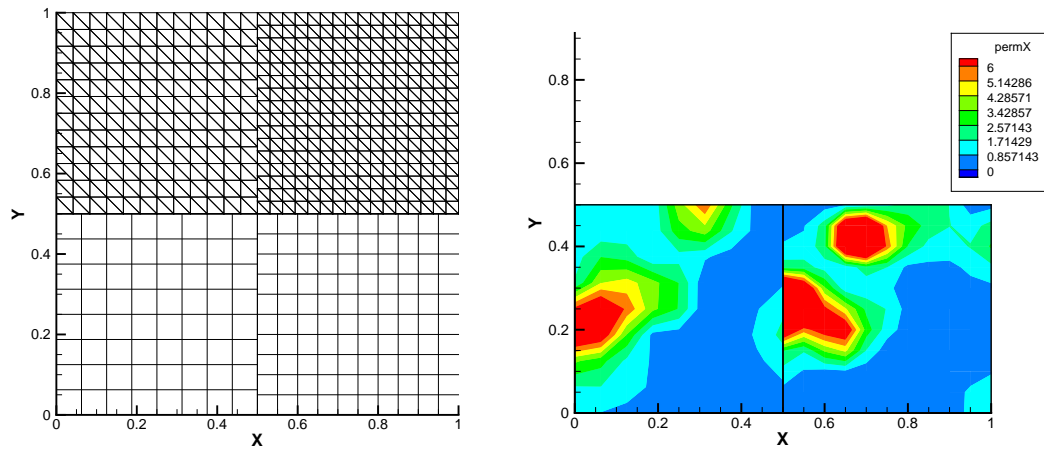


Figure 5.1: Mortar multiscale example. Left: four subdomains with non-matching grids, right: permeability field

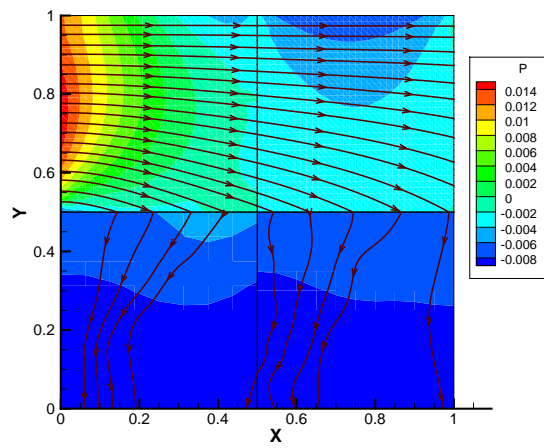


Figure 5.2: Mortar multiscale example. Computed solution.

and large scale geological structures such as faults and layers. Non-matching grids allow for independent refinement of Stokes and Darcy regions. On Figure 5.1 and Figure 5.2 is shown a numerical example of applying the mortar multiscale method: the computational domain is partitioned into four subdomains (top row for Stokes, bottom row for Darcy) with non-matching meshes. The mortar grids are chosen to be coarser than the traces of the subdomain grids. Our preliminary analysis indicates the following error bound for the mortar multiscale method:

$$\|\mathbf{u} - \mathbf{u}^h\|_X + \|p - p^h\|_Q \leq C(h^{r_f} + h^{r_p+1} + H_{fp}^{r_{fp}+1} + H_{pp}^{r_{pp}+1/2} + H_{ss}^{r_{ss}+1/2}), \quad (5.2)$$

where h_α , $\alpha = f, p$, represents the size of the subdomain mesh for each model; H_{fp} , H_{pp} and H_{ff} denote the sizes of the mortar meshes on the Stokes-Darcy, Darcy-Darcy and Stokes-Stokes interfaces, respectively; and the degree of the polynomials in the corresponding finite dimensional spaces are denoted by r . The development of the mortar multiscale method for the Stokes-Darcy flow problem is in progress [54].

- (4) The effectiveness of the domain decomposition depends on the rate at which the interface iterations converge. The latter is characterized by the condition number of the algebraic problem. In Section 3.4 we investigated the dependence of the condition number on the subdomain mesh size, permeability and the interface type. The number of subdomains also has effect on the convergence. Due to the lack of global information exchange between the subdomains the condition number increases rapidly as the number of subdomain increases. Therefore, in order to be able to solve in parallel a large scale problem by employing a large number of processors, one for each subdomain, we need a suitable preconditioning technique. Developing a balancing preconditioner for the method in Section 3.3 is a topic for future work.
- (5) Stochastic modeling is often employed to address a wide range of physical problems whose complexity makes the deterministic analysis impossible or too expensive. In groundwater flow models the heterogeneity of the porous medium can be dealt in probabilistic sense. Specifically, the permeability is represented by a second order stochastic process with a known covariance function. The fact that the permeability is a stochastic function makes the velocity and the pressure of the flow to be stochastic. In [51] MFE method is used in combination with a stochastic

collocation method to analyze the uncertainty of the flow variables for a given random permeability field. Incorporating such a technique in the treatment of the coupled flow-transport problem (1.12)–(1.19) is another challenging direction to extend this work.

BIBLIOGRAPHY

- [1] AWWA *Manual M50*, American Water Works Association, 6666 West Quincy Avenue, Denver, CO 80235, USA, 2 ed., 2007.
- [2] R. ADAMS, *Sobolev Spaces*, Academic Press, New York, 1975.
- [3] V. AIZINGER, C. N. DAWSON, B. COCKBURN, AND P. CASTILLO, *The local discontinuous Galerkin method for contaminant transport*, *Advances in Water Resources*, 24 (2000), pp. 73–87.
- [4] T. ARBOGAST, L. C. COWSAR, M. F. WHEELER, AND I. YOTOV, *Mixed finite element methods on non-matching multiblock grids*, *SIAM J. Numer. Anal.*, 37 (2000), pp. 1295–1315.
- [5] T. ARBOGAST, M. F. WHEELER, AND I. YOTOV, *Mixed finite elements for elliptic problems with tensor coefficients as cell-centered finite differences*, *SIAM J. Numer. Anal.*, 34 (1997), pp. 828–852.
- [6] D. ARNOLD, *An interior penalty finite element method with discontinuous elements*, *SIAM J. Numer. Anal.*, 19 (1982), pp. 742–760.
- [7] D. ARNOLD, F. BREZZI, B. COCKBURN, AND D. MARINI, *Discontinuous Galerkin methods for elliptic problems*, in *Discontinuous Galerkin Methods. Theory, Computation and Applications*, B. Cockburn, G. Karniadakis, and C.-W. Shu, eds., vol. 11, Springer Verlag, 2000, pp. 89–101.
- [8] D. N. ARNOLD, F. BREZZI, AND M. FORTIN, *A stable finite element for the Stokes equations*, *Calcolo*, 21 (1984), pp. 337–344.
- [9] K. ATKINSON AND W. HAN, *Theoretical Numerical Analysis*, vol. 39 of *Texts in Applied Mathematics*, Springer-Verlag, New York, 2001. A Functional Analysis Framework.
- [10] F. BASSI AND S. REBAY, *A high-order accurate discontinuous finite element method for the numerical solution of the compressible Navier-Stokes equations*, *J. Comput. Phys*, 131 (1997), pp. 267–279.
- [11] G. BEAVERS AND D. JOSEPH, *Boundary conditions at a naturally impermeable wall*, *J. Fluid. Mech*, 30 (1967), pp. 197–207.

- [12] L. BEIRÃO DA VEIGA, V. GYRYA, K. LIPNIKOV, AND G. MANZINI, *Mimetic finite difference method for the Stokes problem on polygonal meshes*, J. Comp. Phys, 228 (2009), pp. 7215–7232.
- [13] L. BEIRÃO DA VEIGA AND K. LIPNIKOV, *A mimetic discretization of the Stokes problem with selected edge bubbles*, SIAM J. Sci. Comp., 32 (2010), pp. 875–893.
- [14] M. BERNDT, K. LIPNIKOV, J. D. MOULTON, AND M. SHASHKOV, *Convergence of mimetic finite difference discretizations of the diffusion equation*, East-West J. Numer. Math., 9 (2001), pp. 253–284.
- [15] M. BERNDT, K. LIPNIKOV, M. SHASHKOV, M. WHEELER, AND I. YOTOV, *Superconvergence of the velocity in mimetic finite difference methods on quadrilaterals*, SIAM J. Numer. Anal., 43 (2005), pp. 1728–1749.
- [16] P. BOCHEV AND J. HYMAN, *Principles of mimetic discretizations of differential operators*, in Compatible Spatial Discretizations, vol. 142 of The IMA Volumes in Mathematics and its Applications, Springer-Verlag, New York, 2007, pp. 89–119.
- [17] D. BRAESS, *Finite Elements. Theory, fast solvers, and applications in solid mechanics*, University Press, Cambridge, 2 ed., 2001.
- [18] S. BRENNER, *Korn's inequalities for piecewise h^1 vector fields*, Math. Comp., 73 (2004), pp. 1067–1087.
- [19] S. C. BRENNER AND L. R. SCOTT, *The mathematical theory of finite element methods*, vol. 15 of Texts in Applied Mathematics, Springer-Verlag, New York, 2002.
- [20] F. BREZZI, J. DOUGLAS, JR., R. DURÀN, AND M. FORTIN, *Mixed finite elements for second order elliptic problems in three variables*, Numer. Math., 51 (1987), pp. 237–250.
- [21] F. BREZZI, J. DOUGLAS, JR., M. FORTIN, AND L. D. MARINI, *Efficient rectangular mixed finite elements in two and three space variables*, RAIRO Modèl. Math. Anal. Numèr., 21 (1987), pp. 581–604.
- [22] F. BREZZI, J. DOUGLAS, JR., AND L. D. MARINI, *Two families of mixed elements for second order elliptic problems*, Numer. Math., 88 (1985), pp. 217–235.
- [23] F. BREZZI AND M. FORTIN, *Mixed and hybrid finite element methods*, Springer-Verlag, New York, 1991.
- [24] F. BREZZI, K. LIPNIKOV, AND M. SHASHKOV, *Convergence of mimetic finite difference method for diffusion problems on polyhedral meshes*, SIAM J. Numer. Anal., 43 (2005), pp. 1872–1896.
- [25] ———, *Convergence of mimetic finite difference method for diffusion problems on polyhedral meshes with curved faces*, Math. Mod. Meth. Appl. Sci., 16 (2006), pp. 275–297.

- [26] F. BREZZI, K. LIPNIKOV, AND V. SIMONCINI, *A family of mimetic finite difference methods on polygonal and polyhedral meshes*, *Math. Mod. Meth. Appl. Sci.*, 15 (2005), pp. 1533–1552.
- [27] H. C. BRINKMAN, *A calculation of the viscous force exerted by a flowing fluid on a dense swarm of particles*, *Appl. Sci. Res. A*, 1 (1947), pp. 27–34.
- [28] P. CASTILLO, B. COCKBURN, I. PERUGIA, AND D. SCHÖTZAU, *An a priori error analysis of the local discontinuous Galerkin method for elliptic problems*, *SIAM J. Numer. Anal.*, 38 (2000), pp. 1676–1706 (electronic).
- [29] P. CASTILLO, B. COCKBURN, D. SCHÖTZAU, AND C. SCHWAB, *Optimal a priori error estimates for the hp-version of the local discontinuous Galerkin method for convection-diffusion problems*, *Math. Comp.*, 71 (2002), pp. 455–478 (electronic).
- [30] Z. CHEN AND J. DOUGLAS, JR., *Prismatic mixed finite elements for second order elliptic problems*, *Calcolo*, 26 (1989), pp. 135–148.
- [31] P. CIARLET, *The finite element method for elliptic problems*, North-Holland, Amsterdam, 1978.
- [32] B. COCKBURN AND C. DAWSON, *Some extensions of the local discontinuous Galerkin method for convection-diffusion equations in multidimensions*, in *The mathematics of finite elements and applications*, X, MAFELAP 1999 (Uxbridge), Elsevier, Oxford, 2000, pp. 225–238.
- [33] B. COCKBURN, S. HOU, AND C.-W. SHU, *The Runge-Kutta local projection discontinuous Galerkin finite element method for conservation laws. IV. The multidimensional case*, *Math. Comp.*, 54 (1990), pp. 545–581.
- [34] B. COCKBURN AND C.-W. SHU, *The local discontinuous Galerkin method for time-dependent convection-diffusion systems*, *SIAM J. Numer. Anal.*, 35 (1998), pp. 2440–2463.
- [35] B. COCKBURN AND C.-W. SHU, *Runge-Kutta discontinuous Galerkin methods for convection-dominated problems*, *J. Sci. Comput.*, 16 (2001), pp. 173–261.
- [36] M. CROUZEIX AND R. FALK, *Non conforming finite elements for the Stokes problem*, *Math. Comp.*, 52 (1989), pp. 437–456.
- [37] M. CROUZEIX AND P.-A. RAVIART, *Conforming and nonconforming finite element methods for solving the stationary Stokes equations. I*, *Rev. Française Automat. Informat. Recherche Opérationnelle Sér. Rouge*, 7 (1973), pp. 33–75.
- [38] H. P. G. DARCY, *Les Fontaines Publiques de la Ville de Dijon*, Victor Dalmont, Paris, 1856.
- [39] C. DAWSON, *Conservative, shock-capturing transport methods with nonconservative velocity approximations*, *Comput. Geosci.*, 3 (1999), pp. 205–227 (2000).

- [40] C. DAWSON AND J. PROFT, *A priori error estimates for interior penalty versions of the local discontinuous Galerkin method applied to transport equations*, Numer. Methods Partial Differential Equations, 17 (2001), pp. 545–564.
- [41] C. DAWSON, S. SUN, AND M. F. WHEELER, *Compatible algorithms for coupled flow and transport*, Comput. Methods Appl. Mech. Engrg., 193 (2004), pp. 2565–2580.
- [42] M. DISCACCIATI, E. MIGLIO, AND A. QUARTERONI, *Mathematical and numerical models for coupling surface and groundwater flows*, Appl. Numer. Mathematics, (2002).
- [43] M. DISCACCIATI AND A. QUARTERONI, *Convergence analysis of a subdomain iterative method for the finite element approximation of the coupling of Stokes and Darcy equations*, Comput Visual Sci, 6 (2004), pp. 93–103.
- [44] M. DISCACCIATI, A. QUARTERONI, AND A. VALLI, *Robin-robin domain decomposition methods for the Stokes-Darcy coupling*, SIAM J. Numer. Anal., 45 (2007), pp. 1246–1268.
- [45] J. DONEA AND A. HUERTA, *Finite Element Methods for Flow Problems*, John Wiley & Sons Ltd., 2003.
- [46] J. DRONIOU AND R. EYMARD, *Study of the mixed finite volume method for Stokes and Navier-Stokes equations*, Numerical methods for partial differential equations, 25 (2008), pp. 137–171.
- [47] L. DURLOFSKY AND J. F. BRADY, *Analysis of the Brinkman equation as a model for flow in porous media*, Phys. Fluids, 30 (1987).
- [48] C. FARHAT AND F. ROUX, *A method of finite element tearing and interconnecting and its parallel solution algorithm*, Internat. J. Methods Engrg., 32 (1991), pp. 1205–1227.
- [49] M. FORTIN AND M. SOULIE, *A non-conforming piecewise quadratic finite element on triangles*, Internat. J. Numer. Methods Engrg., 19 (1983), pp. 505–520.
- [50] J. GALVIS AND M. SARKIS, *Non-matching mortar discretization analysis for the coupling Stokes-Darcy equations*, Electron. Trans. Numer. Anal., 26 (2007), pp. 350–384.
- [51] B. GANIS, H. KLIE, M. F. WHEELER, T. WILDEY, I. YOTOV, AND D. ZHANG, *Stochastic collocation and mixed finite elements for flow in porous media*, Comput. Methods Appl. Mech. Engrg., 197 (2008), pp. 3547–3559.
- [52] V. GIRAULT AND P.-A. RAVIART, *Finite element methods for Navier-Stokes equations*, Springer-Verlag, Berlin, 1986. Theory and algorithms.
- [53] V. GIRAULT, B. RIVIÈRE, AND M. WHEELER, *A discontinuous galerkin method with non-overlapping domain decomposition for the Stokes and Navier-Stokes problems*, Mathematics of Computation, 74 (2004), pp. 53–84.

- [54] V. GIRAULT, I. YOTOV, AND D. VASSILEV, *A mortar multiscale finite element method for Stokes-Darcy flows*, (In preparation).
- [55] R. GLOWINSKI AND M. F. WHEELER, *Domain decomposition and mixed finite element methods for elliptic problems*, in First International Symposium on Domain Decomposition Methods for Partial Differential Equations, R. Glowinski, G. H. Golub, G. A. Meurant, and J. Periaux, eds., SIAM, Philadelphia, 1988, pp. 144–172.
- [56] P. GRISVARD, *Elliptic problems in nonsmooth domains*, Pitman, Boston, 1985.
- [57] R. HERBIN, *An error estimate for a finite volume scheme for a diffusion convection problem on triangular mesh*, Numer. Methods P.D.E., 11 (1995), pp. 165–173.
- [58] ———, *Finite volume methods for diffusion convection equations on general meshes*, in Finite volumes for complex applications, Problems and Perspectives, F. Benkhaldoun and R. Vilsmeier, eds., Hermes, 1996, pp. 153–160.
- [59] H. HOTEIT, P. ACKERER, R. MOSE, J. ERHEL, AND B. PHILIPPE, *New two-dimensional slope limiters for discontinuous Galerkin methods on arbitrary meshes*, Int. J. Numer. Meth. Engng., 61 (2004), pp. 2566–2593.
- [60] J. HYMAN AND M. SHASHKOV, *The approximation of boundary conditions for mimetic finite difference methods*, Computers and Mathematics with Applications, 36 (1998), pp. 79–99.
- [61] ———, *Mimetic discretizations for Maxwell’s equations and the equations of magnetic diffusion*, Progr. Electromagn. Res., 32 (2001), pp. 89–121.
- [62] J. HYMAN, M. SHASHKOV, AND S. STEINBERG, *The numerical solution of diffusion problems in strongly heterogeneous non-isotropic materials*, J. Comput. Phys., 132 (1997), pp. 130–148.
- [63] Y. KUZNETSOV, *Efficient iterative solvers for elliptic finite element problems on non-matching grids*, Russian J. Numer. Anal. Math. Modelling, 10 (1995), pp. 187–211.
- [64] P. LASAINT AND P.-A. RAVIART, *On a finite element method for solving the neutron transport equation*, in Mathematical aspects of finite elements in partial differential equations, vol. 33, Math. Res. Center, Univ. of Wisconsin-Madison, Academic Press, New York, 1974, pp. 89–123.
- [65] W. LAYTON, F. SCHIEWECK, AND I. YOTOV, *Coupling fluid flow with porous media flow*, SIAM J. Numer. Anal., 40 (2003), pp. 2195–2218.
- [66] J. L. LIONS AND E. MAGENES, *Non-homogeneous boundary value problems and applications*, vol. 1, Springer-Verlag, 1972.

- [67] K. LIPNIKOV, M. SHASHKOV, AND D. SVYATSKIY, *The mimetic finite difference discretization of diffusion problem on unstructured polyhedral meshes*, J. Comput. Phys., 211 (2006), pp. 473–491.
- [68] K. LIPNIKOV, M. SHASHKOV, AND I. YOTOV, *Local flux mimetic finite difference methods*, Numerische Mathematik, 112 (2008), pp. 115–152.
- [69] K. LIPNIKOV, D. VASSILEV, AND I. YOTOV, *Discontinuous Galerkin and mimetic finite difference methods for coupled Stokes-Darcy flows on polygonal grids*, (In preparation).
- [70] I. LOMTEV AND G. KARNIADAKIS, *A discontinuous galerkin method for the navier-stokes equations*, Int. J. Numer. Meth. Fluids, 29 (1999), pp. 587–603.
- [71] J. MANDEL, *Balancing domain decomposition*, Communications in Numerical Methods for Engineering, 9 (1993), pp. 233–241.
- [72] K. A. MARDAL, X.-C. TAI, AND R. WINTHER, *A robust finite element method for Darcy-Stokes flow*, SIAM J. Numer. Anal., 40 (2002), pp. 1605–1631 (electronic).
- [73] L. MARGOLIN, M. SHASHKOV, AND P. SMOLARKIEWICZ, *A discrete operator calculus for finite difference approximations*, Comput. Methods Appl. Mech. Engrg., 187 (2000), pp. 365–383.
- [74] T. P. MATHEW, *Domain decomposition and iterative refinement methods for mixed finite element discretizations of elliptic problems*, PhD thesis, Courant Institute of Mathematical Sciences, New York University, 1989. Tech. Rep. 463.
- [75] J. C. NEDELEC, *Mixed finite elements in \mathbf{R}^3* , Numer. Math., 35 (1980), pp. 315–341.
- [76] D. A. NIELD AND A. BEJAN, *Convection in Porous Media*, Springer-Verlag, New York, 1992.
- [77] J. T. ODEN, I. BABUŠKA, AND C. E. BAUMANN, *A discontinuous hp finite element method for diffusion problems*, J. Comput. Phys., 146 (1998), pp. 491–516.
- [78] A. QUARTERONI AND A. VALLI, *Numerical Approximations of Partial Differential Equations*, Springer-Verlag, Berlin Heidelberg New York, 2 ed., 1997.
- [79] P.-A. RAVIART AND J. M. THOMAS, *A mixed finite element method for 2nd order elliptic problems*, in Mathematical Aspects of the Finite Element Method, Lecture Notes in Mathematics, vol. 606, Springer-Verlag, New York, 1977, pp. 292–315.
- [80] W. REED AND T. HILL, *Triangular mesh methods for the neutron transport equation*, Tech. Rep. LA-UR-73-479, Los Alamos Scientific Laboratory, 1973.
- [81] B. RIVIÈRE AND I. YOTOV, *Locally conservative coupling of Stokes and Darcy flows*, SIAM J. Numer. Anal., 42 (2005), pp. 1959–1977.

- [82] T. RUSSELL, M. WHEELER, AND I. YOTOV, *Superconvergence for control-volume mixed finite element methods on rectangular grids*, SIAM J. Numer. Anal., 45 (2007), pp. 223–235.
- [83] T. RUSTEN AND R. WINTHER, *A preconditioned iterative methods for saddle point problems*, SIAM J. Matrix Anal. Appl., 13 (1992), pp. 887–904.
- [84] P. SAFFMAN, *On the boundary condition at the surface of a porous media*, Stud. Appl. Math., L, (1971), pp. 93–101.
- [85] H. SCHWARZ, *Über einen Grenzübergang durch alternierendes Verfahren*, Vierteljahr. Naturforschenden Gesellschaft Zürich, 15 (1870), pp. 272–286.
- [86] M. SHASHKOV AND S. STEINBERG, *Support-operator finite difference algorithms for general elliptic problems*, J. Comput. Phys., 118 (1995), pp. 131–151.
- [87] K. STÜBEN, *Algebraic multigrid (AMG): experiences and comparisons*, Appl. Math. Comput., 13 (1983), pp. 419–452.
- [88] S. SUN AND M. F. WHEELER, *Discontinuous Galerkin methods for coupled flow and reactive transport problems*, Appl. Numer. Math., 52 (2005), pp. 273–298.
- [89] C. TAYLOR AND P. HOOD, *A numerical solution of the Navier-Stokes equations using the finite element technique*, Internat. J. Comput. & Fluids, 1 (1973), pp. 73–100.
- [90] A. TOSELLI AND O. WIDLUND, *Domain Decomposition Methods - Algorithms and Theory*, Springer-Verlag Berlin Heidelberg, 2005.
- [91] D. VASSILEV AND I. YOTOV, *Domain decomposition for coupled Stokes and Darcy flows*, (In preparation).
- [92] ———, *Coupling Stokes-Darcy flow with transport*, SIAM J. Sci. Comput., 31 (2009), pp. 3661–3684.
- [93] T. WARBURTON AND G. KARNIADAKIS, *A discontinuous Galerkin method for the viscous mhd equations*, J. Comput. Phys, 152 (1999), pp. 1–32.
- [94] M. F. WHEELER, *An elliptic collocation-finite element method with interior penalties*, SIAM J. Numer. Anal., 15 (1978), pp. 152–161.